

CALIBRATION OF TURKISH LRFD BRIDGE DESIGN METHOD  
FOR  
SLAB ON STEEL PLATE GIRDERS

A THESIS SUBMITTED TO  
THE GRADUATE SCHOOL OF NATURAL AND APPLIED SCIENCES  
OF  
MIDDLE EAST TECHNICAL UNIVERSITY

BY

AHMET FATİH KOÇ

IN PARTIAL FULFILLMENT OF THE REQUIREMENTS  
FOR  
THE DEGREE OF MASTER OF SCIENCE  
IN  
CIVIL ENGINEERING

SEPTEMBER 2013



Approval of the thesis:

**CALIBRATION OF TURKISH LRFD BRIDGE DESIGN METHOD  
FOR  
SLAB ON STEEL PLATE GIRDERS**

submitted by **AHMET FATİH KOÇ** in partial fulfillment of the requirements for the degree of **Master of Science in Civil Engineering Department, Middle East Technical University** by,

Prof. Dr. Canan Özgen  
Dean, Graduate School of **Natural and Applied Sciences**

\_\_\_\_\_

Prof. Dr. Ahmet Cevdet Yalçın  
Head of Department, **Civil Engineering**

\_\_\_\_\_

Assoc. Prof. Dr. Alp Caner  
Supervisor, **Civil Engineering Dept., METU**

\_\_\_\_\_

**Examining Committee Members:**

Prof. Dr. M. Semih Yüçemen  
Civil Engineering Dept., METU

\_\_\_\_\_

Assoc. Prof. Dr. Alp Caner  
Civil Engineering Dept., METU

\_\_\_\_\_

Assoc. Prof. Dr. Ayşegül Askan Gündoğan  
Civil Engineering Dept., METU

\_\_\_\_\_

Dr. Erhan Karaesmen  
Civil Engineering Dept., METU

\_\_\_\_\_

Gizem Seyhun, M. Sc.  
ZTM Mühendislik ve Müşavirlik Ltd. Şti.

\_\_\_\_\_

**Date:**

\_\_\_\_\_

**I hereby declare that all information in this document has been obtained and presented in accordance with academic rules and ethical conduct. I also declare that, as required by these rules and conduct, I have fully cited and referenced all material and results that are not original to this work.**

Name, Last Name : Ahmet Fatih Koç  
Signature :

## **ABSTRACT**

### **CALIBRATION OF TURKISH LRFD BRIDGE DESIGN METHOD FOR SLAB ON STEEL PLATE GIRDERS**

Koç, Ahmet Fatih  
M.S., Department of Civil Engineering  
Supervisor: Assoc. Prof. Dr. Alp Caner

September 2013, 114 pages

Steel composite I-girder bridges are usually used to span between 50 to 80 meters in Turkey. In a typical Turkish bridge design, a modified version of the AASHTO LFD (Load Factor Design) or ASD (Allowable Stress Design) requirements are used until now. The recent switch of the US bridge codes to LRFD method also necessitates the calibration of the new design of the Turkish bridges according to the LRFD system. The main aim of this study is to define a new type of live (truck) load to be used in the basic gravity load combination, as well as to develop the corresponding load factors to be implemented in the design of steel composite I-girder bridges. In such studies, usually a target reliability index is selected to reflect the safety level of current design practice based on the uncertainties associated with the design parameters. For the basic gravity load combination, which includes the dead and live loads, a minimum target reliability of 4.00 is selected, instead of 3.50 that have been used in US. In the statistical computations of the reliability index, the quantification of uncertainties is made based on local data supplemented by information compiled from relevant international literature.

**Keywords:** Reliability Analysis, Reliability Index, Bridge Live Load Models, Steel Plate Girder Bridges, LRFD

## ÖZ

### ÇELİK KİRİŞLİ KÖPRÜLER İÇİN TÜRK YÜK VE DAYANIM KATSAYILARI TASARIM YÖNTEMİNİN KALİBRASYONU

Koç, Ahmet Fatih  
Yüksek Lisans, İnşaat Mühendisliği Bölümü  
Tez Yöneticisi: Doç. Dr. Alp Caner

Eylül 2013, 114 sayfa

Türkiye’de çelik I-kirişli kompozit köprüler genellikle 50 ile 80 metre arasındaki açıklıklar için kullanılmaktadır. Türk köprü tasarım pratiğinde AASHTO limit durum tasarım kılavuzunun değiştirilmiş versiyonu ve emniyet gerilmeleri tasarım yöntemleri uygulanmış gelmiştir. Günümüzde ise Amerikan köprü şartnamelerinin limit durum tasarımdan, yük ve dayanım katsayıları tasarım yöntemine geçmesi Türkiye’de de yeni yük ve dayanım katsayıları tasarım yönteminin geliştirmesi ihtiyacını doğurmuştur. Bu çalışmadaki esas amaç çelik I-kirişli kompozit köprülerin tasarımında kullanılacak yeni bir hareketli yük modeli tanımlamak ve bu hareketli yüke uygun yük katsayısı belirlemektir. Bu tür çalışmalarda, genellikle mevcut köprülerin güvenilirlik durumları tasarım parametrelerinin belirsizlikleri üzerinden değerlendirilerek bir hedef güvenilirlik indisi belirlenir. Ölü ve hareketli yükleri barındıran temel düşey yük kombinasyonu için asgari hedef güvenilirlik indisi Amerika’da 3.50 seçilmesine karşın, bu çalışmada 4.00 olarak seçilmiştir. Güvenirlik indisinin istatistiksel hesaplarının içerdiği belirsizlikler yerel kaynaklardan elde edilen verilere göre belirlenmiş olup, elde edilemeyen yerel bilgiler için uluslararası ilgili çalışmalardan yararlanılmıştır.

Anahtar Kelimeler: Güvenirlik Analizi, Güvenirlik İndisi, Köprü Hareketli Yük Modeli, Çelik Yapma Kirişli Köprüler, Yük ve Dayanım Katsayıları Tasarım

To My Parents and Sister

## ACKNOWLEDGMENTS

It is great pleasure to acknowledge the support and help of my supervisor Assoc. Prof. Dr. Alp Caner for his continuous guidance, advice, criticism, and insight throughout the research. Without his patience and encouragement this thesis would not have been completed.

I would also like to express my sincere thanks to Prof. Dr. M. Semih Yücemem for sharing his invaluable experience and knowledge during the preparation of the thesis, and to Assoc. Prof. Dr. Ayşegül Askan, Dr. Erhan Karaesmen and Gizem Seyhun for their suggestions and contributions during my thesis defense.

I owe thanks to Yüksel Domaniç Engineering, and my colleagues for their support, insight and patience, while I was both studying and working, and special thanks to Arzu İpek Yılmaz, Berat Ertekin, Nalan Darende Şafak, and Menekşe Canatan for their encouragements.

I should also thank my dearest friends Gülfem İnaner and Kerem Kılıç for their great friendship and for tolerating my stress throughout the year, and Ali Rıza Yücel, Alp Yılmaz, Sadun Tanışer and Serdar Söğüt for sharing my feelings during our graduate journey.

I have special thanks to Cemre Artan for being with me and for her encouragement, patience, and trust.

Finally, I would like to express my deepest thanks, appreciation and gratitude to my parents and my sister for the affection and love they have given me and their dedicated partnership for success in my life.

## TABLE OF CONTENTS

ABSTRACT .....	v
ÖZ .....	vi
ACKNOWLEDGMENTS .....	viii
TABLE OF CONTENTS.....	ix
LIST OF TABLES.....	xi
LIST OF FIGURES .....	xiii
LIST OF SYMBOLS AND ABBREVIATIONS .....	xvi
CHAPTERS	
1. INTRODUCTION .....	1
1.1 Aim .....	2
1.2 Scope.....	2
2. LITERATURE REVIEW .....	5
3. STATISTICS OF LOADS.....	17
3.1 Dead Loads .....	17
3.2 Live Loads .....	18
3.2.1 Live Load Models .....	18
3.2.2 Evaluation of Truck Survey Data .....	23
3.2.3 Assessment of Statistical Parameters of Live Load .....	28
3.3 Dynamic Load.....	43
3.4 Girder Distribution Factor .....	46
3.5 Summary of Statistical Parameters of Load.....	47
4. STATISTICS OF RESISTANCE.....	49
4.1 Nominal Flexural Resistance Capacity of Composite Steel Girder Based On AASHTO LRFD Design Specifications .....	49
4.2 Quantification of Uncertainties Related to Resistance Variables .....	53
4.2.1 Material Properties.....	53
4.2.2 Dimensions and Theoretical Behavior.....	60
4.2.3 Summary of Statistical Parameters of Resistance.....	60
5. DESIGN OF BRIDGE GIRDERS.....	61

5.1	Designs Using Spreadsheet .....	62
5.1.1	Input Parameters.....	62
5.1.2	Design Algorithm.....	63
5.2	Design Results.....	66
5.2.1	Cross Sectional Dimensions of Steel Girders.....	66
5.2.2	Total Weight of Steel Used in Designed Bridges.....	74
6.	RELIABILITY EVALUATION .....	77
6.1	Reliability Models .....	77
6.1.1	First-Order Second-Moment Methods .....	78
6.1.2	Second-Order Reliability Method .....	84
6.2	Failure Function .....	87
6.3	Target Reliability Index .....	87
6.4	Load and Resistance Factors .....	88
6.5	Comparison of Results of Different Reliability Analysis Methods.....	95
6.6	Change in Reliability Indices with respect to Total Steel Weight.....	97
7.	CONCLUSION.....	101
7.1	Summary and Concluding Comments.....	101
7.2	Recommendations for Future Studies .....	104
	REFERENCES.....	107
	APPENDICES	
A.	DESIGN EXAMPLE .....	111

## LIST OF TABLES

### TABLES

Table 2-1 Recommended Target Reliability Indices (Kun and Qilin, 2012).....	11
Table 2-2 Recommended Resistance Factors (Kun and Qilin, 2012).....	11
Table 3-1 Statistical Parameters of Dead Load.....	18
Table 3-2 Statistical Parameters of Live Load HL93 (Arginhan, 2010).....	20
Table 3-3 Maximum Moments due to HL93 and AYK45 per Lane.....	22
Table 3-4 Truck Types Based on Axle Configuration (Arginhan, 2010).....	24
Table 3-5 Truck Axle Distances Assumed by Arginhan (2010).....	24
Table 3-6 Number of Trucks vs. Time Period and Probability.....	34
Table 3-7 Mean Maximum Moment Ratios (Overall).....	34
Table 3-8 Mean Maximum Moment Ratios (Upper Tail).....	35
Table 3-9 Mean Maximum Moment Ratios (Extreme).....	35
Table 3-10 Gumbel Distribution Parameters, Mean Values, Standard Deviations and Coefficients of Variation of Moment Ratios (Overall) According to Gumbel Distribution.....	39
Table 3-11 Gumbel Distribution Parameters, Mean Values, Standard Deviations and Coefficients of Variation of Moment Ratios (Upper Tail) According to Gumbel Distribution.....	40
Table 3-12 Gumbel Distribution Parameters, Mean Values, Standard Deviations and Coefficients of Variation of Moment Ratios (Extreme) According to Gumbel Distribution.....	40
Table 3-13 One Lane Truck Maximum Moment Ratios (Overall Case).....	42
Table 3-14 One Lane Truck Maximum Moment Ratios (Extreme Case).....	42
Table 3-15 Dynamic Load Allowance, IM (AASHTO LRFD Table 3.6.2.1-1).....	45
Table 3-16 Summary of Statistical Parameters of Loads.....	47
Table 4-1 Statistics of 28-Day Cubic Compressive Strength of Concrete (that involves different grades together) through the Years (Firat, 2006).....	56
Table 4-2 Statistics of 28-Day Cubic Compressive Strength of Different Concrete Grades (Firat, 2006).....	56
Table 4-3 Summary of Findings on C30 Grade of Concrete.....	58
Table 4-4 Strength Values of Steel (TS648, 1980).....	59
Table 4-5 Summary of Statistical Parameters of Resistance.....	60
Table 5-1 Section Dimensions (LL: 1.50, $\Phi_f = 0.90$ ; HL93).....	66
Table 5-2 Section Dimensions (LL: 1.50, R: 0.95; HL93).....	66
Table 5-3 Section Dimensions (LL: 1.50, R: 1.00; HL93).....	66
Table 5-4 Section Dimensions (LL: 1.75, R: 0.90; HL93).....	67
Table 5-5 Section Dimensions (LL: 1.75, R: 0.95; HL93).....	67
Table 5-6 Section Dimensions (LL: 1.75, R: 1.00; HL93).....	67
Table 5-7 Section Dimensions (LL: 2.00, R: 0.90; HL93).....	67

Table 5-8 Section Dimensions (LL: 2.00, R: 0.95; HL93).....	68
Table 5-9 Section Dimensions (LL: 2.00, R: 1.00; HL93).....	68
Table 5-10 Section Dimensions (LL: 2.25, R: 0.90; HL93).....	68
Table 5-11 Section Dimensions (LL: 2.25, R: 0.95; HL93).....	68
Table 5-12 Section Dimensions (LL: 2.25, R: 1.00; HL93).....	69
Table 5-13 Section Dimensions (LL: 2.50, R: 0.90; HL93).....	69
Table 5-14 Section Dimensions (LL: 2.50, R: 0.95; HL93).....	69
Table 5-15 Section Dimensions (LL: 2.50, R: 1.00; HL93).....	69
Table 5-16 Section Dimensions (LL: 1.50, R: 0.90; AYK45) .....	70
Table 5-17 Section Dimensions (LL: 1.50, R: 0.95; AYK45) .....	70
Table 5-18 Section Dimensions (LL: 1.50, R: 1.00; AYK45) .....	70
Table 5-19 Section Dimensions (LL: 1.75, R: 0.90; AYK45) .....	70
Table 5-20 Section Dimensions (LL: 1.75, R: 0.95; AYK45) .....	71
Table 5-21 Section Dimensions (LL: 1.75, R: 1.00; AYK45) .....	71
Table 5-22 Section Dimensions (LL: 2.00, R: 0.90; AYK45) .....	71
Table 5-23 Section Dimensions (LL: 2.00, R: 0.95; AYK45) .....	71
Table 5-24 Section Dimensions (LL: 2.00, R: 1.00; AYK45) .....	72
Table 5-25 Section Dimensions (LL: 2.25, R: 0.90; AYK45) .....	72
Table 5-26 Section Dimensions (LL: 2.25, R: 0.95; AYK45) .....	72
Table 5-27 Section Dimensions (LL: 2.25, R: 1.00; AYK45) .....	72
Table 5-28 Section Dimensions (LL: 2.50, R: 0.90; AYK45) .....	73
Table 5-29 Section Dimensions (LL: 2.50, R: 0.95; AYK45) .....	73
Table 5-30 Section Dimensions (LL: 2.50, R: 1.00; AYK45) .....	73
Table 5-31 Alternative Girder designed for HL93 (LL: 2.50 and R: 1.0).....	74
Table 6-1 Reliability Index and the Corresponding Probability of Failure.....	80
Table 6-2 Reliability Indices for Different Sets of Load and Resistance Factors (HL93) (Based on the Statistics of Live Load from Overall Case).....	88
Table 6-3 Reliability Indices for Different Sets of Load and Resistance Factors (HL93) (Based on the Statistics of Live Load from Extreme Case) .....	89
Table 6-4 Reliability Indices for Different Sets of Load and Resistance Factors (AYK45) (Based on the Statistics of Live Load from Overall Case).....	89
Table 6-5 Reliability Indices for Different Sets of Load and Resistance Factors (AYK45) (Based on the Statistics of Live Load from Extreme Case).....	90
Table 6-6 Comparison of Results of Different Reliability Analysis Methods .....	96

## LIST OF FIGURES

### FIGURES

Figure 2-1 Original and Extrapolated CDF's of Moment Ratio from Truck Survey (Nowak, 1999) .....	6
Figure 2-2 Bias Factor for One Lane Loaded, Simple Span Moment; Ratio $M(75)/M(HL93)$ and $M(75)/M(HS20)$ , ADTT = 1000 (Nowak, 1999) .....	7
Figure 2-3 Reliability Indices for AASHTO (1992): Simple Span Moment in Composite Steel Girders (Nowak, 1999) .....	9
Figure 2-4 Reliability Indices for LRFD Code, Simple Span Moments in Composite Steel Girders (Nowak, 1999) .....	10
Figure 2-5 Reliability Analysis and Calibration Process (Kwon et al., 2011) .....	12
Figure 2-6 Reliability Indices for Representative Bridges (Kwon et al., 2011) .....	13
Figure 2-7 Average Reliability Indices for Different ADTT Values (Kwon et al., 2011) .....	14
Figure 2-8 Reliability Indices for Different Sets of Load and Resistance Factors (HL93) (Arginhan, 2010) .....	15
Figure 3-1 HL93 Live Load Model .....	19
Figure 3-2 HL93 Design Truck (AASHTO LRFD) .....	19
Figure 3-3 H30S24 Truck Loading .....	20
Figure 3-4 H30S24 Lane Loading .....	20
Figure 3-5 The Ratio of Midspan Moment Effect of H30S24 Design Truck to Lane Loading .....	21
Figure 3-6 AYK45 Live Load Model .....	21
Figure 3-7 The Ratio of Midspan Moments of AYK45 Loading to Current Turkish Design Live Load .....	22
Figure 3-8 Comparison of Moments of HL93 and AYK45 per Lane .....	23
Figure 3-9 Histogram of Vehicles Based on Axle Configurations (Arginhan, 2010) ..	25
Figure 3-10 Histogram of Gross Vehicle Weights (GVW) of Surveyed Trucks .....	25
Figure 3-11 Histogram of Moments of Surveyed Trucks for Span Length of 50 m .....	26
Figure 3-12 Histogram of Moments of Surveyed Trucks for Span Length of 60 m .....	26
Figure 3-13 Histogram of Moments of Surveyed Trucks for Span Length of 70 m .....	27
Figure 3-14 Histogram of Moments of Surveyed Trucks for Span Length of 80 m .....	27
Figure 3-15 Straight Lines Fitted to Overall Moment Ratios on Normal (NP) and Gumbel (GP) Probability Papers for 50 m Span Length .....	29
Figure 3-16 Straight Lines Fitted to Overall Moment Ratios on Normal (NP) and Gumbel (GP) Probability Papers for 60 m Span Length .....	30
Figure 3-17 Straight Lines Fitted to Overall Moment Ratios on Normal (NP) and Gumbel (GP) Probability Papers for 70 m Span Length .....	30
Figure 3-18 Straight Lines Fitted to Overall Moment Ratios on Normal (NP) and Gumbel (GP) Probability Papers for 80 m Span Length .....	30

Figure 3-19 Straight Lines Fitted to Upper Tail of Moment Ratios on Normal (NP) and Gumbel (GP) Probability Papers for 50 m Span Length.....	31
Figure 3-20 Straight Lines Fitted to Upper Tail of Moment Ratios on Normal (NP) and Gumbel (GP) Probability Papers for 60 m Span Length.....	31
Figure 3-21 Straight Lines Fitted to Upper Tail of Moment Ratios on Normal (NP) and Gumbel (GP) Probability Papers for 70 m Span Length.....	31
Figure 3-22 Straight Lines Fitted to Upper Tail of Moment Ratios on Normal (NP) and Gumbel (GP) Probability Papers for 80 m Span Length.....	32
Figure 3-23 Straight Lines Fitted to Extreme Surveyed Truck Moment Ratios on Normal (NP) and Gumbel (GP) Probability Papers for 50 m Span Length .....	32
Figure 3-24 Straight Lines Fitted to Extreme Surveyed Truck Moment Ratios on Normal (NP) and Gumbel (GP) Probability Papers for 60 m Span Length .....	32
Figure 3-25 Straight Lines Fitted to Extreme Surveyed Truck Moment Ratios on Normal (NP) and Gumbel (GP) Probability Papers for 70 m Span Length .....	33
Figure 3-26 Straight Lines Fitted to Extreme Surveyed Truck Moment Ratios on Normal (NP) and Gumbel (GP) Probability Papers for 80 m Span Length .....	33
Figure 3-27 Extrapolated Moment Ratios (Overall) .....	36
Figure 3-28 Extrapolated Moment Ratios (Upper Tail).....	37
Figure 3-29 Extrapolated Moment Ratios (Extreme).....	38
Figure 3-30 An Example of How to Calculate Gumbel Distribution Parameters for the Case of 50 m Span Length (Overall Case).....	39
Figure 3-31 Comparison of Moment Ratios Based on Different Assumptions .....	41
Figure 3-32 Comparison of Coefficients of Variation Based on Different Assumptions .....	41
Figure 3-33 One Truck Followed Behind by Another Truck.....	42
Figure 3-34 Two Trucks in Adjacent Lanes.....	43
Figure 3-35 Static and Dynamic Response of an Actual Bridge Due to an Actual Truck (Nassif and Nowak, 1995).....	44
Figure 3-36 Dynamic Load Factors for One Truck and Two Trucks (Hwang and Nowak, 1991).....	45
Figure 4-1 Cross-Section of Isolated Composite Steel Girder (AASHTO LRFD 2010) .....	49
Figure 4-2 Location of PNA: in Web (CASE I), in Flange (CASE II), and in Deck (CASE III) (AASHTO LRFD 2010).....	53
Figure 4-3 RMC Production per Capita in Europe (ERMCO, 2013).....	54
Figure 4-4 Concrete Production (%) with respect to Years .....	55
Figure 4-5 Distribution of Steel Structures (Altay and Güneyisi, 2008).....	59
Figure 5-1 Typical Cross-Section of Designed Bridges.....	61
Figure 5-2 Common Input Parameters Substituted to the Program .....	62
Figure 5-3 Further Input Parameters Put into the Program .....	63
Figure 5-4 Design Algorithm Flowchart.....	65
Figure 5-5 Total Weight of Steel (HL93).....	74
Figure 5-6 Total Weight of Steel (AYK45) .....	75

Figure 6-1 Fundamentals of Reliability Analysis .....	77
Figure 6-2 Hasofer-Lind Reliability Index: Nonlinear Failure Function.....	82
Figure 6-3 Nonlinear and Linear Failure Functions .....	85
Figure 6-4 Rotation of Coordinates (Haldar and Mahadevan, 2000) .....	86
Figure 6-5 Reliability Indices for Different Sets of Load and Resistance Factors (HL93) (Based on Statistics of Live Load from Overall Case) .....	91
Figure 6-6 Reliability Indices for Different Sets of Load and Resistance Factors (HL93) (Based on Statistics of Live Load from Extreme Case).....	92
Figure 6-7 Reliability Indices for Different Sets of Load and Resistance Factors (AYK45) (Based on Statistics of Live Load from Overall Case).....	93
Figure 6-8 Reliability Indices for Different Sets of Load and Resistance Factors (AYK45) (Based on Statistics of Live Load from Extreme Case) .....	94
Figure 6-9 Comparison of Results of Different Reliability Analysis Methods (HL93; R: 0.90, LL: 1.50) (Based on Extreme Case).....	95
Figure 6-10 Comparison of Results of Different Reliability Analysis Methods (HL93; R: 0.90, LL: 1.50) (Based on Extreme Case).....	96
Figure 6-11 Change in Reliability Indices with Respect to Total Steel Weight (HL93) (Extreme Case) .....	97
Figure 6-12 Change in Reliability Indices with Respect to Total Steel Weight (HL93) (Overall Case).....	98
Figure 6-13 Change in Reliability Indices with Respect to Total Steel Weight (AYK45) (Extreme Case) .....	98
Figure 6-14 Change in Reliability Indices with Respect to Total Steel Weight (AYK45) (Overall Case).....	99
Figure 7-1 Set of Load and Resistance Factors Considered and Corresponding Reliability Indices (Based on Statistical Parameters Obtained from Extreme Case for Live Load) .....	102
Figure 7-2 Load and Resistance Factor Considered and Corresponding Reliability Index (Based on Statistical Parameters Obtained from Overall Case for Live Load)	103
Figure 7-3 Total Weight of Steel Used in Design of Bridge (AYK45, LL: 1.75) .....	104

## LIST OF SYMBOLS AND ABBREVIATIONS

$A$	Cross sectional area of noncomposite girder
AASHTO	American Association of State Highway and Transportation Officials
ADDT	Average daily truck traffic
AFOSM	Advanced first order second moment
$b_c$	Width of compression flange
$b_e$	Effective width of the concrete deck
$b_s$	Effective width of the concrete deck
$b_t$	Width of tension flange
CDF	Cumulative distribution function
COV	Coefficient of variation
D	Dead load
$D$	Web depth
$D_A$	Dead load due to asphalt
DC	Dead load of structural and non-structural members
$d_c$	Distance from the PNA to the midthickness of the compression flange
$D_{dyn}$	Dynamic deflection
DLF	Dynamic load factor
$D_p$	Distance from the top of the concrete deck to the neutral axis of the composite section at the plastic moment
$d_s$	Distance from the PNA to the midthickness of the concrete deck
$D_{sta}$	Maximum static deflection
$D_t$	Total depth of the composite section
$d_t$	Distance from the PNA to the midthickness of the tension flange
DW	Dead load due to asphalt
$d_w$	Distance from the PNA to the midthickness of the web
$E_B$	Modulus of elasticity of beam material
$E_D$	Modulus of elasticity of deck material
$e_g$	Distance between the centers of gravity of the basic girder and deck
ERMCO	European Ready Mixed Concrete Organization
$f'_c$	Minimum specified 28-day compressive strength of concrete
FHWA	Federal Highway Administration
FORM	First order reliability method
$F_y$	Specified minimum yield strength of steel

GDF	Girder distribution factor
GP	Gumbel probability paper
I	Impact
$I$	Moment of inertia of noncomposite girder
IM	Dynamic impact factor
$K_g$	Longitudinal stiffness parameter
L	Live load; Span length
LFD	Load factor design
LL	Live load; Live load factor
LRFD	Load and resistance factor design
$M_n$	Nominal flexural resistance
$M_p$	Plastic moment of the composite section
MVFOSM	Mean value first order second moment
$\bar{N}$	Mean correction factor
NBI	National Bridge Inventory
NP	Normal probability paper
$P_c$	Plastic force in the compression flange
PNA	Plastic neutral axis
$P_s$	Plastic compressive force in the concrete deck
$P_t$	Plastic force in the tension flange
$P_w$	Plastic force in the web
R	Resistance; Resistance factor
$R$	Rate of loading (psi/sec)
RMC	Ready-mixed concrete
$S$	Girder spacing
SORM	Second order reliability method
$t_c$	Thickness of compression flange
$t_h$	Average thickness of haunch
THBB	Turkish Ready Mixed Concrete Association
$t_s$	Thickness of the concrete deck
$t_t$	Thickness of tension flange
$t_w$	Web thickness
WIM	Weigh-in-motion
$Y$	Distance from the PNA to the top of the element where the PNA is located
$z$	Standard normal variate
$\beta$	Reliability index

$\beta_T$	Target reliability index
$\gamma$	Live load factor
$\gamma_{LL+IM}$	Live load factor
$\delta$	Scale parameter of Gumbel distribution
$\Delta$	Prediction error
$\eta$	Reduced variate
$\lambda$	Location parameter of Gumbel distribution
$\mu$	Mean value
$\sigma$	Standard deviation
$\Phi$	Resistance factor; Standard normal cumulative distribution function
$\Phi_f$	Resistance factor
$\Omega$	Total coefficient of variation

## CHAPTER 1

### INTRODUCTION

Bridges are one of the most significant components of the modern transportation system. Hence, it is essential to ensure that they withstand without any damage during their design lifetime. For that reason, there are some specifications to be followed in design and construction of highway bridges. For instance, “AASHTO (American Association of State Highway and Transportation Officials) LRFD (Load and Resistance Factor Design) Bridge Design Specifications” are used in the US and “Eurocode” is used in the European Union.

In Turkey, a modified version of “AASHTO Standard Specifications for Highway Bridges”, which was used early in the US, is used for the design of typical highway bridges. That design code is based on load factor design (LFD). However, due to the shift in design concept from LFD to LRFD (probability-based design method) throughout the world, General Directorate of Highways of Turkey has decided to use a modified version of AASHTO LRFD requirements in design of Turkish bridges.

In LFD concept, load and resistance factors are calibrated based on experience and judgment, whereas in LRFD concept, load and resistance factors are calibrated based on statistical parameters belonging to load and resistance. LRFD method has been developed in order to maintain a uniform and consistent safety margin for various types of structures. In calibration of AASHTO LRFD method, statistical parameters pertaining to engineering design and construction practice have been used in the USA. Therefore, in a similar way, the LRFD method should be calibrated to be used in Turkey based on Turkish engineering practice.

Two main components used in calibration of design method are load and resistance. The structural reliability of a bridge is a function of these two components. Basically, the resistance should be high enough to resist loads. However, there is always a chance that the effect of loads can exceed the resistance, which can be quantified by the probability of failure. Uncertainties related to load and resistance should be assessed to develop a design method with a probabilistic approach.

The most popular bridge safety measure in probabilistic approach is reliability index,  $\beta$ , which is an indicator of probability of survival. In calibration, the goal is to choose load and resistance factors so that predefined target reliability index is achieved.

## 1.1 Aim

The aim of this study to calibrate load and resistance factors for the design of composite steel plate girder bridges by considering local conditions of Turkey and by utilizing probabilistic methods.

For that purpose, Strength I limit state of AASHTO LRFD is calibrated for 50 to 80 m long simply supported composite steel plate girder bridges according to uncertainties involved in the design and construction practice in Turkey. In case of lack of data reflecting conditions in Turkey, data available from international literature have been used.

A new design live load, which will be called AYK45 (Ağır Yük Kamyonu (“*Heavy Load Truck*” in Turkish): 45 tons with lane load of 1 ton/m) in the rest of this study, is also proposed to overcome the shortcomings associated with the current Turkish design truck load. For proposed design live load, statistical parameters are calculated using truck survey data for 2005 and 2006 gathered from the Division of Transportation and Cost Studies of the General Directorate of Highways of Turkey. This data base is the same as the one used in the thesis study of Arınhan (2010). In his thesis, Arınhan evaluated statistical parameters of HL93 design live load for Turkey.

A minimum target reliability index of 4.00 is aimed, instead of 3.50, which was used as the minimum value in the calibration of AASHTO LRFD in the USA. For this purpose, flexural designs of a total of 120 simply supported composite steel plate girder bridges having span length varying from 50 to 80 m have been utilized for both HL93 (current AASHTO LRFD live load model) and AYK45 loading with different set of load and resistance factor combinations. In design, AASHTO LRFD requirements have been followed. For each design, reliability indices are evaluated by using the computational algorithms according to MVFOSM (Mean Value First Order Second Moment), AFOSM (Advanced First Order Second Moment), FORM (First Order Reliability Method) and SORM (Second Order Reliability Method).

## 1.2 Scope

Literature is reviewed in Chapter 2. Calibration procedure of AASHTO LRFD is presented. In addition, other researches on calibration of load and resistance factors are summarized.

In Chapter 3, statistical parameters regarding load components are stated. HL93 and AYK45 live load models are explained. The 75-year maximum live load effect is predicted by using the extreme value theory. For that purpose, truck survey data is

processed. Moreover, statistical parameters of dead loads, girder distribution factor and dynamic load factor are presented.

Nominal flexural resistance capacity of composite steel girder is derived based on AASHTO LRFD Bridge Design Specifications in Chapter 4. Then, uncertainties regarding resistance are introduced considering conditions in Turkey.

In Chapter 5, typical geometrical properties of cross section of designed bridges are given. Design algorithm and design results in terms of dimensions and estimated total weights are presented.

Different reliability analysis methods are introduced in Chapter 6. Furthermore, reliability analysis of girders designed for both HL93 and AYK45 are conducted. Reliability indices are given with respect to span length and set of load and resistance factors. The comparison of results of different reliability analysis is done.

Finally, main findings of the study are presented in Chapter 7. A conclusion is drawn. Further study to be conducted in future is also recommended.



## CHAPTER 2

### LITERATURE REVIEW

It is not possible to maintain uniform safety level in design of different bridges with allowable stress design and load factor design. Therefore, a new design concept is needed in order to provide consistent and uniform safety level. This new design concept is called LRFD which is based on probabilistic analysis (Nowak, 1999).

The report of National Cooperative Highway Research Program named “Report 368: Calibration of LRFD Bridge Design Code” by Nowak aims to describe the calibration procedure of LRFD – in other words, it aims to show how to calculate load and resistance factors (Nowak, 1999). In this report, calibration procedure, load models, resistance models, reliability analysis and the development of load and resistance factors are presented. This report provides the main guideline for this thesis study.

Calibration procedure described in the Calibration Report includes six main steps, which are selection of representative bridges, establishing the statistical data base for load and resistance parameters, development of load and resistance models, development of the reliability analysis procedure, selection of the target reliability index, and calculation of load and resistance factors.

About 200 bridges which were not very old were selected from different regions of the United States for design evaluation. Load effects including moments, shears, tensions and compressions as well as load carrying capacities were calculated for each selected bridge and its members. The available data on loads and resistance were gathered using results of surveys, material tests, component tests and field measurements. Considering load and resistance were random variables, their variations were defined in terms of cumulative distribution functions (CDF) and correlations. Thereby, live load model including multiple presence of trucks in one lane and in adjacent lanes, dynamic load for single trucks and two trucks side-by-side, resistance models for girder bridges were developed. Next, the reliabilities of structures were calculated in terms of reliability index ( $\beta$ ) by defining limit states as mathematical formulas. An iterative procedure described by Rackwitz and Fiessler was used in the calculation of reliability index. Next, a target reliability index ( $\beta_T$ ) was chosen by considering that reliability level of existing structures was adequate. Finally, load and resistance factors were calculated so that predefined target reliability index was achieved (Nowak, 1999).

The effect of live load is a function of many variables which are the span length, truck weight, axle loads and configuration, position of the vehicle on the bridge (transverse and longitudinal), multiple presence of vehicles on the bridge, girder spacing, and stiffness of structural members (slab and girders) (Nowak, 1999).

HL93 live load model is used in the current AASHTO LRFD 2010. Design live load model of early versions of AASHTO is standard HS20 truck or lane loading, whichever governs. HL93 and HS20 trucks are the same except that HL93 truck is combined with a uniform lane load, whereas HS20 truck is not.

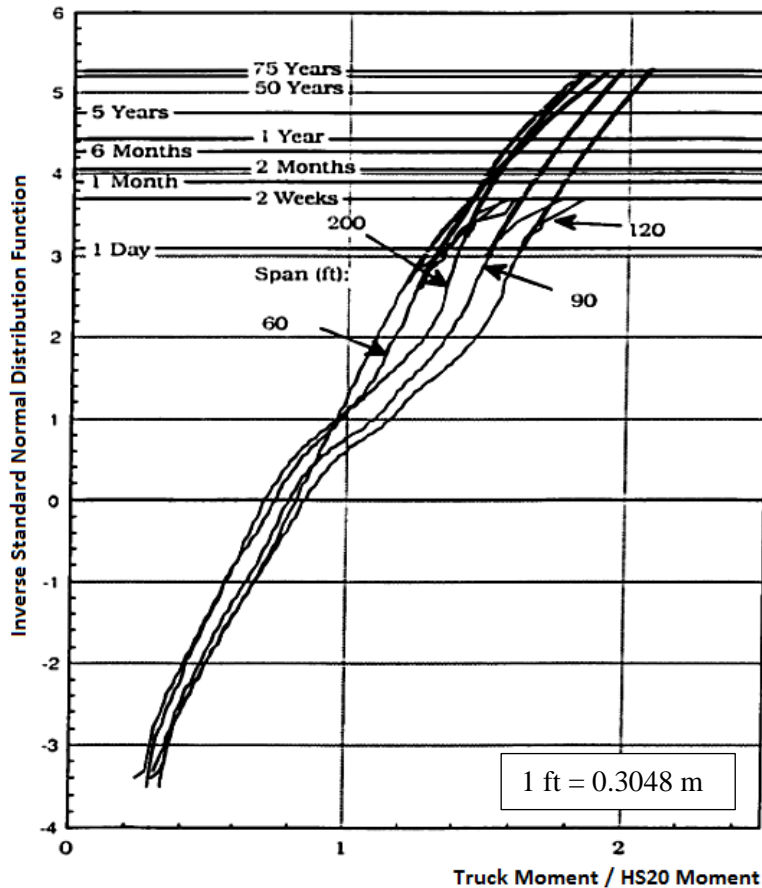


**Figure 2-1** Original and Extrapolated CDF's of Moment Ratio from Truck Survey (Nowak, 1999)

In the Calibration Report, data of truck survey performed in 1975 by the Ontario Ministry of Transportation is used. The considered survey data covered approximately 10,000 trucks, which is very small compared to the actual number of heavy vehicles in

a 75 year life time. To estimate maximum truck moment for various time periods, the available survey data is extrapolated (Nowak, 1999).

Simple span moments of all surveyed trucks were calculated for spans from 30 to 200 feet (9.144 to 60.96 meters), so were moments of HS20 truck or lane loading, whichever governs. After that, the cumulative distribution function (CDF) of moment ratio of surveyed truck to HS20 was plotted on normal probability paper (Figure 2-1). Finally, these distributions were extrapolated for various time periods (Figure 2-1). Extrapolation is carried out by assuming number of trucks passing through the bridge in different time periods. For example, considering the surveyed trucks represent about two week traffic, a total of 20 million trucks are assumed to pass in 75 year time period (Nowak, 1999).

In the Calibration Report, a new live load model, which is currently called HL93, was proposed. A comparison on effects of HL93 live load model and HS20 truck model was made for various span lengths in terms of bias factor, which is the ratio of moment of maximum 75 year live load to that of HL93 or HS20. In Figure 2-2, calculated bias factors for HL93 and HS20 are shown. HL93 live load model is more uniform in terms of bias factor compared with HS20 load model.

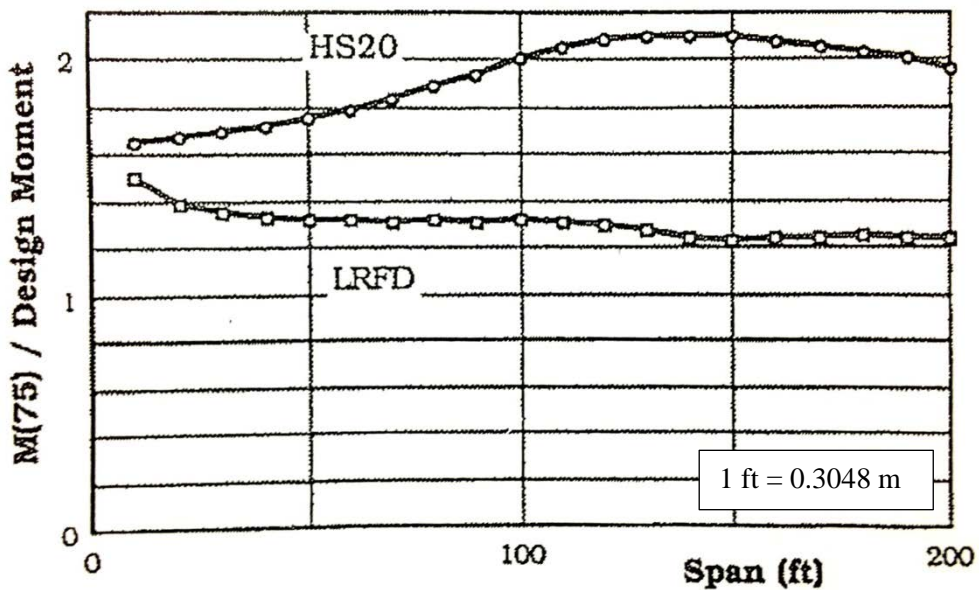


**Figure 2-2** Bias Factor for One Lane Loaded, Simple Span Moment; Ratio  $M(75)/M(HL93)$  and  $M(75)/M(HS20)$ , ADTT = 1000 (Nowak, 1999)

Other variables related to live load are dynamic factor and girder distribution factors. In the Calibration Report and update of the Calibration Report, these are explained in detail. In the following chapters, they will be presented.

Resistance,  $R$  is taken as nominal resistance,  $R_n$  multiplied by three random variables, which are strength factor ( $M$ ), fabrication factor ( $F$ ) and analysis factor ( $P$ ).  $M$ ,  $F$  and  $P$  take uncertainties regarding strength of materials, dimensions and analysis methods into account (Nowak, 1999). The formulation is shown below.

$$R = R_n M F P \quad (2-1)$$

The basic design limit state based on AASHTO (Load Factor Design) is described in terms of moments and shears as the following.

$$1.3 D + 2.17 (L + I) < \Phi R \quad (2-2)$$

where  $D$ ,  $L$  and  $I$  are moments (shears) created by dead load, live load and impact, respectively.  $R$  is moment (shear) carrying capacity, and  $\Phi$  is the resistance factor, which is 1.00 for moment and shear design of composite and non-composite steel girders.

In calibration of AASHTO LRFD, reliability analysis was performed for a selected set of structures. Structural type, material and geographical location were taken into consideration for selection. The required minimum resistance was calculated based on equation (2-2) for given loads, namely  $D$ ,  $L$  and  $I$ . The reliability indices calculated for composite steel girders are displayed in Figure 2-3 (Nowak, 1999).

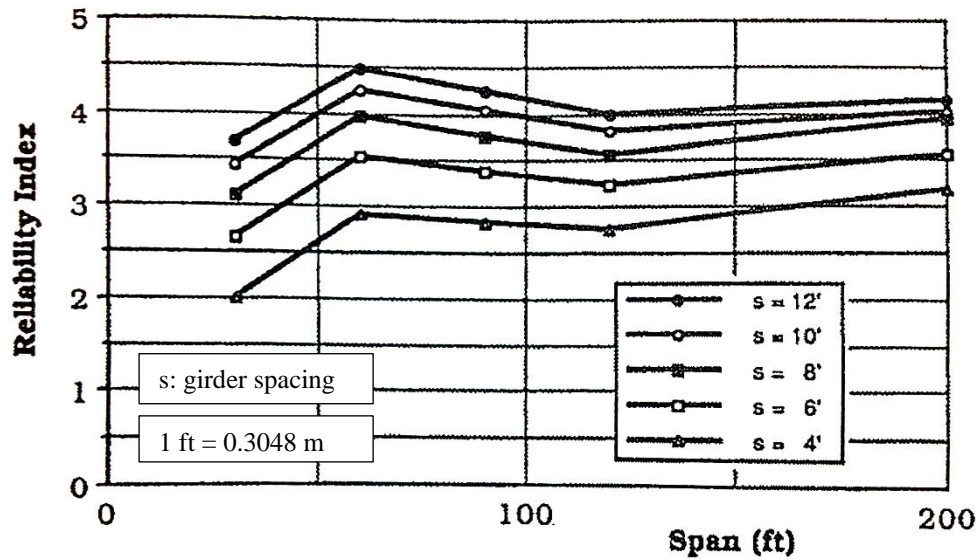


Figure 2-3 Reliability Indices for AASHTO (1992): Simple Span Moment in Composite Steel Girders (Nowak, 1999)

Girders designed based on AASHTO (LFD) does not provide a consistent and uniform safety level as shown in Figure 2-3. Since LFD method, design is very much affected from selected girder spacing and span length. In order to maintain uniform safety level, factors in limit state design equation were tried with different values so that predefined target reliability is achieved. Target reliability index was chosen based on reliability level of existing structures, some part of which is shown in Figure 2-3. Calculated reliability index of girder having span length of 60 ft (18.29 m) and spacing of 6 ft (1.83 m) was accepted as target reliability index, which is  $\beta_T = 3.5$ . For different sets of load and resistance factor, reliability indices were calculated (Nowak, 1999). Results are shown in Figure 2-4.

In the Calibration Report, reliability analysis was carried out using average daily truck traffic (ADTT) = 1000. That resulted in an initial live load factor of 1.7, the alternative of which was 1.6. However, after the Calibration Report had been written, it was decided to use an ADTT = 5000. That means the number of vehicles throughout the calculations had to be multiplied by 5. This change of ADTT from 1000 to 5000 caused an increase in live load force effects by amount of 2.5% for moment and 3.5% for shear (Kulicki et al., 2007). After this adjustment on ADTT, AASHTO LRFD currently uses the design equation below.

$$1.25 D + 1.50 D_A + 1.75 (1 + I)L < \Phi R \quad (2-3)$$

where  $D$  is moment (shear) due to sum of weight of factory made elements and cast-in place concrete,  $D_A$  is moment (shear) due to sum of weight of the wearing surface (asphalt) and miscellaneous weight (e.g. railing, luminaries) and  $(1+I)L$  is moment (shear) due to live load including impact, with the impact factor,  $I$ .

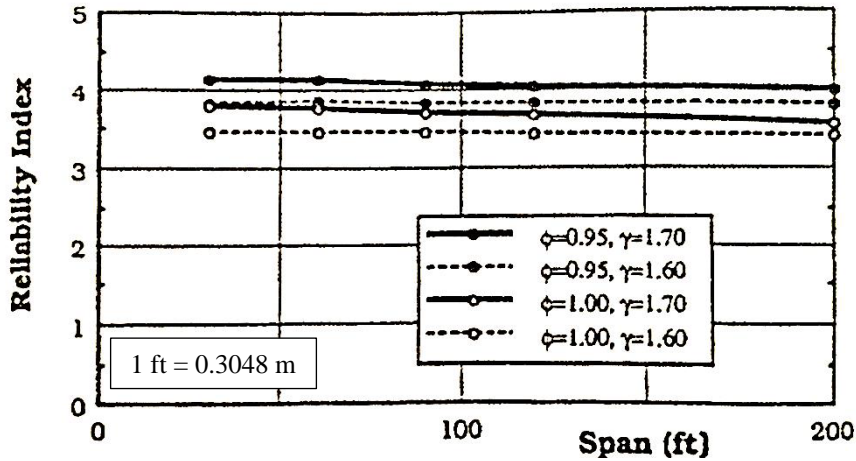


**Figure 2-4** Reliability Indices for LRFD Code, Simple Span Moments in Composite Steel Girders (Nowak, 1999)

In another research conducted by Kun and Qilin (2012) in China, target reliability index of steel highway bridge was calibrated and recommended resistance factors of two commonly used steels for bridges in China (Q235q and Q345qD) were calculated for various type of failure modes, namely axial tensile, axial compression, eccentric compression, flexure and shear. The study was conducted in order to establish a new national design specification for steel highway bridges in China.

For calibration, load combinations including only dead load and live load were considered. Statistical parameters of dead load were determined based on measurements of thickness and unit weight of asphalt concrete and cement concrete pavement from 36 bridges built in different years and based on investigation of the weight admissible errors for self-weight of steel bridge members. It was concluded that dead load follows normal distribution. For live load statistical parameters, the data of more than 60,000 cars were gathered from different testing points on four main national highways. It was seen that live load shows two kinds of distribution, which are extreme value of type 1 and normal. Statistical parameters of resistance consisting of three main uncertainties, which are material properties, geometrical dimensions and calculation models, were obtained from steel plants in China and available literature (Kun and Qilin, 2012).

Reliability indices were calculated by first-order secondary-moment method based on current design specification used in China, which employs the allowable stress design. In reliability analysis, six different ratios of live load to dead load were used, and then averages of their reliability indices were taken. Calculations were done for two kinds of distribution model of live load, which were normal and extreme value type 1; and for two kinds of operation status of live loads, which were normal and intensive car operations; and also for two kinds of load combinations, which were primary and adjunctive load combinations. Hence, eight groups of reliability indices could be calculated. In addition, two different commonly used steel grades were taken into consideration. After all, recommended target reliability indices were determined, which are shown in Table 2-1 (Kun and Qilin, 2012).

**Table 2-1** Recommended Target Reliability Indices (Kun and Qilin, 2012)

Load Combination	Safety of structure					
	Class I		Class II		Class III	
	Ductile failure	Brittle failure	Ductile failure	Brittle failure	Ductile failure	Brittle failure
Primary	5.7	7.2	5.2	6.7	4.7	6.2
Adjunctive	4.2	5.7	3.7	5.2	3.2	4.7

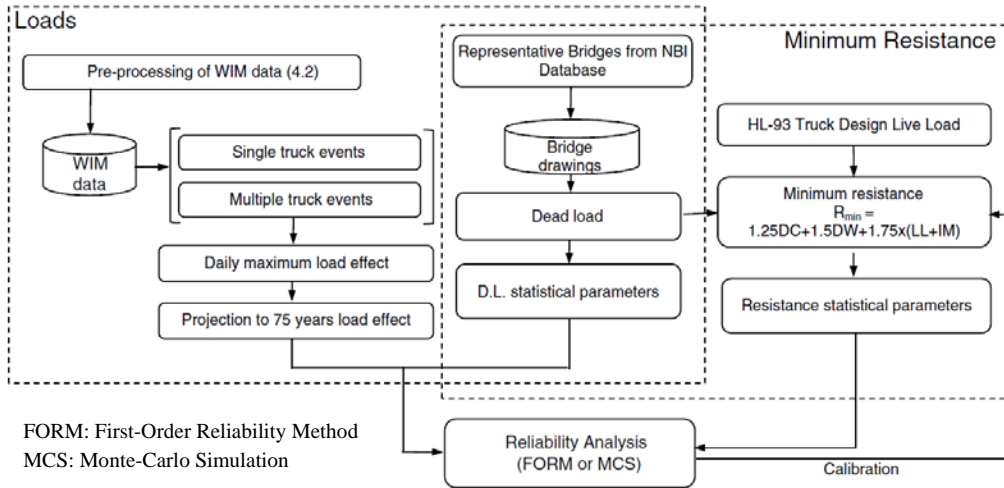
Based on target reliability indices determined, resistance factors were calculated for different load combinations and steel grades and loading state of members, which could be axial tension, axial compression, eccentric compression, flexural, and shear members. Calculated resistance factors,  $\gamma_{Ri}$  are presented in Table 2-2.

**Table 2-2** Recommended Resistance Factors (Kun and Qilin, 2012)

Steel	Load Combination	Resistance factor, $\gamma_{Ri}$				
		$\gamma_{R1}$	$\gamma_{R2}$	$\gamma_{R3}$	$\gamma_{R4}$	$\gamma_{R5}$
Q235q	Primary	1.2687	1.2996	1.3431	1.3592	1.8895
	Adjunctive	1.2034	1.2273	1.3027	1.3150	1.8009
Q345qD	Primary	1.2629	1.3804	1.3654	1.3656	2.1806
	Adjunctive	1.2049	1.3194	1.3217	1.3248	2.1302

In another research conducted by Kwon et al. (2011), the live load factor in the Strength I Limit State in the AASHTO LRFD Bridge Design Specifications was calibrated considering state-specific traffic data and bridge configurations. Live load

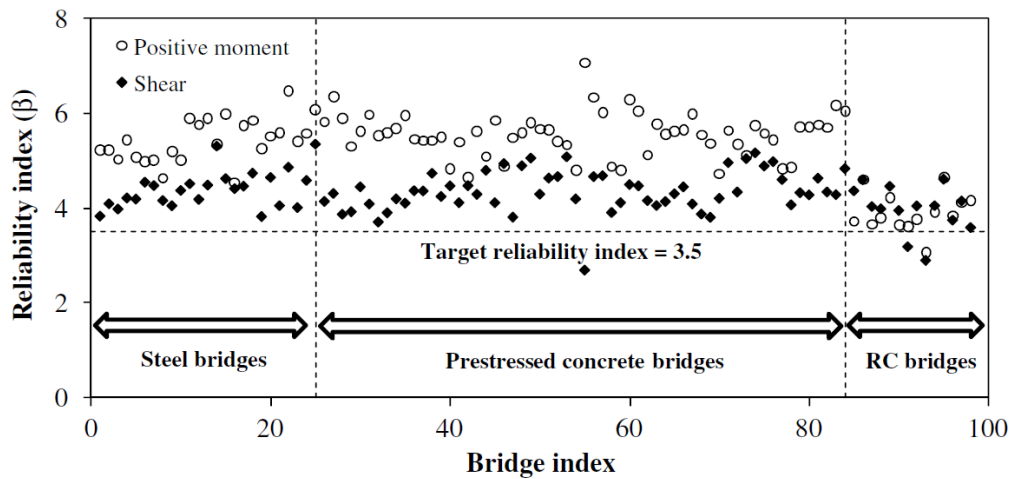
factors were proposed as a function of ADTT. Reliability analysis and calibration process are illustrated in Figure 2-5.



**Figure 2-5** Reliability Analysis and Calibration Process (Kwon et al., 2011)

In Kwon et al.'s (2011) study, about 41 million weigh-in-motion (WIM) data collected between 2004 and 2008 from different WIM stations in Missouri were used, 84% of which were recorded on interstate highways. Only a subset of the heaviest trucks were used in calculation of maximum load effects. For example, when assuming ADTT is 5,000, 5,000 trucks were randomly selected from WIM database and the top 5% heaviest of those selected trucks were used in simulation of heavy single-truck events for each day. Then the mean maximum 75-year load effects were extrapolated by using extreme value theory. Multiple presences of trucks were also taken into consideration. Statistical parameters of dead loads and resistance were taken from Nowak (1999)'s study.

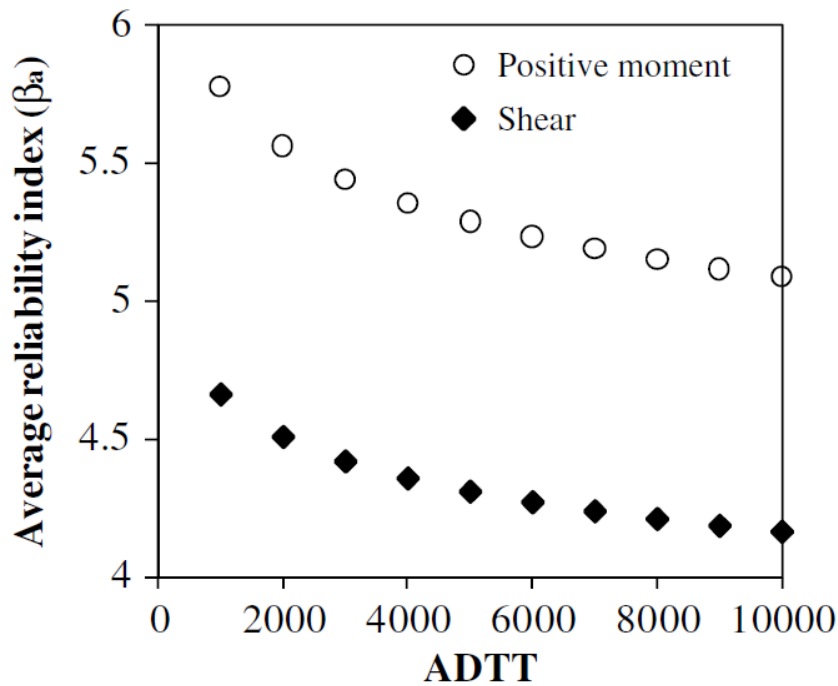
Reliability indices of 98 bridges from the US Federal Highway Administration's (FHWA) National Bridge Inventory (NBI) database were calculated by first order reliability method (FORM). Nominal dead load effects were calculated based on drawings of bridges and required minimum design strength were calculated according to the load combination for the Strength 1 Limit State in AASHTO-LRFD. Assuming dead load, live load and resistance follows normal, the Gumbel and lognormal distributions, respectively, reliability indices were calculated (Kwon et al., 2011). Figure 2-6 shows the calculated reliability indices when ADTT is 5,000.



**Figure 2-6** Reliability Indices for Representative Bridges (Kwon et al., 2011)

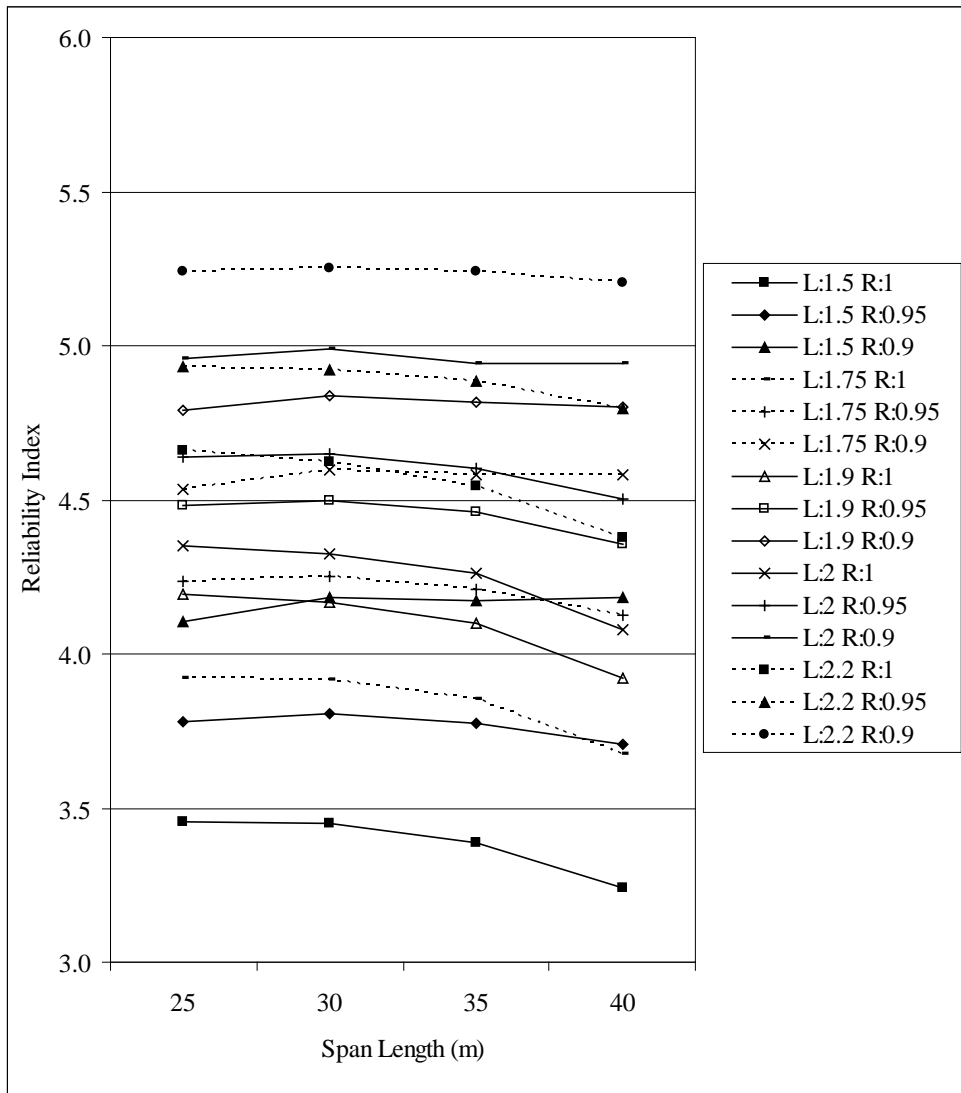
As shown in Figure 2-6, the reliability indices are much higher than target reliability index of 3.5. The average reliability indices are 5.3 and 4.3 for positive moment and shear, respectively, which means that current AASHTO LRFD brings about an overdesigned bridge superstructure for Missouri and the live load factor in the specification can be adjusted to achieve target reliability index (Kwon et al., 2011).

Figure 2-7 shows the change in average reliability index with respect to ADTT. As can be seen, the average reliability index increases rapidly as ADTT decreases. To adjust the design of bridges considering different ADTT, a live load factor of 1.75 in current AASHTO LRFD was calibrated with a factor,  $\alpha$ , which is a function of ADTT. With this calibration factor, live load factor in the load combination of Strength 1 Limit State,  $\gamma_{LL}$  would be  $1.75\alpha$ . Proposed live load calibration factors are between 0.80 and 1.00. Calibration factors of 0.80, 0.85, 0.90 and 1.00 were proposed for ADTT less than 1,000, for ADTT between 1,000 and 5,000, for ADTT between 5,000 and 10,000 and for ADTT more than 10,000, respectively.



**Figure 2-7** Average Reliability Indices for Different ADTT Values (Kwon et al., 2011)

Argınhan (2010) evaluated reliability based safety level of Turkish type precast prestressed concrete bridge girders designed in accordance with load and resistance factor design. He considered four different types of girders varying span lengths of 25 to 40 m, which are most commonly used in Turkey. Statistical parameters regarding load and resistance were obtained from local data supplemented by information compiled from relevant international literature. He designed the girders with different sets of load and resistance factors in order to see change in reliability indices. Current Turkish live load model, H30S24 and AASHTO LRFD live load model, HL93 were considered in the design. After designing girders, he conducted reliability analysis for each of the designed girders by using four different reliability analysis methods, namely mean value first order second moment method, advanced first order second moment method, first order reliability method and second order reliability method. Final reliability indices were selected based on minimum values obtained from those methods. In Figure 2-8, reliability indices of 60 girders designed for HL93 loading by 15 different sets of load and resistance factors can be seen.



**Figure 2-8** Reliability Indices for Different Sets of Load and Resistance Factors (HL93) (Arginhan, 2010)



## CHAPTER 3

### STATISTICS OF LOADS

Dead load, live load (static and dynamic), environmental loads (temperature, wind, earthquake) and other loads (collision, emergency breaking) are the major design load effects that can act on components of highway bridges. Using the available statistical data, surveys and other observations, the loads are modeled. These load components are considered as random variables, and are defined by their statistical distribution, bias factor (ratio of mean value to nominal) and coefficient of variation.

AASHTO LRFD contains different load combinations. Strength I limit state is basic load combination relating to vehicular use of the bridge without wind (AASHTO LRFD 3.4.1). The load combination for this limit state is specified as the following.

$$Q = 1.25 DC + 1.50 DW + 1.75 LL (1+IM) GDF \quad (3-1)$$

where DC is dead load of structural and non-structural components, DW is dead load of wearing surface, LL is vehicular live load, IM is dynamic impact factor, and GDF is girder distribution factor. Note that GDF is taken as 1.0 if a detailed finite element analysis is used to determine the forces in girders. GDF is used only with hand analysis type computations.

In this study, bridge designs are utilized based on this load combination except that factor of vehicular live load is tested with different values.

#### 3.1 Dead Loads

Nowak (1999) considered four different components of dead load due to different degrees of variation. These components are

- $D_1$  = weight of factory made elements
- $D_2$  = weight of cast-in-place concrete
- $D_3$  = weight of the wearing surface
- $D_4$  = miscellaneous weight

In this study, statistical parameters regarding dead loads are taken from Nowak's calibration report (1999). All four components of dead load are considered normally distributed. The parameters are listed in Table 3-1.

**Table 3-1** Statistical Parameters of Dead Load

Component	Bias Factor	Coefficient of Variation
D1	1.03	0.08
D2	1.05	0.10
D3	1.0	0.25
D4	1.03~1.05	0.08~0.10

## 3.2 Live Loads

Live load includes a range of forces generated by vehicles travelling on the bridge. The static and dynamic effects of live load are generally considered separately. Hence, only static component of live load is going to be covered in this section of study. Dynamic effects will be reviewed in the following sections.

The effect of live load is function of many parameters such as span length, truck weight, axle loads, axle configuration, position of the vehicle on the bridge (transverse and longitudinal), traffic volume (ADDT), multiple presence of vehicles on the bridge, girder spacing, and stiffness of structural members (slab and girders), and future growth (Moses and Ghosn, 1985, as cited in Nowak and Hong, 1991).

### 3.2.1 Live Load Models

In this section, official live load model of AASHTO LRFD Bridge Design Specifications (2010), which is HL93, and the live load model to be implemented in Turkish LRFD bridge design code are being introduced.

#### 3.2.1.1 HL93 Loading

In AASHTO LRFD Specifications, design model of live load is HL93 loading. HL93 is composed of a truck plus lane load. The truck has 3 axles separated by a distance of 4.3 m from each other. Distance between two rear axles may be spaced up to 9.15 meters if it is possible to create more extreme force effects. Leading axle weighs 35 kN and each rear axles weighs 145 kN. The transverse spacing of wheels is taken as 1.8 meters. The lane load is uniformly distributed load of 9.3 kN/m. The lane load is assumed to occupy 3.0 m transversely within a design lane. The model and truck itself are presented in Figure 3-1 and Figure 3-2, respectively.

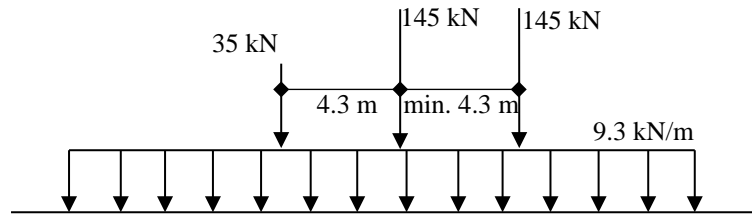


**Figure 3-1** HL93 Live Load Model

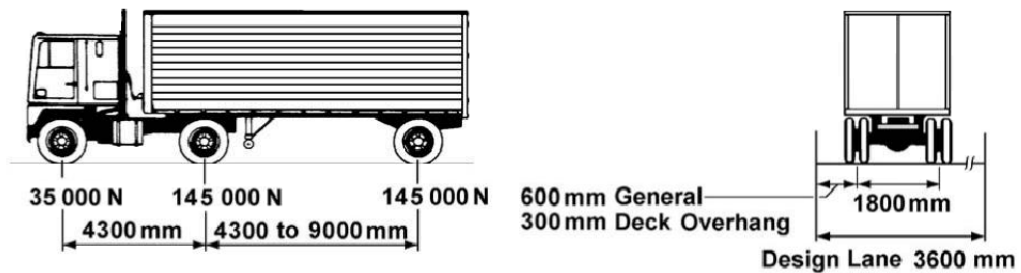


**Figure 3-2** HL93 Design Truck (AASHTO LRFD)

It should be noted that AASHTO LRFD Bridge Design Specifications (2010) also define a design tandem, which consists of a pair of 110 kN axles spaced 1.2 meters apart and transverse spacing of wheels is taken as 1.8 meters. Design tandem is used as an alternative to design truck. Maximum of load effects due to design truck or tandem is used in design of bridge. Based on calculations, it is also be noted that design tandem governs the design for span lengths of approximately less than 15 meters.

In the study of Arginhan (2010), he evaluated statistical parameters of live load HL93 by processing truck survey data of years 2005 and 2006 obtained from the Division of Transportation and Cost Studies of the General Directorate of Highways of Turkey. The parameters are calculated for span lengths varying from 25 m to 40 m. In this study, these calculated parameters will be used assuming these are also valid for span lengths of 50 m to 80 m. The statistical parameters regarding HL93 live load reflecting conditions in Turkey are listed in Table 3-2.

**Table 3-2** Statistical Parameters of Live Load HL93 (Argınhan, 2010)

Parameter	Bias Factor	Coefficient of Variation
LL-HL93 (for one lane) (Overall Case)	1.10	0.306
LL-HL93 (for two lanes) (Overall Case)	0.77	0.306
LL-HL93 (for one lane) (Extreme Case)	1.12	0.165
LL-HL93 (for two lanes) (Extreme Case)	0.86	0.165

### 3.2.1.2 AYK45 Loading

In the calibration of AASHTO LRFD for Turkey, a new live load model is going to be implemented. The new model is called AYK45, in which AYK stands for “Ağır Yük Kamyonu” meaning “Heavy Load Truck” in Turkish and “45” is total weight of truck in units of ton. Similar to HL-93 truck model philosophy, AYK45 needs to be used with a uniform lane load of 10 kN/m.

Design live load model of current design practice in Turkey is standard H30S24 truck or lane loading, whichever governs (Karayolları Genel Müdürlüğü, 1982). The live load model is illustrated in Figure 3-3 and Figure 3-4.

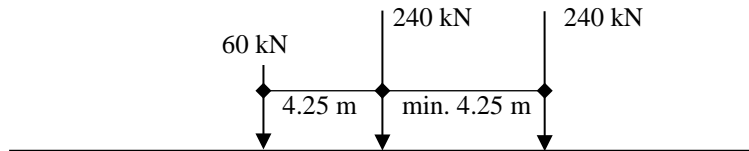


**Figure 3-3** H30S24 Truck Loading

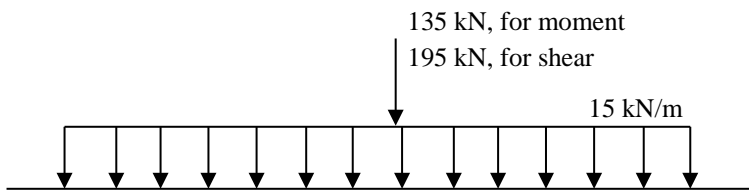


**Figure 3-4** H30S24 Lane Loading

Considering only static effect of live load, H30S24 truck loading governs for span length up to approximately 46 meters. For longer spans, H30S24 lane loading controls the design. In Figure 3-5, the ratio of midspan moment effect of H30S24 truck loading

to that of lane loading is plotted. It can be observed that H30S24 truck loading is not very appropriate to be used in design of bridges with span lengths in excess of 50 meters.

Since this study covers bridges having span length longer than 50 meters, implementation of a new design live load is necessitated. Therefore, a design truck combined with lane load as a new live load model is decided to be created as in the case with calibration of AASHTO LRFD.

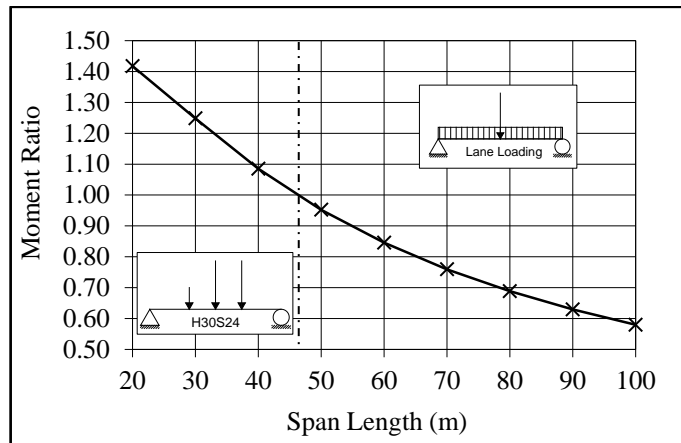


**Figure 3-5** The Ratio of Midspan Moment Effect of H30S24 Design Truck to Lane Loading

The moment and shear survey of existing Turkish trucks indicated that H30S24 truck is a considerably heavy truck. Therefore, selecting a more realistic truck is decided instead of using H30S24 truck based on the statistical study. In addition, uniform 10 kN/m lane load is combined with this truck load. The new design live load model is illustrated in Figure 3-6.

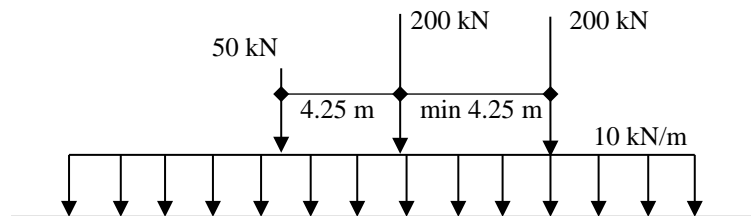


**Figure 3-6** AYK45 Live Load Model

Comparison of AYK45 loading and current Turkish design live loading based on their midspan moment effects for span lengths of 20 to 100 meters is illustrated in Figure 3-7. AYK45 loading is observed to be safer in comparison to the current Turkish design live load model.

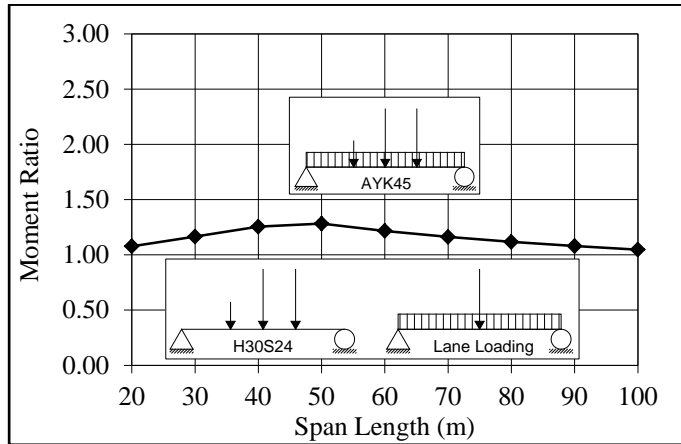


**Figure 3-7** The Ratio of Midspan Moments of AYK45 Loading to Current Turkish Design Live Load

### 3.2.1.3 Maximum Midspan Moments Due to HL93 and AYK45

Maximum midspan moments have been calculated based on HL93 and AYK45 loading for span length of 50 to 80 meters with an increment of 10 meters. Moving load analysis has been utilized so that position of truck on the bridge that creates maximum moment has been determined. The results are shown in Table 3-3. AYK45 loading gives up to 25% higher results. The comparison is illustrated as a bar graph in Figure 3-8.

**Table 3-3** Maximum Moments due to HL93 and AYK45 per Lane

Span Length	Maximum Moment (kNm)	
	HL93	AYK45
50 m	6585.2	8223.3
60 m	8675.9	10722.5
70 m	10999.2	13472.0
80 m	13555.2	16471.6

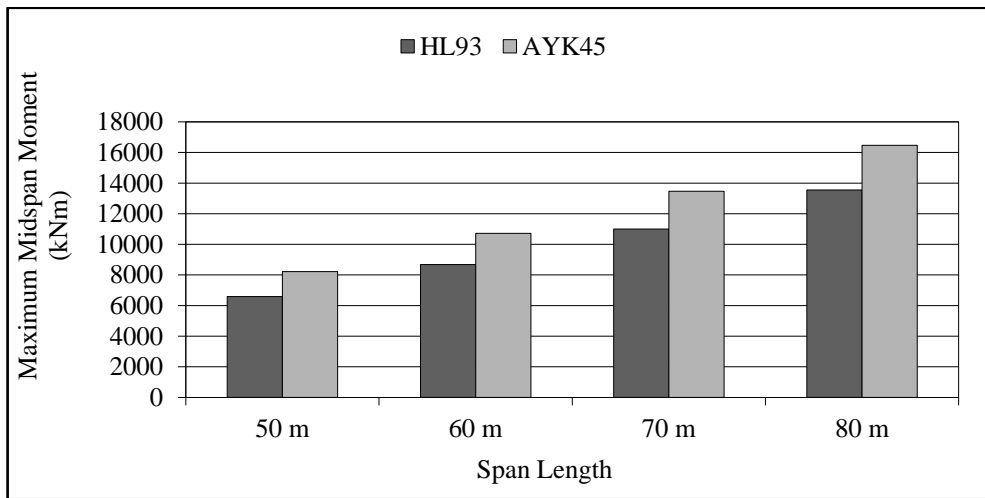


**Figure 3-8** Comparison of Moments of HL93 and AYK45 per Lane

### 3.2.2 Evaluation of Truck Survey Data

The truck survey data was obtained from the Turkish General Directorate of Highways to determine the statistics regarding live load in Turkey. The survey was conducted in different highway stations of Turkey in years between 1997 and 2006. However, only 2005 and 2006 data were used in this study. Truck survey data includes more than 20,000 trucks' axle weights and number of axles they have. Same survey data was used by Argınhan (2010) to investigate reliability-based safety level of most commonly used types of precast prestressed concrete bridge girders, which are designed based on LRFD method, in Turkey.

The span moments due to surveyed trucks are calculated. However, although survey data includes number of axles of surveyed trucks, it does not include axle spacing of surveyed trucks, which is essential to compute moment effects. According to survey data, it is possible to categorize the trucks into 19 groups based on axle configurations as can be seen in Table 3-4. Based on this categorization, Argınhan (2010) determined the axle spacing distance by searching commercial truck catalogs. He matched the types of surveyed trucks with the trucks with same axle configuration in catalogs and estimated the axle spacing distance of surveyed trucks (Table 3-5).

**Table 3-4** Truck Types Based on Axle Configuration (Arginhan, 2010)

Notation	Figure	Notation	Figure
1.1		1.2+2	
1.2		1.2+21	
1.21		1.2+11 (1.2+22)	
1.22		1.22+11 (1.22+22)	
1.121 (1.122)		1.2+111	
11.21		1.2+122 (1.2+222)	
11.22		1.22+111 (1.22+222)	

**Table 3-5** Truck Axle Distances Assumed by Arginhan (2010)

Truck Type	Distance Between Each Axles (m)		
	D1-D2	D2-D3	D3-D4
1.21 and 1.22	3.80 (3.60 ≤ 5.00)	1.35 (1.15 ≤ 1.40)	-
11.22	1.70 (1.70 ≤ 1.95)	2.80 (2.80 ≤ 3.40)	1.35
1.121	3.80 (3.80 ≤ 5.00)	1.35 (1.15 ≤ 1.40)	1.35 (1.15 ≤ 1.40)

Note that Arginhan (2010) excluded “1.1”, “1.2” and “1.21” type trucks from the computations due the fact that they weigh lighter in comparison with other trucks. He also excluded wrecker and wreckers plus half trailer, which are shown on the right hand side of the Table 3-4. They have not been taken into consideration in the calculations of this study, either. By the exclusion of those trucks, total number of trucks considered becomes approximately 11,000. In Figure 3-9, frequency distribution of truck types based on axle configurations is illustrated.

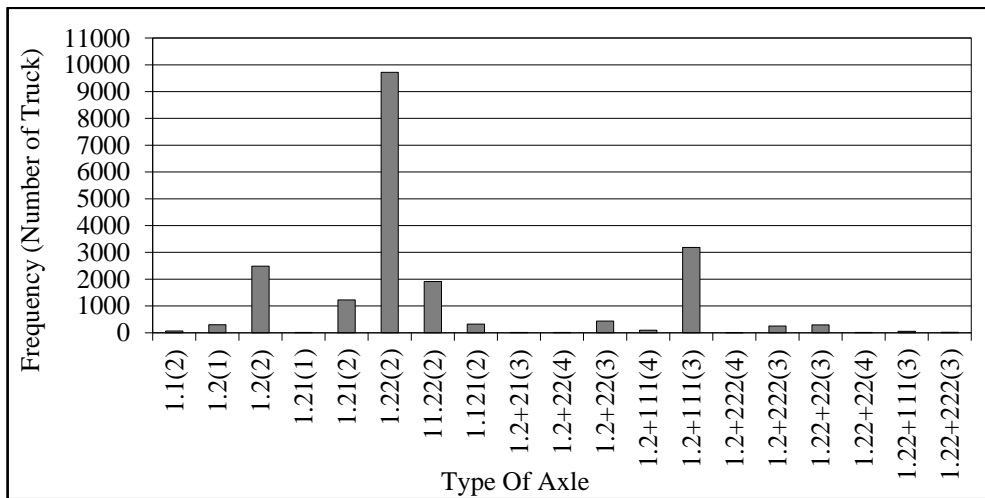


**Figure 3-9** Histogram of Vehicles Based on Axle Configurations (Arginhan, 2010)

Gross weight of trucks considered in calculations varied from 2.9 to 30.48 tons. Mean value of the gross weight is 11 tons (Arginhan, 2010). In Figure 3-10, frequency distribution of gross vehicle weights is illustrated.

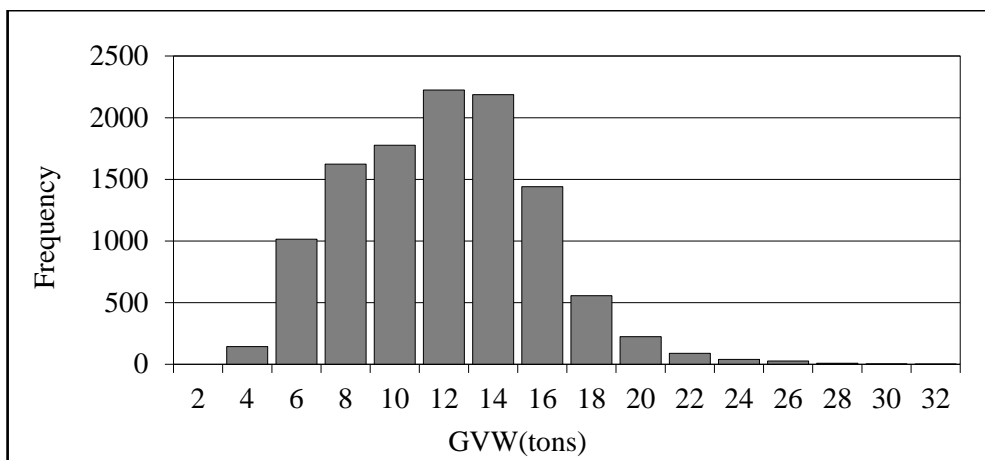


**Figure 3-10** Histogram of Gross Vehicle Weights (GVW) of Surveyed Trucks

Maximum span moment effects of those 11,000 trucks have been calculated for 50 m, 60 m, 70 m and 80 m span lengths. The histograms are plotted in Figure 3-11 to Figure 3-14. All moments are given per lane.

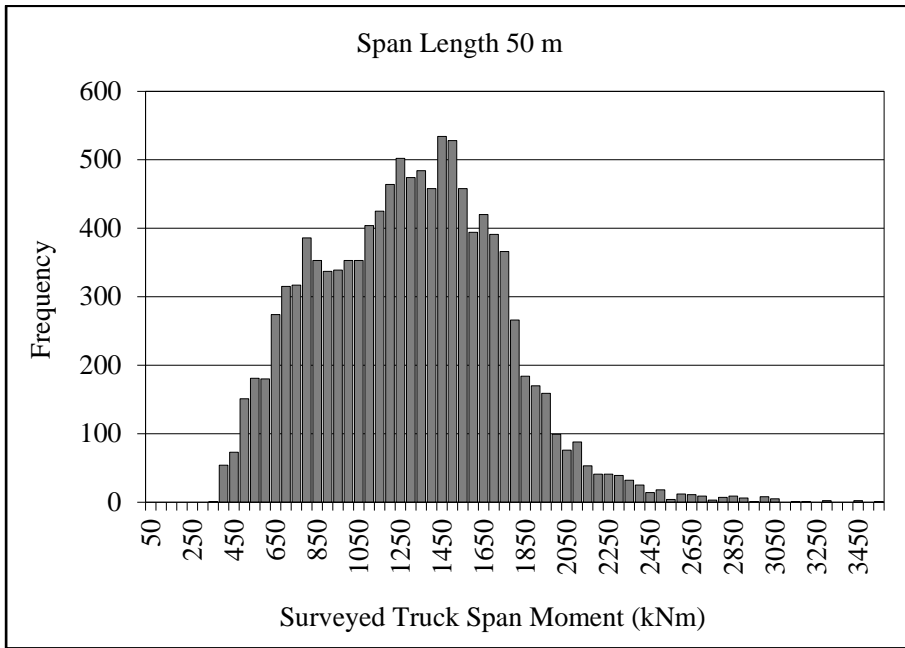


**Figure 3-11** Histogram of Moments of Surveyed Trucks for Span Length of 50 m

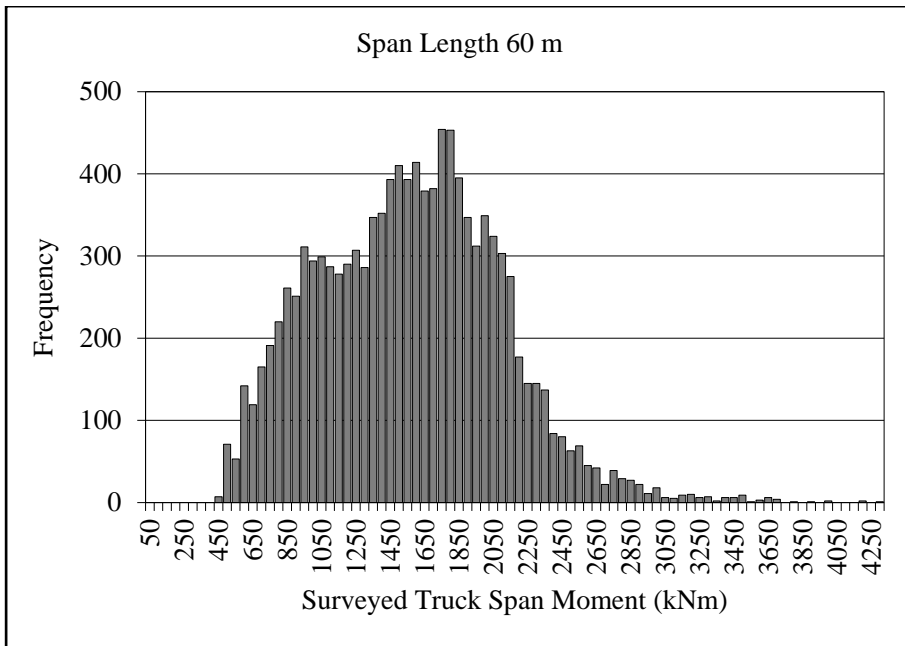


**Figure 3-12** Histogram of Moments of Surveyed Trucks for Span Length of 60 m

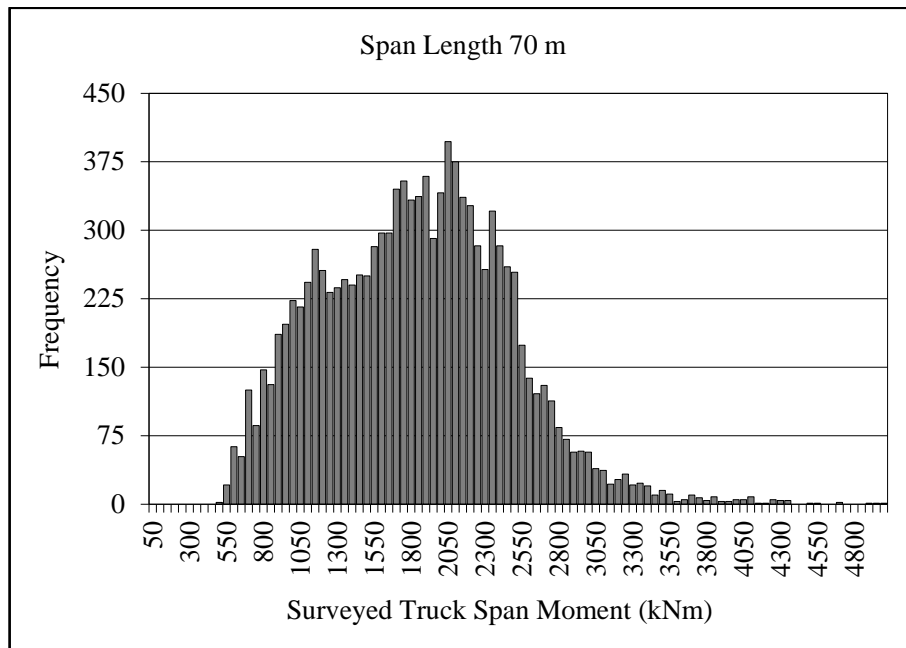


**Figure 3-13** Histogram of Moments of Surveyed Trucks for Span Length of 70 m

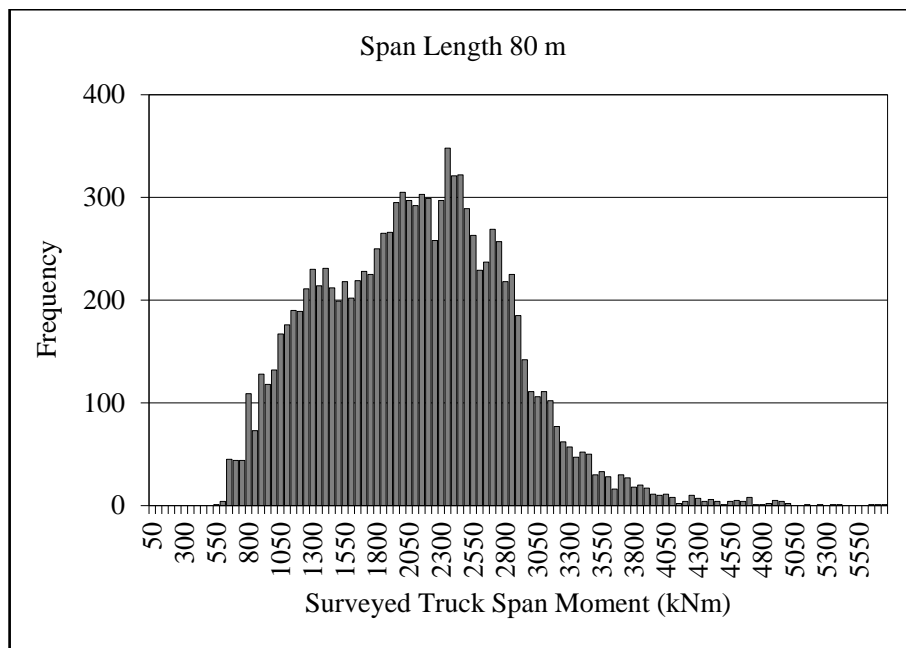


**Figure 3-14** Histogram of Moments of Surveyed Trucks for Span Length of 80 m

### 3.2.3 Assessment of Statistical Parameters of Live Load

Statistical parameters regarding live load is being evaluated based on extreme value theory, which is also used in calibration of AASHTO LRFD (Nowak, 1999). The main aim of this theory is to estimate future data that are more extreme than any previously observed based on available data.

In previous sections, it was mentioned that Argınhan (2010) calculated statistical parameters of HL93 loading for span length of 25 to 40 meter with an increment of 5 meters. Same parameters will be utilized in this study for span lengths of 50 to 80 m. Statistical parameters of AYK45 loading have also been determined.

The moment ratios of surveyed trucks to AYK45 are plotted on both normal probability papers and Gumbel probability papers. For that purpose, three cases are considered. Complete data, part of exceeding 90-percentile values of complete data, and isolated 10 percent highest values of data are used to assess statistical parameters. These cases will be called overall, upper tail and extreme, respectively in the rest of this study.

#### 3.2.3.1 Fitting Straight Lines to the CDFs of Moments of Surveyed Trucks

In “overall” case, all surveyed truck data, which includes 11,000 trucks, are used. Their cumulative distribution functions are plotted on both Gumbel and normal probability papers. Then, straight lines are fitted as best estimate lines. The plots are presented in Figure 3-15 to Figure 3-18.

In “upper tail” case, cumulative distribution functions of all surveyed data are plotted on both Gumbel and normal probability paper. However, this time straight lines are not fitted on complete data but on data exceeding 90-percentile values of complete data, namely on upper tail of data. The plots are shown in Figure 3-19 to Figure 3-22.

In “extreme” case, 10 percent highest values of data are isolated from the complete data and plotted on both normal and Gumbel distribution papers and then straight lines are fitted as best estimate lines. A similar analytical approach is used by Kwon et al. (2011) whom selected top 5% of the data. The plots are shown in Figure 3-23 to Figure 3-26.

In normal probability paper, vertical axis represents the value of the standard normal variate ( $z$ ), and in Gumbel distribution paper, vertical axis represents the reduced variate ( $\eta$ ) (Castillo, 1988).

$$z = \Phi^{-1}[F(M)] \quad (3-2)$$

$$\eta = -\ln[-\ln[F(M)]] \quad (3-3)$$

where  $F(M)$  is cumulative distribution function of moment ratio of surveyed trucks to AYK45, and  $\Phi^{-1}$  is the inverse of cumulative distribution function of standard normal variate.

After plotting the ratios with respect to  $z$  and  $\eta$  for three cases, straight lines are fitted to data points. These lines are needed to extrapolate future data from current data. It is important to estimate maximum live load effect in a 75 year period, which is the design life of a bridge according to AASHTO LRFD Bridge Design Specifications (2010).

As it can be seen from plots shown in Figure 3-15 to Figure 3-26, straight lines on Gumbel probability papers represent the plotted data much better than those on normal data, especially for the overall case. In other words, the plots indicate that Gumbel distribution fits the data quite well. Therefore, it can be concluded that surveyed truck moments follow Gumbel distribution.

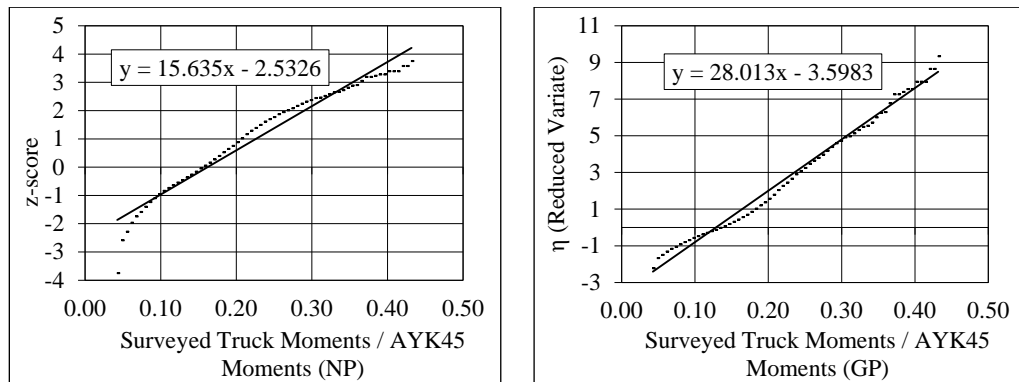


**Figure 3-15** Straight Lines Fitted to Overall Moment Ratios on Normal (NP) and Gumbel (GP) Probability Papers for 50 m Span Length

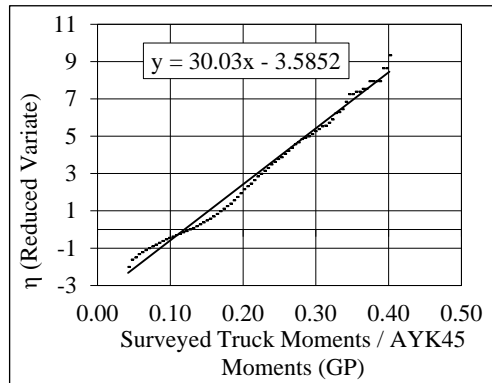
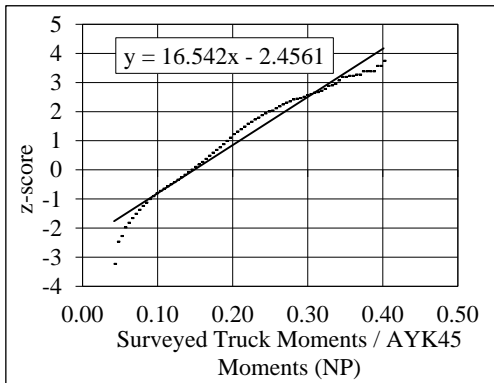


**Figure 3-16** Straight Lines Fitted to Overall Moment Ratios on Normal (NP) and Gumbel (GP) Probability Papers for 60 m Span Length

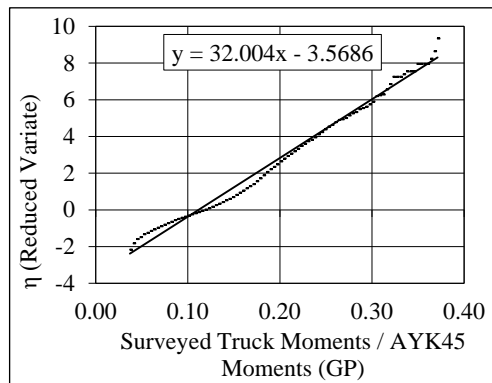
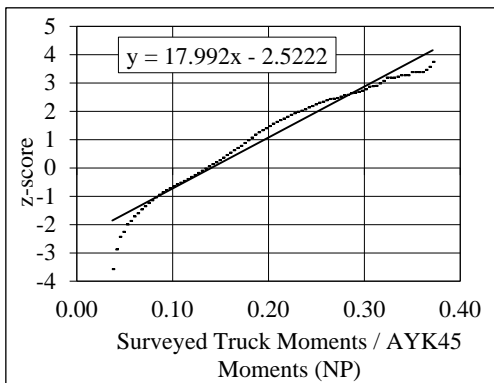


**Figure 3-17** Straight Lines Fitted to Overall Moment Ratios on Normal (NP) and Gumbel (GP) Probability Papers for 70 m Span Length

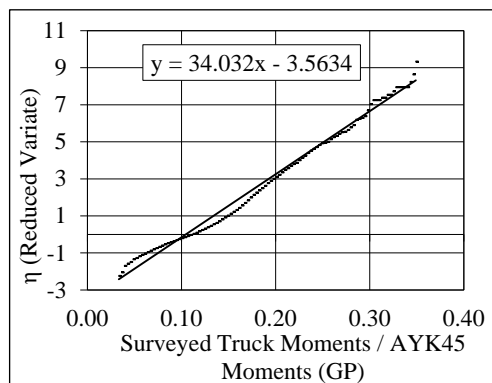
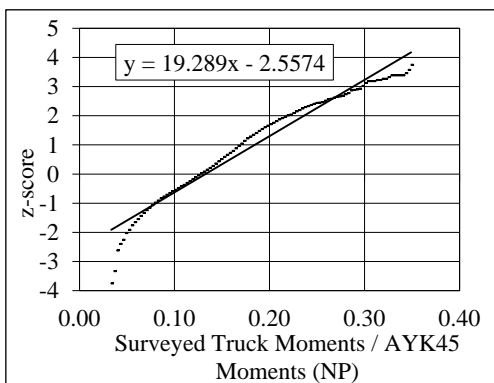


**Figure 3-18** Straight Lines Fitted to Overall Moment Ratios on Normal (NP) and Gumbel (GP) Probability Papers for 80 m Span Length

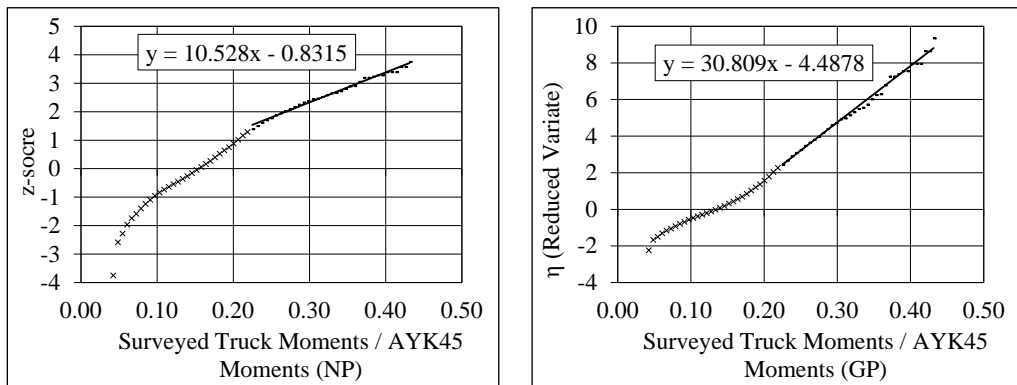


**Figure 3-19** Straight Lines Fitted to Upper Tail of Moment Ratios on Normal (NP) and Gumbel (GP) Probability Papers for 50 m Span Length

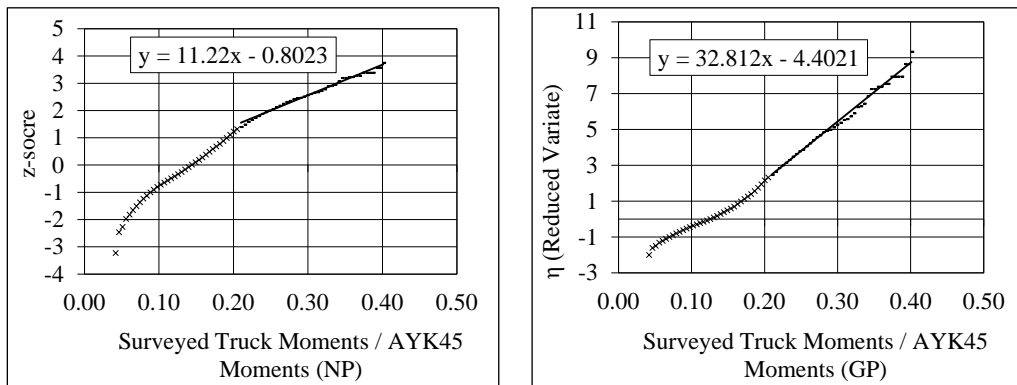


**Figure 3-20** Straight Lines Fitted to Upper Tail of Moment Ratios on Normal (NP) and Gumbel (GP) Probability Papers for 60 m Span Length

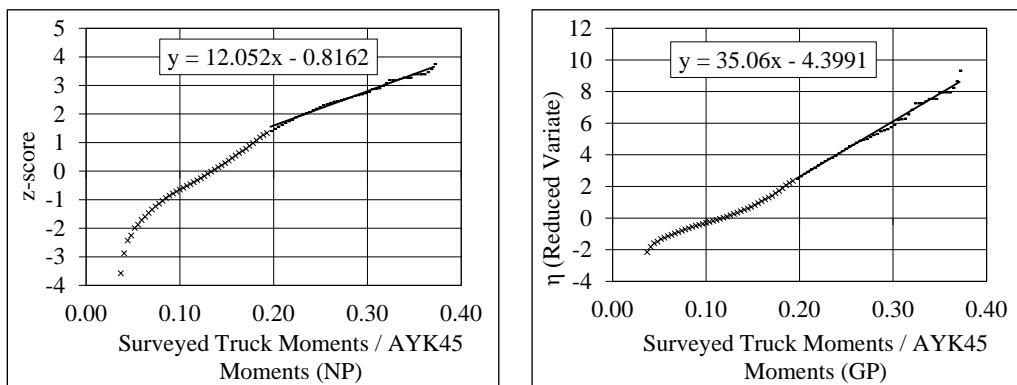


**Figure 3-21** Straight Lines Fitted to Upper Tail of Moment Ratios on Normal (NP) and Gumbel (GP) Probability Papers for 70 m Span Length

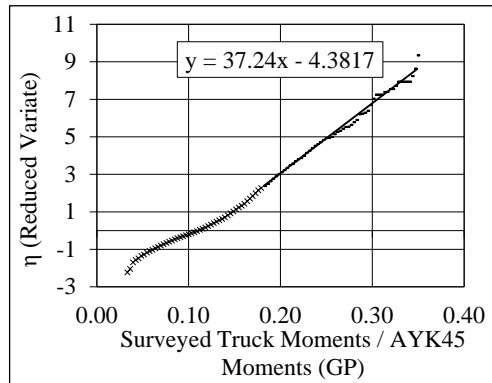
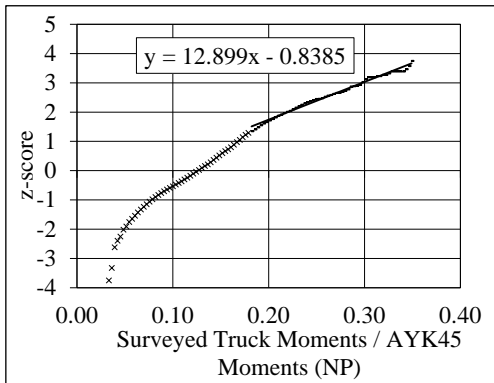


**Figure 3-22** Straight Lines Fitted to Upper Tail of Moment Ratios on Normal (NP) and Gumbel (GP) Probability Papers for 80 m Span Length

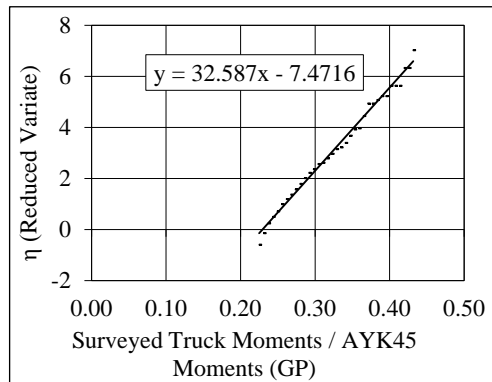
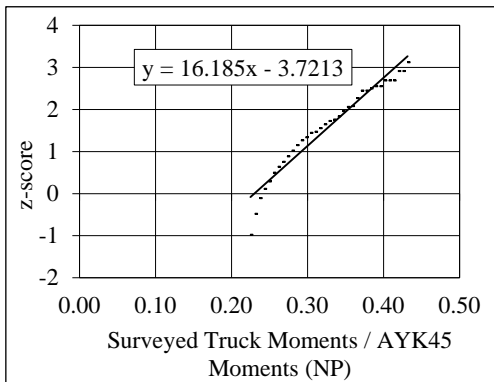


**Figure 3-23** Straight Lines Fitted to Extreme Surveyed Truck Moment Ratios on Normal (NP) and Gumbel (GP) Probability Papers for 50 m Span Length

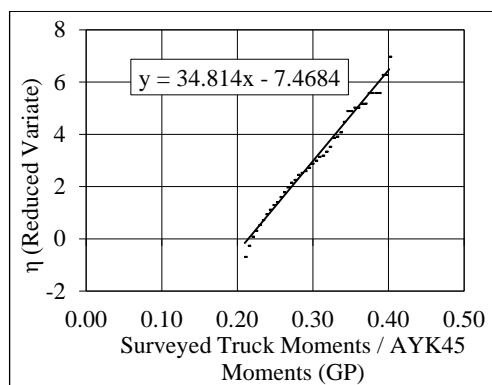
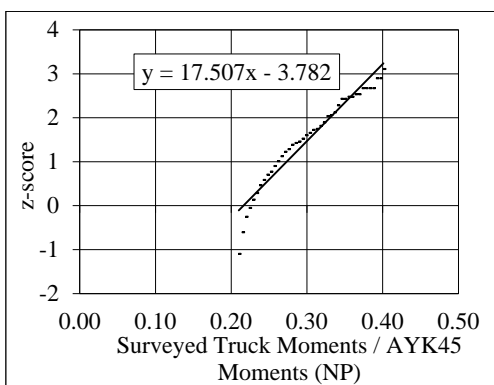


**Figure 3-24** Straight Lines Fitted to Extreme Surveyed Truck Moment Ratios on Normal (NP) and Gumbel (GP) Probability Papers for 60 m Span Length

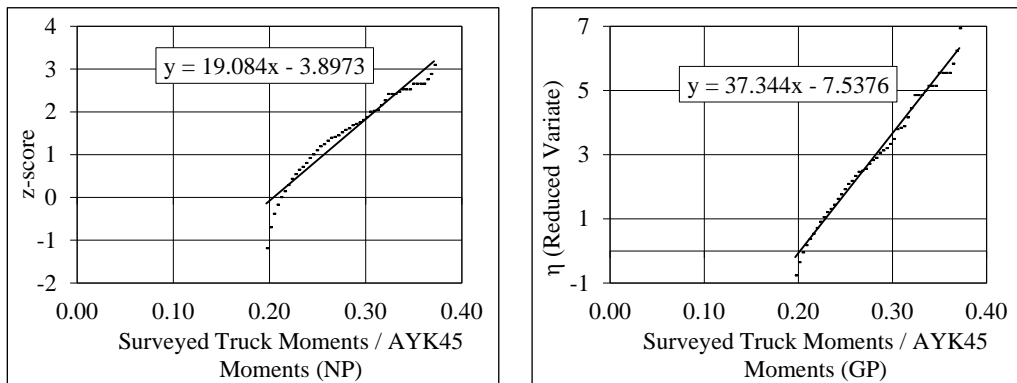


**Figure 3-25** Straight Lines Fitted to Extreme Surveyed Truck Moment Ratios on Normal (NP) and Gumbel (GP) Probability Papers for 70 m Span Length

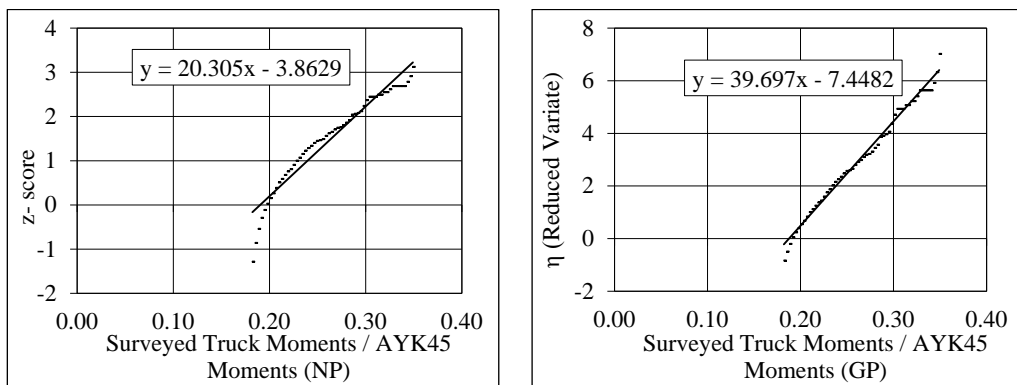


**Figure 3-26** Straight Lines Fitted to Extreme Surveyed Truck Moment Ratios on Normal (NP) and Gumbel (GP) Probability Papers for 80 m Span Length

### 3.2.3.2 Mean Maximum Moment Ratios Predicted by Extrapolation

Extrapolation is going to be carried out to estimate future time conditions regarding moment ratios. For that purpose, in this study, procedure and assumptions in Nowak’s calibration report (1999) are followed. In Table 3-6, the number of trucks that pass through a bridge in different time intervals and corresponding probability of occurrence of the heaviest truck are listed. Corresponding  $z$  and  $\eta$  are indicated as well.

Extrapolation is utilized based on assumption of number of trucks passing through the bridge in different time periods. For instance, considering the surveyed trucks represent about two week traffic, a total of 20 million trucks are assumed to pass in 75 year time period (Nowak, 1999).

**Table 3-6** Number of Trucks vs. Time Period and Probability

Time Period T	# of Trucks N	Probability 1/N	Std. Normal Variate z	Reduced Variate $\eta$
75 years	20,000,000	$5 \times 10^{-8}$	5.33	16.81
50 years	15,000,000	$7 \times 10^{-8}$	5.27	16.52
5 years	1,500,000	$7 \times 10^{-7}$	4.83	14.22
1 year	300,000	$3 \times 10^{-6}$	4.50	12.61
6 months	150,000	$7 \times 10^{-6}$	4.36	11.92
2 months	50,000	$2 \times 10^{-5}$	4.11	10.82
1 month	30,000	$3 \times 10^{-5}$	3.99	10.31
2 weeks	10,000	$1 \times 10^{-4}$	3.71	9.21
1 day	1,000	$1 \times 10^{-3}$	3.09	6.91

Extrapolation has been carried out by replacing  $\eta$  values into the equation of fitted lines on Gumbel distribution and obtaining corresponding moment ratio values. For example,  $\eta$  value corresponding to 75-year time period is 16.81. In overall case, the equation of fitted line on Gumbel paper is “ $y = 28.013x - 3.5983$ ” for 50 m span length. If  $\eta = 16.81$  is substituted for  $y$  in the equation, one can get  $x = 0.729$ , which is the moment ratio of 75-year truck for span length of 50 m.

Extrapolation has been done for all three cases. Results are tabulated in Table 3-7 to Table 3-9. Moreover, extrapolated data is shown on normal distribution papers in Figure 3-27 to Figure 3-29.

**Table 3-7** Mean Maximum Moment Ratios (Overall)

Span (m)	Surveyed Truck Moments / AYK45 Moment								
	1 day	2 weeks	1 month	2 months	6 months	1 year	5 years	50 years	75 years
50	0.375	0.457	0.496	0.515	0.554	0.579	0.636	0.718	0.729
60	0.349	0.426	0.463	0.480	0.516	0.539	0.593	0.670	0.679
70	0.327	0.399	0.434	0.450	0.484	0.506	0.556	0.628	0.637
80	0.308	0.375	0.408	0.423	0.455	0.475	0.523	0.590	0.599

**Table 3-8 Mean Maximum Moment Ratios (Upper Tail)**

Span (m)	Surveyed Truck Moments / AYK45 Moment								
	1 day	2 weeks	1 month	2 months	6 months	1 year	5 years	50 years	75 years
50	0.370	0.445	0.480	0.497	0.533	0.555	0.607	0.682	0.691
60	0.345	0.415	0.448	0.464	0.497	0.519	0.568	0.638	0.647
70	0.322	0.388	0.420	0.434	0.465	0.485	0.531	0.597	0.605
80	0.303	0.365	0.394	0.408	0.438	0.456	0.500	0.561	0.569

**Table 3-9 Mean Maximum Moment Ratios (Extreme)**

Span (m)	Surveyed Truck Moments / AYK45 Moment								
	1 day	2 weeks	1 month	2 months	6 months	1 year	5 years	50 years	75 years
50	0.441	0.512	0.546	0.561	0.595	0.616	0.666	0.736	0.745
60	0.413	0.479	0.511	0.525	0.557	0.577	0.623	0.689	0.697
70	0.387	0.448	0.478	0.492	0.521	0.540	0.583	0.644	0.652
80	0.362	0.420	0.447	0.460	0.488	0.505	0.546	0.604	0.611

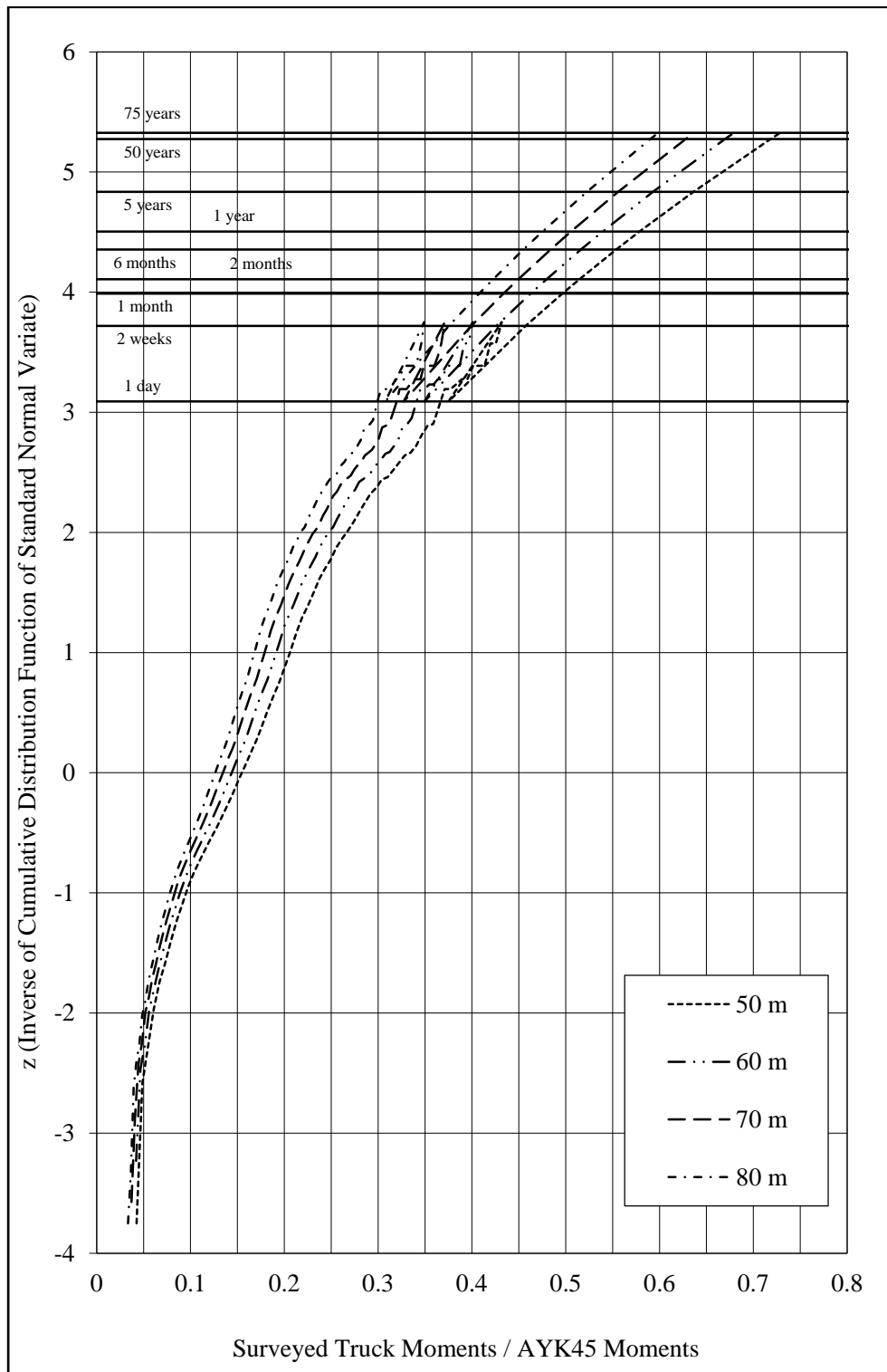


**Figure 3-27** Extrapolated Moment Ratios (Overall)

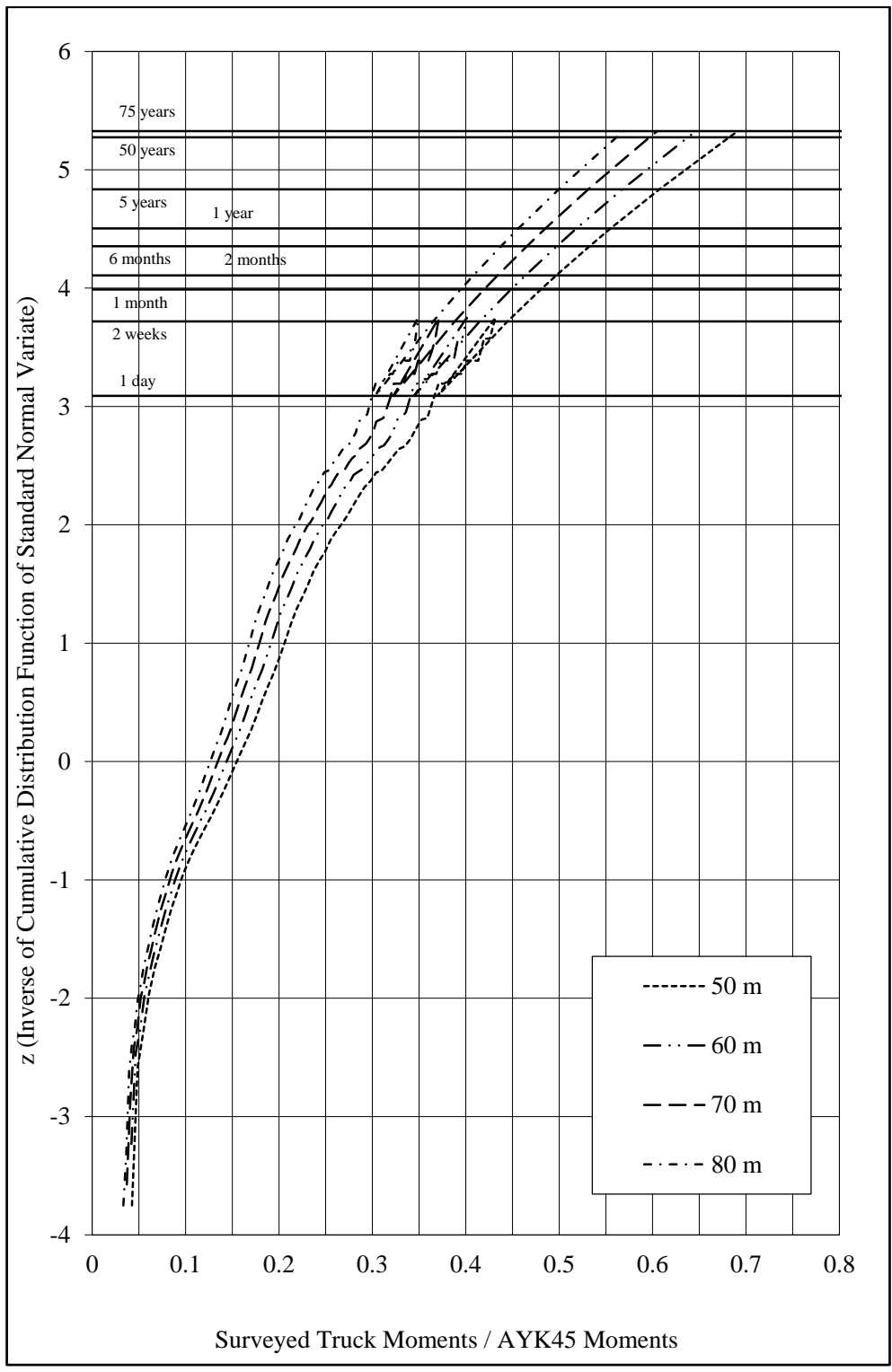


**Figure 3-28** Extrapolated Moment Ratios (Upper Tail)

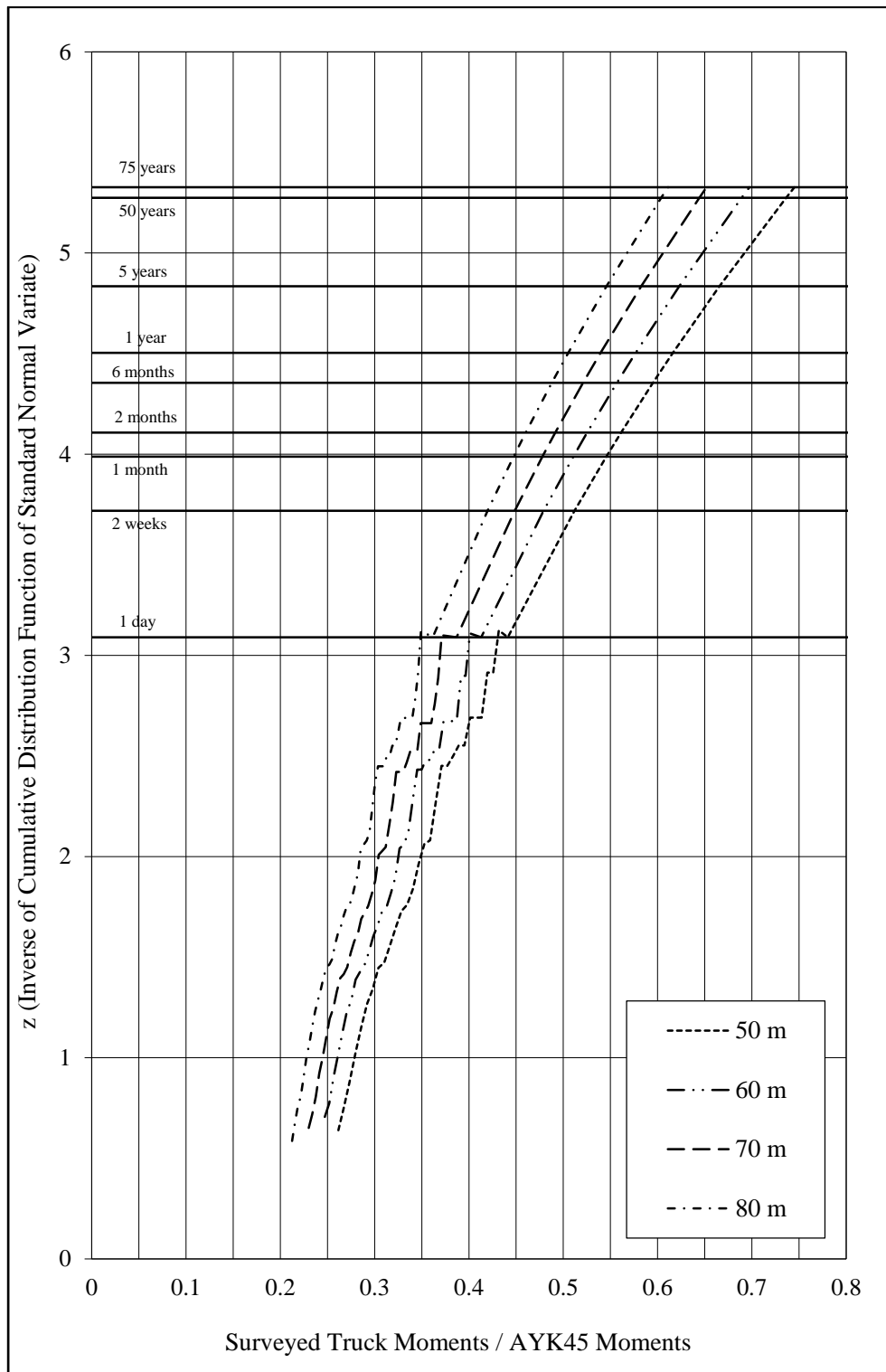


**Figure 3-29** Extrapolated Moment Ratios (Extreme)

### 3.2.3.3 Estimation of Coefficient of Variation

The mean value  $\mu$  can be expressed as  $\lambda + 0.5772\delta$ , where  $\lambda$  and  $\delta$  are Gumbel distribution parameters. The abscissa corresponding to  $\eta = 0$  on the Gumbel distribution paper is  $\lambda$ , and the abscissa corresponding to  $\eta = 1$  on Gumbel distribution paper is  $\lambda + \delta$ . Moreover, standard deviation  $\sigma$  can be stated as square root of  $\pi^2\delta^2/6$  (Castillo, 1988). An example of how to calculate Gumbel distribution parameter is illustrated in Figure 3-30.

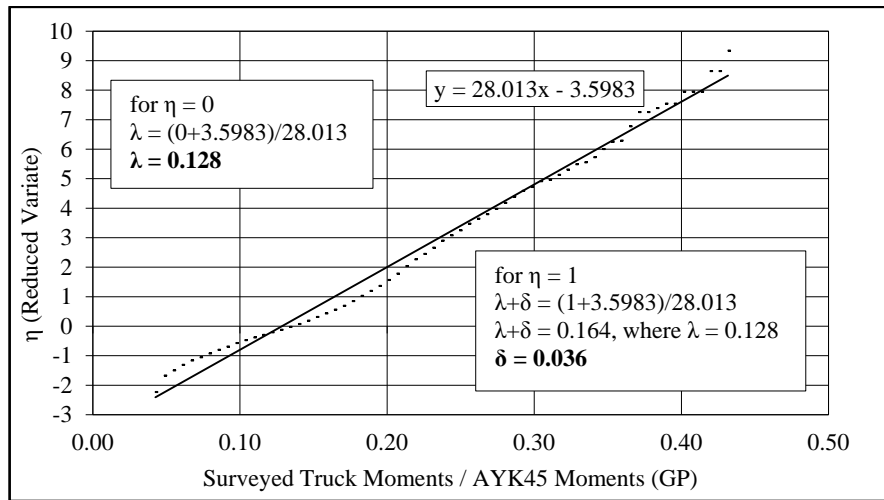


**Figure 3-30** An Example of How to Calculate Gumbel Distribution Parameters for the Case of 50 m Span Length (Overall Case)

By making these calculations, mean values and standard deviations of moment ratios are computed and shown in Table 3-10 to Table 3-12.

**Table 3-10** Gumbel Distribution Parameters, Mean Values, Standard Deviations and Coefficients of Variation of Moment Ratios (Overall) According to Gumbel Distribution

Span	$\lambda$	$\delta$	$\mu$	$\sigma$	COV
50 m	0.128	0.036	0.149	0.046	0.307
60 m	0.119	0.033	0.139	0.043	0.308
70 m	0.112	0.031	0.130	0.040	0.309
80 m	0.105	0.029	0.122	0.038	0.310

**Table 3-11** Gumbel Distribution Parameters, Mean Values, Standard Deviations and Coefficients of Variation of Moment Ratios (Upper Tail) According to Gumbel Distribution

Span	$\lambda$	$\delta$	$\mu$	$\sigma$	COV
50 m	0.146	0.032	0.164	0.042	0.253
60 m	0.134	0.030	0.152	0.039	0.258
70 m	0.125	0.029	0.142	0.037	0.258
80 m	0.118	0.027	0.133	0.034	0.259

**Table 3-12** Gumbel Distribution Parameters, Mean Values, Standard Deviations and Coefficients of Variation of Moment Ratios (Extreme) According to Gumbel Distribution

Span	$\lambda$	$\delta$	$\mu$	$\sigma$	COV
50	0.229	0.031	0.247	0.039	0.159
60	0.215	0.029	0.231	0.037	0.159
70	0.202	0.027	0.217	0.034	0.158
80	0.188	0.025	0.202	0.032	0.160

#### 3.2.3.4 Comparison of the Results Obtained from Different Extrapolation Cases

In Figure 3-31, 75-year maximum moment ratios are plotted with respect to span lengths for all three cases, and coefficients of variation are shown in Figure 3-32. 75-year maximum moment ratios based on extreme case are higher than the others as expected. However, coefficients of variation are remarkably higher for the case in which whole trucks are considered, which is also expected due to the fact that light trucks together with heavy trucks make the data heterogeneous. It is known that using higher bias factor of live load results in less reliability index and using higher coefficient of variation of live load also results in less reliability index. In previous studies such as Arginhan (2010) and Kwon et al. (2011), extreme case was considered to determine statistical parameters regarding live load. However, while bias factor is higher in extreme case, coefficient of variation is higher in overall case. Therefore, overall case also needs to be considered. Accordingly, in this study, both results obtained from extreme and overall cases are going to be considered in reliability analyses.

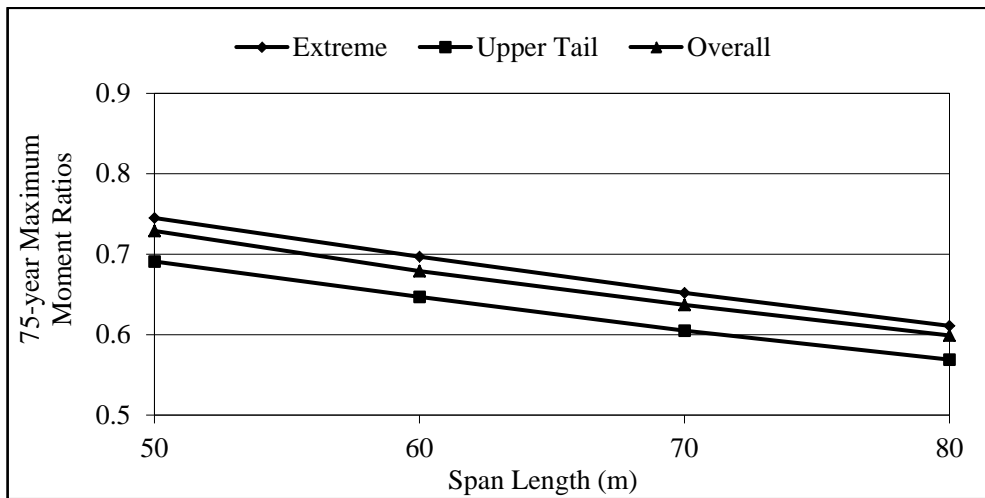


**Figure 3-31** Comparison of Moment Ratios Based on Different Assumptions

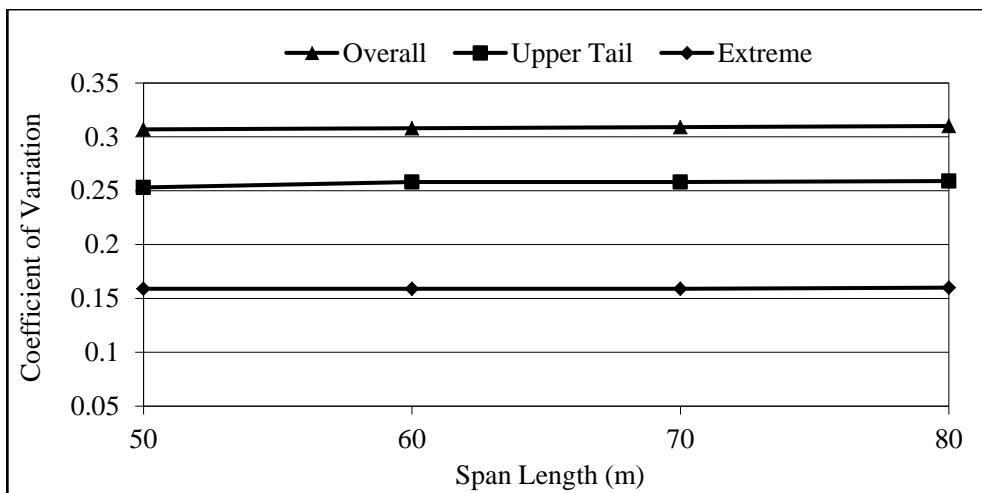


**Figure 3-32** Comparison of Coefficients of Variation Based on Different Assumptions

### 3.2.3.5 Consideration of Multiple Presences of Vehicles on a Bridge

The probability of multiple presences of trucks on the same bridge should also be considered. Nowak (1999) indicates that there are two possible situations: either one truck followed behind by another truck in a single lane (Figure 3-33) or two trucks are in adjacent lanes (Figure 3-34).



**Figure 3-33** One Truck Followed Behind by Another Truck

To decide statistical parameters regarding one truck followed behind by another truck, headway distance and correlation between trucks should be known. Unfortunately, there is no data available for these variables. Therefore, some assumptions are made. The distance between centers of gravity of two trucks is assumed to be 15 meter, which is believed to be a conservative value. For correlation of trucks, assumptions of Nowak (1999) are used. Nowak assumes three different combinations: maximum 1-year truck followed by an average truck from survey, maximum 6-month truck followed by a maximum 1-day truck, and maximum 1-month truck followed by another maximum 1-month truck.

Moment ratios of multiple presences of trucks (i.e. one followed behind by another one) are calculated based on specified assumptions above and tabulated in Table 3-13 and Table 3-14 for overall and extreme cases, respectively. In these tables also maximum 75-year truck moment ratios are stated. As a result, the worst cases are selected in the last column.

**Table 3-13** One Lane Truck Maximum Moment Ratios (Overall Case)

Span	Max 75-year	Max 1-year and average	Max 6-month and 1-day	Two max 1-month	Envelope
50 m	0.729	0.640	0.704	0.695	0.729
60 m	0.679	0.611	0.691	0.694	0.694
70 m	0.637	0.582	0.671	0.681	0.681
80 m	0.599	0.554	0.647	0.662	0.662

**Table 3-14** One Lane Truck Maximum Moment Ratios (Extreme Case)

Span	Max 75-year	Max 1-year and average	Max 6-month and 1-day	Two max 1-month	Envelope
50 m	0.745	0.678	0.772	0.764	0.772
60 m	0.697	0.648	0.763	0.766	0.766
70 m	0.652	0.616	0.742	0.751	0.751
80 m	0.611	0.584	0.714	0.727	0.727

For the probability of occurrence of side-by-side trucks, Nowak (1999) states that the case with fully correlated side-by-side trucks governs, with each truck equal to the maximum 2-month truck. In this study, 2-month truck ratios are also used for the case of multiple presences of two trucks in adjacent lanes.

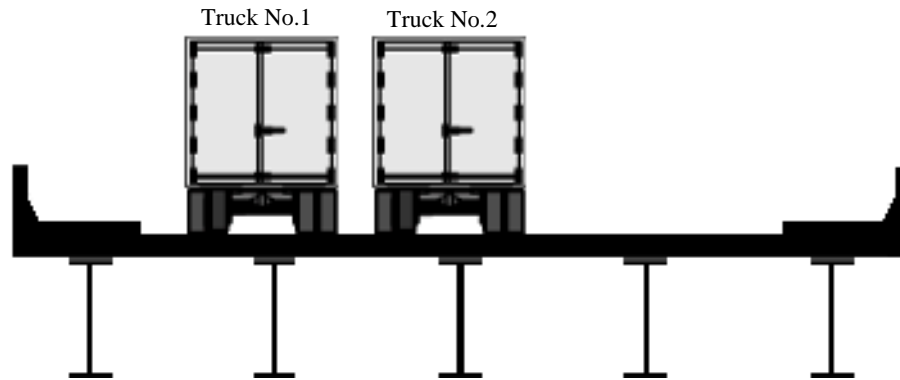


**Figure 3-34** Two Trucks in Adjacent Lanes

### **3.3 Dynamic Load**

The dynamic load is time-variant, random in nature and it has dependency on the vehicle type, vehicle weight, axle configuration, bridge span length, road roughness and transverse position of truck on the bridge. The dynamic load is usually considered as an equivalent static live load and it is expressed in terms of a dynamic load factor (DLF). There are different definitions for DLF. It may be taken as the ratio of dynamic and static responses:  $DLF = D_{dyn} / D_{sta}$ , in which  $D_{dyn}$  is the absolute maximum dynamic response at any point (e.g. stress, strain or deflection) measured from the test data and  $D_{sta}$  is the maximum static response from the filtered dynamic response (Nassif and Nowak, 1995). The actual bridge behavior due to a 5 axle actual truck traveling at a speed of 104 km/h is illustrated in Figure 3-35.

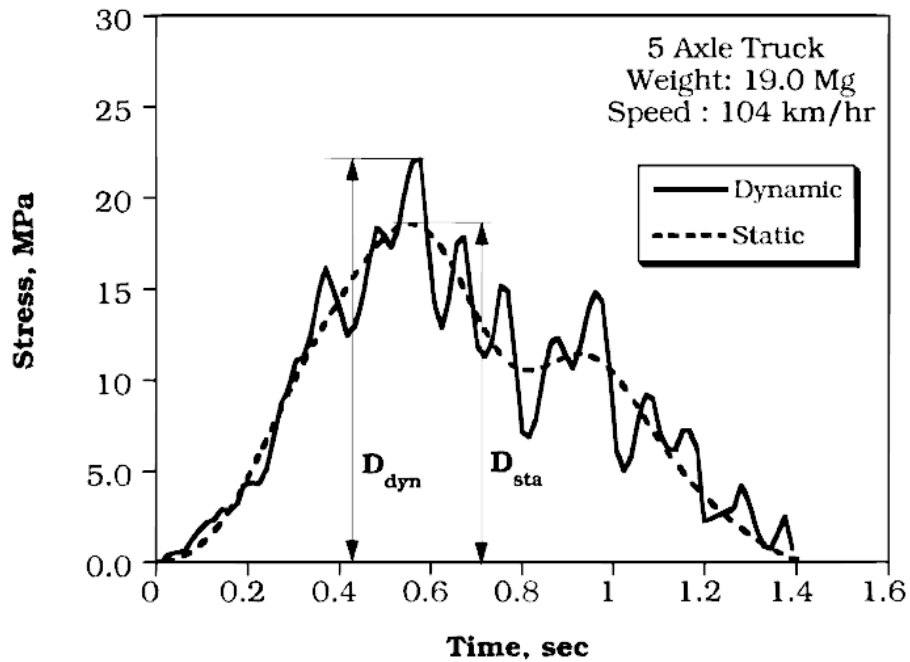


**Figure 3-35** Static and Dynamic Response of an Actual Bridge Due to an Actual Truck (Nassif and Nowak, 1995)

For the calibration of design codes, it is vital to determine statistical parameters of the dynamic load. The comparison of static and corresponding dynamic load shows that dynamic load does not have dependency on static load. For heavier trucks, the static response increases while dynamic response remains constant. Since the DLF is the ratio of dynamic response to static response, the heavier the truck is, the less the DLF is (Nowak et al., 1999).

Based on Hwang and Nowak's study (1991), depending on the span length of the bridge, the coefficient of variation varies from 0.40 to 0.70. The dynamic load factors for one truck are higher than two side-by-side trucks as illustrated in Figure 3-36.

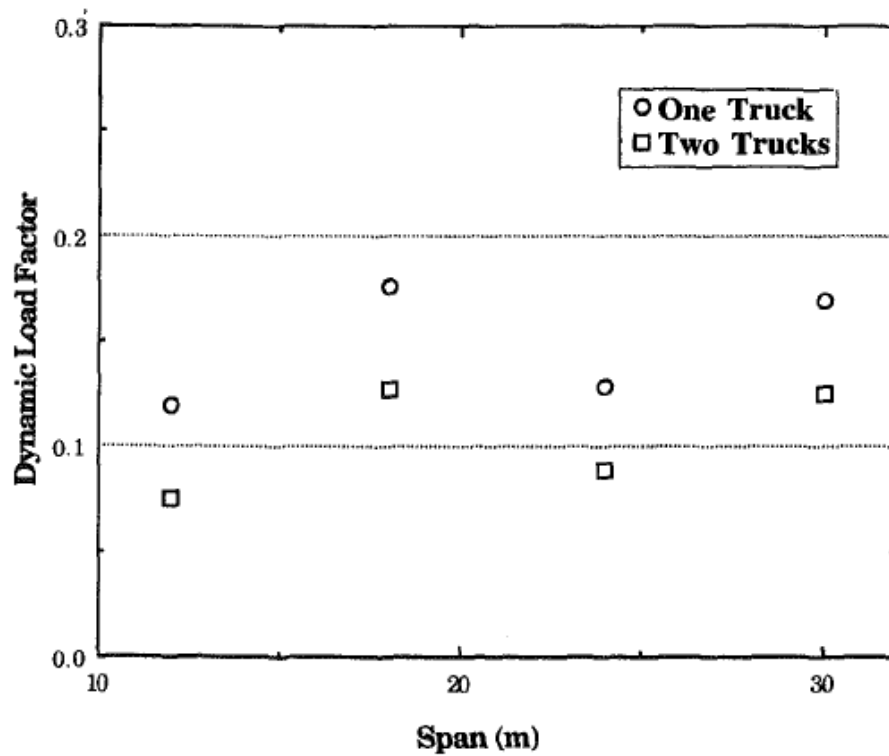


**Figure 3-36** Dynamic Load Factors for One Truck and Two Trucks (Hwang and Nowak, 1991)

In AASHTO LRFD Bridge Design Specification, the static effect of the design truck is increased by 33% for dynamic load allowance in Strength I limit state. The factor to be applied to static load shall be taken as  $(1+IM/100)$ , where IM is dynamic load factor. Table provided in AASHTO LRFD for IM is shown in Table 3-15. It should be noted that dynamic load factor is not applied to lane load.

**Table 3-15** Dynamic Load Allowance, IM (AASHTO LRFD Table 3.6.2.1-1)

Component	IM
Deck Joints – All Limit States	%75
All Other Components:	
• Fatigue and Fracture Limit State	%15
• All Other Limit States	%33

In Nowak's calibration report (1999), mean dynamic load factor is indicated as 0.10 for two side-by-side trucks and 0.15 for a single truck. The corresponding coefficient of variation is 0.80. In this study, these values are used.

### 3.4 Girder Distribution Factor

In bridge design, the maximum moment in the girders is determined by solving a three-dimensional problem involving complex behavior of load transfer from concrete slab to steel girder. The AASHTO bridge specification suggests many methods to analyze bridges, i.e., finite element analysis, grillage analysis, and a girder distribution factor (GDF) equation. Finite element analysis is an accurate method; however, it requires much effort in data preparation, bridge modeling and analysis, and interpretation of results. With girder distribution, the maximum moment in the girders is determined by multiplying the moment from a one-dimensional bridge analysis by the value obtained from the GDF equation (Phuvoravan, 2006).

GDF equation for interior girders is given in AASHTO LRFD Table 4.6.2.2.2b-1 as follows:

For one design lane loaded,

$$0.06 + \left(\frac{S}{4300}\right)^{0.4} \left(\frac{S}{L}\right)^{0.3} \left(\frac{K_g}{Lt_s^3}\right)^{0.1} \quad (3-4)$$

For two or more design lanes loaded,

$$0.075 + \left(\frac{S}{2900}\right)^{0.6} \left(\frac{S}{L}\right)^{0.2} \left(\frac{K_g}{Lt_s^3}\right)^{0.1} \quad (3-5)$$

in which  $S$  is girder spacing in mm,  $L$  is span length in mm,  $t_s$  is depth of concrete deck in mm, and  $K_g$  is longitudinal stiffness parameter in  $\text{mm}^4$ . Longitudinal stiffness parameter is defined in AASHTO LRFD 2010 4.6.2.2.1-1.

$$K_g = n(I + Ae_g^2) \quad \text{and} \quad n = \frac{E_B}{E_D} \quad (3-6)$$

where,  $E_B$  is the elastic modulus of girder material in MPa,  $E_D$  is the elastic modulus of slab material in MPa,  $I$  is the moment of inertia of noncomposite girder in  $\text{mm}^4$ ,  $A$  is the cross sectional area of noncomposite girder in  $\text{mm}^2$  and  $e_g$  is the distance between the centers of gravity of the deck and basic girder in mm.

Field measurements show that the actual load distribution is more uniform than what is analytically predicted. For girder distribution factors based on simplified methods (i.e. GDF equation), bias factor and coefficient of variation are 0.93 and 0.12, respectively. For girder distribution factors based on more sophisticated methods, (e.g. finite element analysis and grid analysis), bias factor and coefficient of variation are 0.98 and 0.07, respectively. It is also confirmed that the girder distribution factor can

be considered a normal random variable (Nowak et al., 2001). In the updating calibration report for AASHTO LRFD Code (Kulicki et al., 2007), bias factor and coefficient of variation for girder distribution factor is taken as 1.00 and 0.12, respectively.

In this research, coefficient of variation and bias factor are taken as 0.12 and 0.93 for girder distribution factor, respectively. In addition, GDF is treated as a normal random variable.

### 3.5 Summary of Statistical Parameters of Load

In Table 3-16, statistical parameters for dead loads, live loads, impact factor and girder distribution factor are listed.

**Table 3-16** Summary of Statistical Parameters of Loads

Parameter	Bias Factor	COV	Distribution
D1	1.03	0.08	Normal
D2	1.05	0.10	Normal
D3	1.00	0.25	Normal
D4	1.05	0.10	Normal
HL93	1.10 (single lane) (overall case)	0.306	Gumbel
HL93	0.77 (two lanes) (overall case)	0.306	Gumbel
HL93	1.12 (single lane) (extreme case)	0.165	Gumbel
HL93	0.86 (two lanes) (extreme case)	0.165	Gumbel
AYK45	0.69 (0.66~0.73) (single lane) (overall case)	0.309	Gumbel
AYK45	0.47 (0.42~0.52) (two lanes) (overall case)	0.309	Gumbel
AYK45	0.75 (0.73~0.77) (single lane) (extreme case)	0.160	Gumbel
AYK45	0.51 (0.46~0.56) (two lanes) (extreme case)	0.160	Gumbel
IM	mean = 0.15	0.80	Normal
GDF	0.93	0.12	Normal



## CHAPTER 4

### STATISTICS OF RESISTANCE

Flexural resistance capacity of composite steel bridge girders have been calculated based on nominal resistance values. In this study, only Strength I limit state is considered. AASHTO LRFD Bridge Design Specifications describe calculation of flexural resistance capacity and state some limits that should be considered in design. In this chapter, how to calculate flexural capacity of a composite steel girder is given and the limitations are introduced. Furthermore, statistical parameters regarding resistance such as material properties, dimensions and theoretical behavior are stated. The statistical parameters are obtained from both international and local research. Assessments of these parameters as well as calculation of nominal resistance capacities are essential in order to be able to conduct reliability analysis.

#### 4.1 Nominal Flexural Resistance Capacity of Composite Steel Girder Based On AASHTO LRFD Design Specifications

It is possible to design a bridge's superstructure composed of girders and a slab on them by simplifying the superstructure into an isolated single composite girder. In Figure 4-1, the simplification is illustrated.

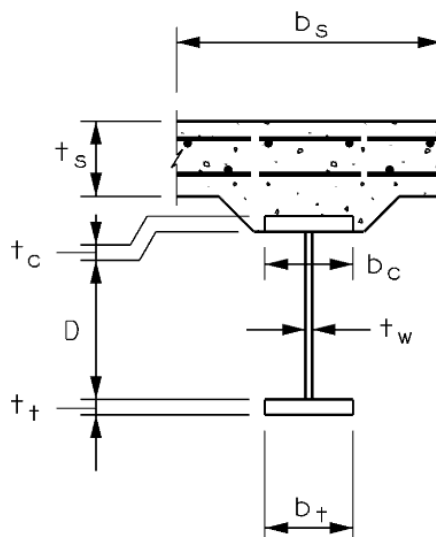


**Figure 4-1** Cross-Section of Isolated Composite Steel Girder (AASHTO LRFD 2010)

where  $b_s$  is effective width of the concrete deck,  $t_s$  is thickness of the concrete deck,  $D$  is web depth,  $t_w$  is web thickness,  $b_c$  and  $b_t$  are full width of flange, and  $t_c$  and  $t_t$  are flange thickness.

According to AASHTO LRFD 2010, effective width  $b_s$  may be taken as one-half the distance to the adjacent girder on each side of the component, or one-half the distance to the adjacent girder plus the full overhang width. AASHTO LRFD 2007 gives some additional statements, namely for interior girders, the effective flange width may be taken as the least of:

- one-quarter of the effective span length;
- 12.0 times the average depth of the slab, plus the greater of web thickness or one-half the width of the top flange of the girder; or
- The average spacing of the adjacent beams.

In this thesis study, effective flange width is taken as the average spacing of adjacent girders, as defined in AASHTO LRFD 2010.

Cross-section proportion limits are defined in Article 6.10.2 (AASHTO LRFD 2010). The limits should be as shown below:

$$\frac{D}{t_w} \leq 150 \quad (4-1a)$$

$$\frac{b_f}{2t_f} \leq 12.0 \quad (4-1b)$$

$$b_f \geq D/6 \quad (4-1c)$$

$$t_f \geq 1.1t_w \quad (4-1d)$$

Since only single span simply supported bridges are considered, only positive flexural carrying capacity of composite girder is going to be introduced.

According to Article 6.10.7.1.2, the nominal flexural resistance of the section shall be taken as:

If  $D_p \leq 0.1D_t$ , then,

$$M_n = M_p \quad (4-2a)$$

Otherwise,

$$M_n = M_p \left( 1.07 - 0.7 \frac{D_p}{D_t} \right) \quad (4-2b)$$

where  $D_p$  is the distance from the top of the concrete deck to the neutral axis of the composite section at the plastic moment,  $D_t$  is total depth of the composite section, and  $M_p$  is plastic moment of the composite section.

Plastic moment of composite section shall be calculated based on Article D6.1 of AASHTO LRFD. There are seven possible cases depending on location of plastic neutral axis (PNA). However, due to neglecting the contribution of longitudinal reinforcement conservatively in the deck in calculation of plastic moment capacities, number of cases considered will be reduced from seven to three, namely PNA is located either in web or in top flange or in concrete deck.

If PNA is in the web,

$$P_t + P_w \geq P_c + P_s \quad (4-3a)$$

$$M_p = \frac{P_w}{2D} [Y^2 + (D - Y)^2] + P_s d_s + P_c d_c + P_t d_t \quad (4-3b)$$

$$Y = \left(\frac{D}{2}\right) \left[ \frac{P_t - P_c - P_s}{P_w} + 1 \right] \quad (4-3c)$$

in which  $P_w$  is plastic force in the web ( $D \times t_w \times F_y$ ),  $P_s$  is plastic compressive force in the concrete deck ( $0.85f'_c \times t_s \times b_e$ ),  $P_c$  is plastic force in the compression flange ( $t_c \times b_c \times F_y$ ),  $P_t$  is plastic force in the tension flange ( $t_t \times b_t \times F_y$ ),  $Y$  is distance from the plastic neutral axis to the top of the web,  $d_s$  is distance from the plastic neutral axis to the mid-thickness of the concrete deck ( $Y + t_c + t_h + t_s/2$ ),  $d_c$  is distance from the plastic neutral axis to the mid-thickness of the compression flange ( $Y + t_c/2$ ),  $d_t$  is distance from the plastic neutral axis to the mid-thickness of the tension flange ( $D - Y + t_t/2$ ),  $t_h$  is average thickness of haunch,  $b_e$  is effective width of the concrete deck,  $F_y$  is specified minimum yield strength of steel, and  $f'_c$  is minimum specified 28-day compressive strength of concrete.

If one rewrites the formula, it yields

$$M_p = \frac{F_y}{2} (t_w D^2 + b_c t_c^2 + b_t t_t^2 + 2t_t b_t D) + 0.85f'_c t_s b_e \left( t_c + t_h + \frac{t_s}{2} \right) - \frac{(t_t b_t F_y - t_c b_c F_y - 0.85f'_c t_s b_e + D t_w F_y)^2}{4t_w F_y} \quad (4-3d)$$

If PNA is in the top flange,

$$P_t + P_w + P_c \geq P_s \quad (4-4a)$$

$$M_p = \frac{P_c}{2t_c} [Y^2 + (t_c - Y)^2] + P_s d_s + P_w d_w + P_t d_t \quad (4-4b)$$

$$Y = \left(\frac{t_c}{2}\right) \left[ \frac{P_w + P_t - P_s}{P_c} + 1 \right] \quad (4-4c)$$

in which  $Y$  is distance from the plastic neutral axis to the top of the flange,  $d_s$  is distance from the plastic neutral axis to the mid-thickness of the concrete deck ( $Y + t_h + t_s/2$ ),  $d_w$  is distance from the plastic neutral axis to the mid-thickness of the web ( $t_c - Y + D/2$ ),  $d_t$  is distance from the plastic neutral axis to the mid-thickness of the tension flange ( $t_c - Y + D + t_t/2$ ).

Rewriting the formula, it results in

$$M_p = \frac{F_y}{2} (t_c^2 b_c + t_t^2 b_t + 2Dt_w t_c + t_w D^2 + 2t_t b_t t_c + 2t_t b_t D) + 0.85f'_c t_s b_e (t_h + t_s/2) - \frac{(Dt_w F_y + t_t b_t F_y - 0.85f'_c t_s b_e + t_c b_c F_y)^2}{4b_c F_y} \quad (4-4d)$$

If PNA is in the reinforced concrete deck,

$$P_s > P_t + P_w + P_c \quad (4-5a)$$

$$M_p = \frac{Y^2 P_s}{2t_s} + P_c d_c + P_w d_w + P_t d_t \quad (4-5b)$$

$$Y = t_s \left[ \frac{P_c + P_w + P_t}{P_s} \right] \quad (4-5c)$$

in which  $Y$  is distance from the plastic neutral axis to the top of the deck,  $d_c$  is distance from the plastic neutral axis to the mid-thickness of the compression flange ( $t_s - Y + t_h + t_c/2$ ),  $d_w$  is distance from the plastic neutral axis to the mid-thickness of the web ( $t_s - Y + t_h + t_c + D/2$ ),  $d_t$  is distance from the plastic neutral axis to the mid-thickness of the tension flange ( $t_s - Y + t_h + t_c + D + t_t/2$ ).

Rewriting the formula, it yields

$$M_p = F_y \left[ t_c b_c \left( t_s + t_h + \frac{t_c}{2} \right) + D t_w \left( t_s + t_h + t_c + \frac{D}{2} \right) + t_t b_t \left( t_s + t_h + t_c + D + \frac{t_t}{2} \right) \right] - \frac{F_y^2 (t_c b_c + D t_w + t_t b_t)^2}{1.7 f'_c b_e} \quad (4-5d)$$

In Figure 4-2, these three cases described above are illustrated.

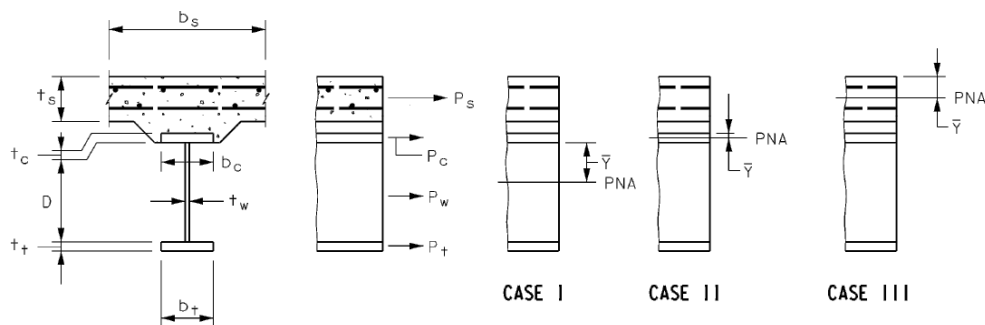


**Figure 4-2** Location of PNA: in Web (CASE I), in Flange (CASE II), and in Deck (CASE III) (AASHTO LRFD 2010)

## 4.2 Quantification of Uncertainties Related to Resistance Variables

Resistance variables can be grouped into three, which are material properties, dimensional properties and theoretical behaviors.

### 4.2.1 Material Properties

The main material property is strength. Composite steel plate girders are made of steel and concrete together.

#### 4.2.1.1 Concrete

Concrete is a composition of sand and gravel (crushed rock or other aggregates) bound together by a hardened paste of portland cement and water. The ingredients, when properly proportioned, form a plastic mass that can be molded or cast into predefined size and shape (Ersoy, 1999). It is the most widely used construction material in Turkey. According to European Ready Mixed Concrete Organization (ERMCO)'s ready-mixed concrete industry statistics report (2013), Turkey seems one of the top

ready-mixed concrete (RMC) manufacturers in Europe. In Figure 4-3, country RMC production per capita in Europe is shown. Note that Turkey is abbreviated as “TK”.

The water–cement ratio (W/C) by weight is the single most significant factor that affects strength of concrete. The lower the W/C ratio, the greater is the strength of concrete. It is clear that increasing the cement content increases the strength for a given amount of water in the mixture. Excess water content, which is not used in the chemical reaction with the cement, may not be desirable due to wetting the surface of the aggregate, eventually evaporates and causes excessive shrinkage and less durable concrete (Barker and Puckett, 2007).

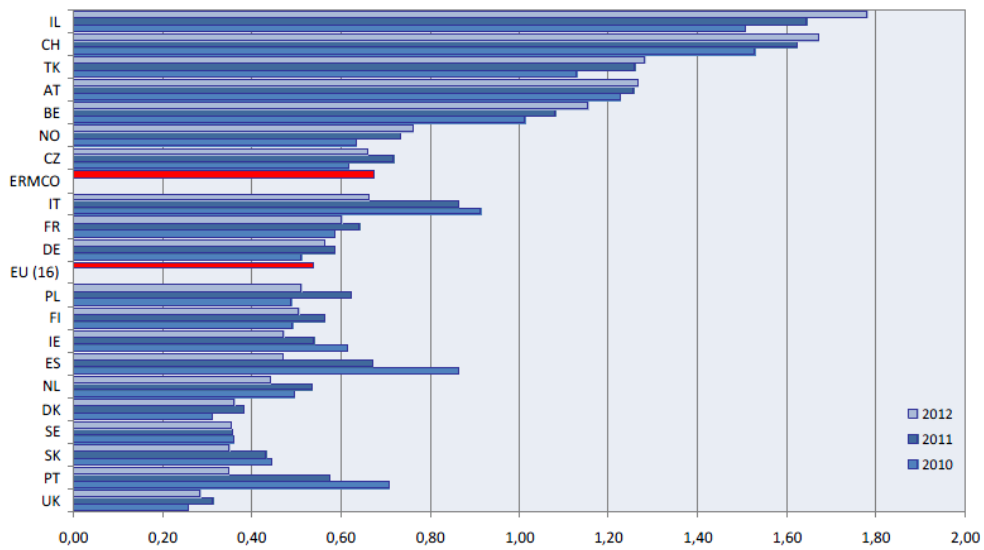


**Figure 4-3** RMC Production per Capita in Europe (ERMCO, 2013)

In Turkey, production percentage of high strength concrete has increased through the years. Turkish Ready Mixed Concrete Association (THBB) (2013) announced concrete grades’ production percentages with respect to years. In Figure 4-4, these values are shown on the graph. As seen, through the years, concrete grades with higher strengths have become more preferable, which indicates the development in construction in Turkey.

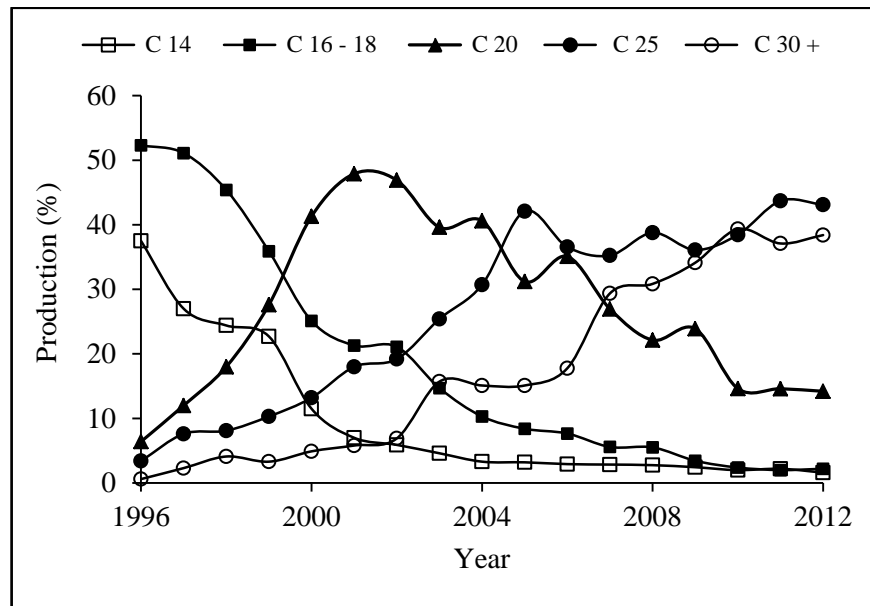


**Figure 4-4** Concrete Production (%) with respect to Years

The most important and useful mechanical property of concrete is compressive strength, and it is one of the most easily determined characteristic. In most cases, concrete is responsible primarily to cope with compressive stress. In other cases where concrete in tension or in shear, the compressive strength is generally used as a measure of these properties as well as the overall quality of concrete (Kesler, 1966). Hence, statistical parameters regarding uncertainties in compressive strength of concrete are investigated.

The specified concrete strength for decks is limited to minimum 4.0 ksi (27.6 MPa) per AASHTO LRFD 2010 5.4.2.1. In Turkey, C30 grade of concrete is frequently used in bridge decks. Therefore, only C30 class concrete is taken into account in this study.

Firat (2006) aimed to investigate the quality of concrete produced in Turkey. He obtained results of 28-day compressive strength of 150x150x150 mm cubic test specimens of concrete taken from different test laboratories located in different parts of Turkey. Tests were performed in the period of 2000 and 2005. He also compared the results with available test results from earlier researches. In Table 4-1 and Table 4-2, the results of his study are tabulated.

**Table 4-1** Statistics of 28-Day Cubic Compressive Strength of Concrete (that involves different grades together) through the Years (Firat, 2006)

Year	Number of Samples	Mean (MPa)	COV	Number of Values under the Limit	Percentage of Values under the Limit (%)
94/95	417	20.60	-	58	13
2000	732	26.97	0.142	40	5.46
2001	535	30.97	0.107	23	4.30
2002	465	31.21	0.104	10	2.15
2003	644	30.78	0.131	36	5.59
2004	1283	28.87	0.123	30	2.34
2005	615	29.97	0.120	24	3.90

**Table 4-2** Statistics of 28-Day Cubic Compressive Strength of Different Concrete Grades (Firat, 2006)

Grade of Concrete	Number of Samples	$f'_{c,cube}$ (MPa)	Mean (MPa)	COV	Number of Values under the Limit	Percentage of Values under the Limit (%)
C14	137	18	20.04	0.143	1	0.83
C16	755	20	25.11	0.144	13	1.73
C18	739	22	25.82	0.120	23	3.11
C20	5817	25	28.46	0.104	118	2.7
C25	2767	30	32.48	0.100	53	2.81
C30	870	37	40.07	0.079	14	2.47

In this study, the main focus is on C30 grade of concrete, which is widely used in bridge decks in Turkey as mentioned before. Firat (2006) has shown that C30 grade of concrete is of mean 28-day cubic compressive strength of 40.07 MPa and coefficient of variation of 0.079, in which additional epistemic uncertainties are not included.

Epistemic uncertainties in strength of concrete results from human errors, rate of loading, discrepancies between in-situ conditions and laboratory test conditions, and specimens not exactly belonging to actual mix.

In order to consider the difference between the in-situ actual strength and the strength obtained from control cylinders, a correction factor,  $N_1$ , will be introduced. Bloem (1968, as cited in Ang and Tang, 1984) reported that strength of field concrete is 10 to 21% lower than that of laboratory concrete. In addition, Firat (2007) introduced epistemic uncertainties from different researches. As cited in his study, Mirza et al.

(1979) indicated the average ratios of core strength to standard cylinder strength reported in different studies varied within the range of 0.74 and 0.96 with an overall average value of 0.87, and similarly Ellingwood and Ang (1972) presented this ratio varied from 0.83 to 0.92. Firat (2007) has taken the mean correction factor as 0.86, which is the average value of the ranges. Furthermore, Argınhan (2010) assumed an upper triangular distribution between lower limit and upper limit of ranges due to the fact that the quality control in a bridge construction is generally high in comparison to that in regular building construction, and concluded the mean correction factor,  $\bar{N}_1$ , as 0.89. Coefficient of variation,  $\Delta_1$ , of  $N_1$ , is suggested as 0.1 by Mirza et al. (1979, as cited in Firat, 2007). In this study, mean correction factor,  $\bar{N}_1$  and corresponding COV,  $\Delta_1$ , are taken as 0.89 and 0.1, respectively.

Effect of rate of loading is another source of uncertainty. To account this uncertainty, a correction factor,  $N_2$ , was introduced by Mirza et al. (1979, as cited in Firat, 2007). He used an empirical formula to express value of  $N_2$  as the following:

$$N_2 = 0.89(1 + 0.08 \log_{10}(R)) \quad (4-6)$$

in which  $R$  is the rate of loading in unit of psi/sec. Using the value 1 psi per second for  $R$ ,  $N_2$  is computed as 0.89. Kömürçü (1995, as cited in Firat, 2007) suggested that the mean value of 0.88 for mean correction factor,  $\bar{N}_2$ , with no prediction uncertainty, i.e.  $\Delta_2 = 0$ . The same values are taken into account for rate of loading in this study.

Human error is an additional source of uncertainty. The specimens may be selected from a special batch instead of randomly taken from actual mix. In addition, standard testing procedures may not be utilized properly. In order to account this uncertainty, Kömürçü (1995, as cited in Firat, 2007) introduced a mean correction factor,  $\bar{N}_3$ , as 0.95 and a prediction uncertainty,  $\Delta_3$ , as 0.05. Argınhan (2010) used this correction factor as 1.0 due to the fact that quality control in bridge construction is high. Mean correction factor,  $\bar{N}_3$  and corresponding coefficient of variation,  $\Delta_3$ , are taken as 1.0 and 0.05, respectively, in this study.

Epistemic uncertainties can be combined as the following:

$$\bar{N}_{f_c'} = \bar{N}_1 \times \bar{N}_2 \times \bar{N}_3 = 0.89 \times 0.88 \times 1.0 \cong 0.8 \quad (4-7a)$$

$$\Delta_{f_c'} = \sqrt{\Delta_1^2 + \Delta_2^2 + \Delta_3^2} = \sqrt{0.1^2 + 0^2 + 0.05^2} = 0.11 \quad (4-7b)$$

True value of compressive strength of C30 grade of concrete can be calculated as  $0.8 \times 40.07 = 32.1$  MPa. C30 grade of concrete has a cylindrical compressive strength of 30 MPa, which corresponds to a cubic compressive strength of 37 MPa. Since

laboratory tests are utilized with cubic specimens, bias factor for compressive strength of C30 grade of concrete is  $32.1/37 = 0.87$ .

Total coefficient of variation can be calculated as the following:

$$\Omega_{f_c'} = \sqrt{\delta_{f_c'}^2 + \Delta_{f_c'}^2} = \sqrt{0.079^2 + 0.11^2} = 0.135 \quad (4-8)$$

in which  $\delta_{f_c'}$  is inherent (aleatory) uncertainty and  $\Delta_{f_c'}$  is the total prediction (epistemic) uncertainty. In Table 4-3, all findings related with statistical parameters on C30 grade of concrete is summarized.

**Table 4-3** Summary of Findings on C30 Grade of Concrete

Statistical Parameters (Cubic)	Values
Laboratory Measured Mean (MPa)	40.07
In-situ Mean (MPa)	32.06
Nominal (MPa)	37
Bias Factor (Mean/Nominal)	0.87
Coefficient of Variation	0.135
Standard Deviation (MPa)	4.32

#### 4.2.1.2 Steel

Iron ore, coke, limestone, and chemical additives are the basic raw materials for producing steel. These are the typical ingredients and the chemical admixtures that provide custom-designed products for particular applications, much like the process used for producing concrete. However, it is possible to better control the process and make a more uniformly reliable final product in the case of steelmaking (Barker and Puckett, 2007).

Turkey is the world's 8<sup>th</sup> largest steel producer according to global production data in 2012 (Güreş, 2013). In Turkey, approximately 60 percent of the steel structures are industrial structures. Bridges are the only 3 percent of the steel structures (Altay and Güneyisi, 2008). Distribution of steel structures based on their types is shown in Figure 4-5.

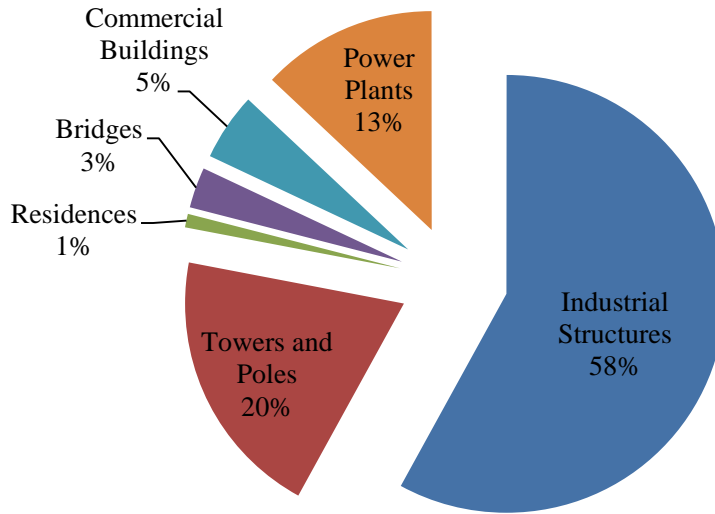


**Figure 4-5** Distribution of Steel Structures (Altay and Güneyisi, 2008)

In comparing the properties of different steels, the terms strength (yield and tensile), ductility, hardness, and toughness are used. These terms are defined below:

- Yield strength is the stress at which an increase in strain occurs without an increase in stress.
- Tensile strength is the maximum stress reached in a tensile test.
- Ductility is an index of the ability of the material to withstand inelastic deformations without fracture and can be expressed as a ratio of elongation at fracture to the elongation at first yield.
- Hardness refers to the resistance to surface indentation from a standard indenter.
- Toughness is the ability of a material to absorb energy without fracture.

In Turkey, mostly Fe 37 and Fe 52 grade of steel are used. Their yield and tensile strength properties are shown in Table 4-4.

**Table 4-4** Strength Values of Steel (TS648, 1980)

Grade	Yield Strength (MPa)	Tensile Strength (MPa)
Fe 37	235	363-491
Fe 52	353	510-608

The yield strength is primary interest in the design of most steel structures.

There is no research on statistics of mechanical properties of steel in Turkey. Statistical yield strength parameters are taken from the paper of Liu (2002). Bias factor and coefficient of variation of yield strength are indicated as 1.12 and 0.0866, respectively. Yield strength shows lognormal distribution.

#### 4.2.2 Dimensions and Theoretical Behavior

Dimension of steel section involves uncertainties due to manufacturing errors. The dimensions of steel sections are assumed to be distributed normally. Dimensions can be classified as thickness and width. Bias factor and coefficient of variation of thickness are 1 and 0.0350, respectively, and 1 and 0.0135 for width (Li, 2007).

Theoretical behavior is another variable that influences resistance. It involves uncertainties due to assumptions or approximations in analyze. Therefore, that should be taken into consideration in reliability analysis. Nowak (1999) describes a multiplier named professional factor to consider this uncertainty. For composite steel girder bridges, bias factor and coefficient of variation of professional factor can be taken as 1.05 and 0.06, respectively. Nominal value of professional factor is taken 1.0 in reliability analysis.

#### 4.2.3 Summary of Statistical Parameters of Resistance

In Table 4-5, statistical parameters for yield strength of steel, compressive strength of concrete, dimension of sections and professional factor are summarized.

**Table 4-5** Summary of Statistical Parameters of Resistance

Parameter	Bias Factor	COV	Distribution
Compressive Strength of Concrete	0.87	0.135	Normal
Yield Strength of Steel	1.12	0.0866	Lognormal
Thickness	1.00	0.0350	Normal
Width	1.00	0.0135	Normal
Professional Factor	1.05	0.06	Normal

## CHAPTER 5

### DESIGN OF BRIDGE GIRDERS

For the purpose of reliability analysis, a total of 120 composite steel bridge girders have been designed. Only single span simply supported bridges have been considered. Span lengths are chosen as 50 m, 60 m, 70 m and 80 m because I-girder composite bridges are usually used to span between 50 to 80 m in Turkey. In design, AASHTO LRFD Bridge Design Specifications are followed; however, different load and resistance factors are used to see change in reliability indices. In Figure 5-1, typical cross section of bridges designed is shown.

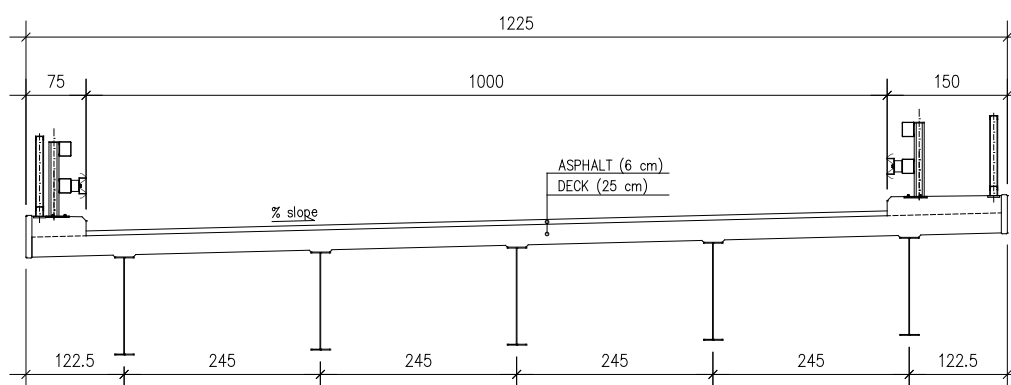


**Figure 5-1** Typical Cross-Section of Designed Bridges

Each bridge has its own design parameters. These bridges can be grouped into two: half of them are those designed for live load HL93 and the other half are those designed for live load AYK45. This combination of different live load models, span lengths, and load and resistance factors results in a total of 120 bridges.

Bridges have 5 girders spaced at 245 cm. Note that only interior girders have been designed. Barrier weight is assumed to be 4.4 kN/m. The unit weight of concrete, asphalt and steel are taken from AASHTO LRFD 2010 Table 3.5.1-1.

The forces in the longitudinal reinforcement in the deck are conservatively neglected in calculation of plastic moment capacities.

## 5.1 Designs Using Spreadsheet

Design of that many bridge girders by hand is very time-consuming job; therefore, it is reasonable to develop a computer program to design these bridge girders. For that purpose, a macro-based Microsoft Excel spreadsheet has been designed. This spreadsheet is called computer program in the rest of this study. By the help of this program, it has become possible to design as many girders as desired with a single click in a few minutes, provided that input parameters are submitted into the program.

### 5.1.1 Input Parameters

Material properties such as yield strength of steel and compressive strength of concrete, width and thickness of deck, thickness of wearing surface, girder spacing, number of girders and barrier weight are common for all bridges designed. These parameters are put into the program as seen in Figure 5-2.

	A	B	C	D	E	F	G
1	<b>Bridge Geometry</b>			<b>Density of Materials</b>			
2	Bridge Width	12.25 m			Concrete	2400 kg/m <sup>3</sup>	
3	Deck Depth	0.25 m			Steel	7850 kg/m <sup>3</sup>	
4	Wearing Surface Depth	0.06 m			Asphalt	2250 kg/m <sup>3</sup>	
5	Number of Girder	5			<b>Strength of Materials</b>		
6	Girder Spacing	2.45 m			Concrete	30 MPa	
7	Lane Width	3.6 m			Steel (Tension Flange)	345 MPa	
8	Average Haunch Depth	0.025 m			Steel (Bottom Flange)	345 MPa	
9	<b>Additional Weights</b>				Steel (Web)	345 MPa	
10	Barrier Weight	4.4 kN/m			Elastic Modulus of Steel	2000 GPa	

**Figure 5-2** Common Input Parameters Substituted to the Program

The parameters that create the differences between bridges are live load models, span lengths, and load and resistance factors.

Live load model needs to be selected. HL93 and AYK45 live load models have been predefined in the program. But also it is possible to define a custom live load model. The program will design the girders for that selected live load model.

Span lengths should be defined. It is possible to define as many span lengths as desired. Only thing that should be done is to put minimum and maximum span lengths

as well as increment between them into the program. Any increment desired can be set into the program.

And finally, resistance factors and live load factors should be set in terms of minimum and maximum values as well as increment.

	I	J	K	L	M	N
1	Span (m)	50 ~ 80			ΔL (m)	10
2	γ <sub>LL+IM</sub>	1.5 ~ 2.5			Δγ <sub>LL+IM</sub>	0.25
3	Φ	0.9 ~ 1.0			ΔΦ	0.05

**Figure 5-3** Further Input Parameters Put into the Program

### 5.1.2 Design Algorithm

After clicking the “run” button, the program starts designing bridge girders one-by-one. First bridge to be designed is the one having a defined minimum span length and it is designed based on minimum load and resistance factors defined in the program.

The program assigns an initial girder cross-section to the bridge. Initial depth of that girder is decided according to minimum girder depth equation defined in AASHTO LRFD 2010 Table 2.5.2.6.3-1. According to this specification, initial girder depth may be chosen as 0.033 times span length.

The other dimensions of cross-section of girders are determined based on formulas derived from cross section proportion limits given in AASHTO LRFD 2010 6.10.2. Cross section proportion limits in AASHTO are shown below.

$$\frac{D}{t_w} \leq 150 \quad (5-1)$$

$$\frac{b_f}{2t_f} \leq 12.0 \quad (5-2)$$

$$b_f \geq D/6 \quad (5-3)$$

$$t_f \geq 1.1t_w \quad (5-4)$$

where  $D$  is web depth,  $t_w$  is web thickness,  $b_f$  is full width of flange, and  $t_f$  is flange thickness.

Using these inequalities, some formulas are derived to determine cross section dimensions. If inequalities (5-2) and (5-3) are considered, a closed interval can be written as shown below:

$$D/6 \leq b_f \leq 24t_f \quad (5-5)$$

Considering  $b_f$  is in the exact middle of those two extreme limit values,

$$b_f = (D/6 + 24t_f)/2 \quad (5-6)$$

In addition, to satisfy the inequalities (5-1) and (5-4) following equations are derived. Note that units are in mm.

$$t_w = D/150 + 0.001 \quad (5-7)$$

$$t_f = 1.2t_w \quad (5-8)$$

Top and bottom flange dimensions are chosen to be the same for the sake of simplicity.

After program assigns the initial girder cross section, program calculates the resistance capacity of composite steel girder and also both live load and dead load demands. Next, it compares the capacity and demand. Until capacity has become large enough to cope with demand, it continuously increases dimensions of cross section so that final dimensions of cross section are determined. Note that increase increment of depth of girder is user-defined and all other dimensions are function of web depth.

Note that in each step the program takes into account the increase in dead load due to increase in cross sectional area of girder. After dimensions are determined, structural reliability analysis is conducted for that bridge girder. Next, program starts designing following bridge girders with the same procedure.

A flow chart that shows the design algorithm is given in Figure 5-4.

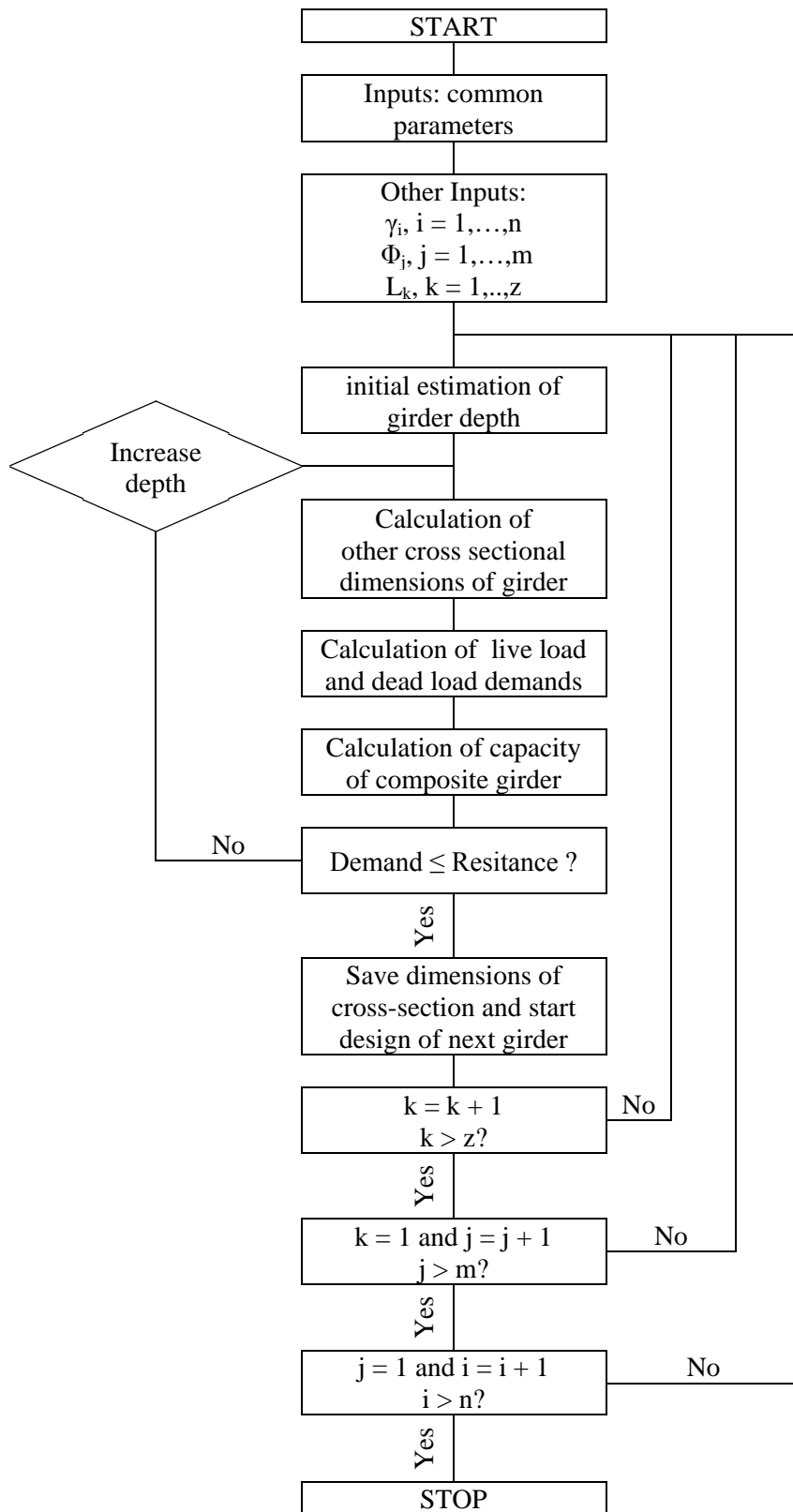


**Figure 5-4** Design Algorithm Flowchart

## 5.2 Design Results

120 steel girders have been designed according to AASHTO LRFD specifications for span lengths of 50 to 80 m with an increment of 10 m. Designs have been utilized based on strength I limit state; however, different resistance and live load factors have been tried in order to see change in reliability level. In addition to HL93, AYK45 model has also been used.

### 5.2.1 Cross Sectional Dimensions of Steel Girders

Cross-sectional dimensions, factored load demands  $M_U$  as well as factored flexural resistance capacity  $\Phi_f M_n$  of girders for different live load and resistance factors are listed in Table 5-1 to Table 5-15 for HL93 and in Table 5-16 to Table 5-30 for AYK45.

**Table 5-1** Section Dimensions (LL: 1.50,  $\Phi_f = 0.90$ ; HL93)

Span	$M_U$ (kNm)	$\Phi_f M_n$ (kNm)	D (mm)	$t_w$ (mm)	$b_f$ (mm)	$t_f$ (mm)
50	15759.5	15785	2032	15	379	18
60	22353	22361	2328	17	432	20
70	30380	30397	2628	19	486	22
80	40674	40675	3019	21	556	25

**Table 5-2** Section Dimensions (LL: 1.50, R: 0.95; HL93)

Span	$M_U$ (kNm)	$\Phi_f M_n$ (kNm)	D (mm)	$t_w$ (mm)	$b_f$ (mm)	$t_f$ (mm)
50	15654	15663	1983	14	370	17
60	22188	22211	2273	16	422	19
70	30033	30038	2546	18	471	22
80	40094	40096	2921	21	538	25

**Table 5-3** Section Dimensions (LL: 1.50, R: 1.00; HL93)

Span	$M_U$ (kNm)	$\Phi_f M_n$ (kNm)	D (mm)	$t_w$ (mm)	$b_f$ (mm)	$t_f$ (mm)
50	15557	15566	1941	14	363	17
60	22021	22021	2225	16	413	19
70	29787	29797	2489	18	461	21
80	39571	39572	2832	20	522	24

**Table 5-4** Section Dimensions (LL: 1.75, R: 0.90; HL93)

Span	$M_U$ (kNm)	$\Phi_f M_n$ (kNm)	D (mm)	$t_w$ (mm)	$b_f$ (mm)	$t_f$ (mm)
50	17012	17021	2098	15	391	18
60	23973	23987	2390	17	443	20
70	32616	32624	2718	19	502	23
80	43474	43489	3118	22	574	26

**Table 5-5** Section Dimensions (LL: 1.75, R: 0.95; HL93)

Span	$M_U$ (kNm)	$\Phi_f M_n$ (kNm)	D (mm)	$t_w$ (mm)	$b_f$ (mm)	$t_f$ (mm)
50	16874	16885	2043	15	381	18
60	23791	23818	2333	17	433	20
70	32179	32204	2632	19	486	22
80	42833	42838	3017	21	555	25

**Table 5-6** Section Dimensions (LL: 1.75, R: 1.00; HL93)

Span	$M_U$ (kNm)	$\Phi_f M_n$ (kNm)	D (mm)	$t_w$ (mm)	$b_f$ (mm)	$t_f$ (mm)
50	16763	16763	1995	14	372	17
60	23624	23641	2285	16	424	20
70	31830	31876	2557	18	473	22
80	42277	42296	2925	21	539	25

**Table 5-7** Section Dimensions (LL: 2.00, R: 0.90; HL93)

Span	$M_U$ (kNm)	$\Phi_f M_n$ (kNm)	D (mm)	$t_w$ (mm)	$b_f$ (mm)	$t_f$ (mm)
50	18294	18313	2157	15	401	19
60	25620	25639	2449	17	454	21
70	34844	34844	2804	20	517	24
80	46316	46322	3213	22	591	27

**Table 5-8** Section Dimensions (LL: 2.00, R: 0.95; HL93)

Span	$M_U$ (kNm)	$\Phi_f M_n$ (kNm)	D (mm)	$t_w$ (mm)	$b_f$ (mm)	$t_f$ (mm)
50	18150	18220	2108	15	392	18
60	25418	25470	2393	17	444	20
70	34411	34417	2717	19	502	23
80	45644	45667	3110	22	572	26

**Table 5-9** Section Dimensions (LL: 2.00, R: 1.00; HL93)

Span	$M_U$ (kNm)	$\Phi_f M_n$ (kNm)	D (mm)	$t_w$ (mm)	$b_f$ (mm)	$t_f$ (mm)
50	17995	18008	2052	15	382	18
60	25227	25229	2341	17	434	20
70	33983	33994	2634	19	487	22
80	45022	45024	3014	21	555	25

**Table 5-10** Section Dimensions (LL: 2.25, R: 0.90; HL93)

Span	$M_U$ (kNm)	$\Phi_f M_n$ (kNm)	D (mm)	$t_w$ (mm)	$b_f$ (mm)	$t_f$ (mm)
50	19561	19597	2213	16	411	19
60	27282	27292	2506	18	464	21
70	37124	37131	2890	20	533	24
80	49308	49321	3308	23	608	28

**Table 5-11** Section Dimensions (LL: 2.25, R: 0.95; HL93)

Span	$M_U$ (kNm)	$\Phi_f M_n$ (kNm)	D (mm)	$t_w$ (mm)	$b_f$ (mm)	$t_f$ (mm)
50	19410	19411	2162	15	402	19
60	27060	27063	2449	17	454	21
70	36642	36658	2798	20	516	24
80	48471	48476	3200	22	588	27

**Table 5-12** Section Dimensions (LL: 2.25, R: 1.00; HL93)

Span	$M_U$ (kNm)	$\Phi_f M_n$ (kNm)	D (mm)	$t_w$ (mm)	$b_f$ (mm)	$t_f$ (mm)
50	19262	19277	2114	15	394	18
60	26863	26869	2394	17	444	20
70	36199	36209	2716	19	502	23
80	47804	47822	3102	22	571	26

**Table 5-13** Section Dimensions (LL: 2.50, R: 0.90; HL93)

Span	$M_U$ (kNm)	$\Phi_f M_n$ (kNm)	D (mm)	$t_w$ (mm)	$b_f$ (mm)	$t_f$ (mm)
50	20840	20848	2268	16	421	19
60	28988	28988	2569	18	475	22
70	39390	39399	2974	21	548	25
80	52228	52228	3399	24	624	28

**Table 5-14** Section Dimensions (LL: 2.50, R: 0.95; HL93)

Span	$M_U$ (kNm)	$\Phi_f M_n$ (kNm)	D (mm)	$t_w$ (mm)	$b_f$ (mm)	$t_f$ (mm)
50	20682	20685	2213	16	411	19
60	28722	28722	2502	18	463	21
70	38889	38905	2881	20	531	24
80	51428	51434	3292	23	605	28

**Table 5-15** Section Dimensions (LL: 2.50, R: 1.00; HL93)

Span	$M_U$ (kNm)	$\Phi_f M_n$ (kNm)	D (mm)	$t_w$ (mm)	$b_f$ (mm)	$t_f$ (mm)
50	20546.9	20615	2168	16	403	19
60	28501	28510	2450	17	454	21
70	38430	38449	2794	20	516	24
80	50641	50669	3188	22	586	27

**Table 5-16** Section Dimensions (LL: 1.50, R: 0.90; AYK45)

Span	$M_U$ (kNm)	$\Phi_f M_n$ (kNm)	D (mm)	$t_w$ (mm)	$b_f$ (mm)	$t_f$ (mm)
50	17790	17800	2136	15	398	18
60	24866	24867	2422	17	449	21
70	33685	33691	2758	19	509	23
80	44694	44726	3158	22	581	27

**Table 5-17** Section Dimensions (LL: 1.50, R: 0.95; AYK45)

Span	$M_U$ (kNm)	$\Phi_f M_n$ (kNm)	D (mm)	$t_w$ (mm)	$b_f$ (mm)	$t_f$ (mm)
50	17647	17676	2078	15	387	18
60	24679	24692	2366	17	439	20
70	33228	33236	2671	19	493	23
80	44036	44094	3057	21	563	26

**Table 5-18** Section Dimensions (LL: 1.50, R: 1.00; AYK45)

Span	$M_U$ (kNm)	$\Phi_f M_n$ (kNm)	D (mm)	$t_w$ (mm)	$b_f$ (mm)	$t_f$ (mm)
50	17527	17539	2032	15	379	18
60	24497	24503	2317	16	430	20
70	32864	32899	2594	18	480	22
80	43458	43476	2963	21	546	25

**Table 5-19** Section Dimensions (LL: 1.75, R: 0.90; AYK45)

Span	$M_U$ (kNm)	$\Phi_f M_n$ (kNm)	D (mm)	$t_w$ (mm)	$b_f$ (mm)	$t_f$ (mm)
50	17527	17539	2207	16	410	19
60	24497	24503	2494	18	462	21
70	32864	32899	2868	20	529	24
80	43458	43476	3278	23	602	27

**Table 5-20** Section Dimensions (LL: 1.75, R: 0.95; AYK45)

Span	$M_U$ (kNm)	$\Phi_f M_n$ (kNm)	D (mm)	$t_w$ (mm)	$b_f$ (mm)	$t_f$ (mm)
50	19280	19284	2156	15	401	18
60	26746	26800	2438	17	452	21
70	36022	36039	2777	20	512	23
80	47498	47523	3169	22	583	27

**Table 5-21** Section Dimensions (LL: 1.75, R: 1.00; AYK45)

Span	$M_U$ (kNm)	$\Phi_f M_n$ (kNm)	D (mm)	$t_w$ (mm)	$b_f$ (mm)	$t_f$ (mm)
50	19131.8	19179	2108	15	392	18
60	26536	26549	2385	17	442	20
70	35568	35587	2693	19	497	23
80	46852	46857	3071	22	565	26

**Table 5-22** Section Dimensions (LL: 2.00, R: 0.90; AYK45)

Span	$M_U$ (kNm)	$\Phi_f M_n$ (kNm)	D (mm)	$t_w$ (mm)	$b_f$ (mm)	$t_f$ (mm)
50	21047.9	21059	2274	16	422	19
60	29104	29108	2573	18	476	22
70	39339	39339	2971	21	547	25
80	51930	51942	3392	24	623	28

**Table 5-23** Section Dimensions (LL: 2.00, R: 0.95; AYK45)

Span	$M_U$ (kNm)	$\Phi_f M_n$ (kNm)	D (mm)	$t_w$ (mm)	$b_f$ (mm)	$t_f$ (mm)
50	20882	20887	2223	16	413	19
60	28824	28869	2507	18	464	21
70	38839	38842	2878	20	531	24
80	51158	51190	3282	23	603	28

**Table 5-24** Section Dimensions (LL: 2.00, R: 1.00; AYK45)

Span	$M_U$ (kNm)	$\Phi_f M_n$ (kNm)	D (mm)	$t_w$ (mm)	$b_f$ (mm)	$t_f$ (mm)
50	20743	20749	2174	16	404	19
60	28615	28675	2453	17	454	21
70	38356	38357	2792	20	515	24
80	50354	50354	3180	22	585	27

**Table 5-25** Section Dimensions (LL: 2.25, R: 0.90; AYK45)

Span	$M_U$ (kNm)	$\Phi_f M_n$ (kNm)	D (mm)	$t_w$ (mm)	$b_f$ (mm)	$t_f$ (mm)
50	22688	22688	2340	17	434	20
60	31335	31335	2665	19	492	23
70	42244	42256	3075	22	566	26
80	55576	55576	3501	24	642	29

**Table 5-26** Section Dimensions (LL: 2.25, R: 0.95; AYK45)

Span	$M_U$ (kNm)	$\Phi_f M_n$ (kNm)	D (mm)	$t_w$ (mm)	$b_f$ (mm)	$t_f$ (mm)
50	22531	22597	2288	16	425	20
60	30984	30992	2585	18	478	22
70	41694	41729	2978	21	549	25
80	54739	54752	3389	24	622	28

**Table 5-27** Section Dimensions (LL: 2.25, R: 1.00; AYK45)

Span	$M_U$ (kNm)	$\Phi_f M_n$ (kNm)	D (mm)	$t_w$ (mm)	$b_f$ (mm)	$t_f$ (mm)
50	22358	22373	2238	16	416	19
60	30686	30699	2516	18	466	21
70	41184	41211	2888	20	532	24
80	53958	53960	3285	22.9	604	28

**Table 5-28** Section Dimensions (LL: 2.50, R: 0.90; AYK45)

Span	$M_U$ (kNm)	$\Phi_f M_n$ (kNm)	D (mm)	$t_w$ (mm)	$b_f$ (mm)	$t_f$ (mm)
50	24357	24369.7	2404	17	446	20
60	33654	33671	2757	19	509	23
70	45205	45208	3175	22	584	27
80	59286	59300	3607	25	661	30

**Table 5-29** Section Dimensions (LL: 2.50, R: 0.95; AYK45)

Span	$M_U$ (kNm)	$\Phi_f M_n$ (kNm)	D (mm)	$t_w$ (mm)	$b_f$ (mm)	$t_f$ (mm)
50	24173	24224	2348	17	436	20
60	33226	33236	2671	19	493	23
70	44575	44583	3074	22	566	26
80	58388	58388	3493	24	641	29

**Table 5-30** Section Dimensions (LL: 2.50, R: 1.00; AYK45)

Span	$M_U$ (kNm)	$\Phi_f M_n$ (kNm)	D (mm)	$t_w$ (mm)	$b_f$ (mm)	$t_f$ (mm)
50	23990	23993	2297	16	426	20
60	32871	32899	2594	18	480	22
70	44031	44070	2982	21	549	25
80	57536	57552	3386	24	622	28

As can be observed, factored flexural resistance capacities of composite girders are as close as possible to factored load demand so that minimum design is maintained. Note that bottom and top flange dimensions are chosen same for the sake of simplicity. It is also possible to choose a wider and thicker bottom flange and shorter web depth so that more vertical clearance is maintained. In Table 5-31, alternative dimensions of an 80 – m girder designed for HL93 loading with LL: 2.50 and R: 1.0 are given. There is not much difference observed in terms of cross sectional area. For small spans, this difference is even smaller.

**Table 5-31** Alternative Girder designed for HL93 (LL: 2.50 and R: 1.0)

Design	D (mm)	t <sub>w</sub> (mm)	b <sub>f,top</sub> (mm)	t <sub>f,top</sub> (mm)	b <sub>f,bottom</sub> (mm)	t <sub>f,bottom</sub> (mm)	Area (m <sup>2</sup> )
Original	3188	22	586	27	586	27	0.1018
Alternative	3054	21	562	26	703	33	0.1019

### 5.2.2 Total Weight of Steel Used in Designed Bridges

Total weight of steel used in each designed bridge is calculated based on some assumptions. Cross sectional dimensions are already determined in design and their lengths and numbers are known. Therefore, it is possible to compute total weight of steel girders. However, weights of secondary members (e.g. bracings) are not known. It is assumed that secondary members weigh 15 percent of total weight of steel girders. Based on this assumption, total weights of steel with respect to load and resistance factor are determined and plotted for different span lengths in Figure 5-5 and Figure 5-6.

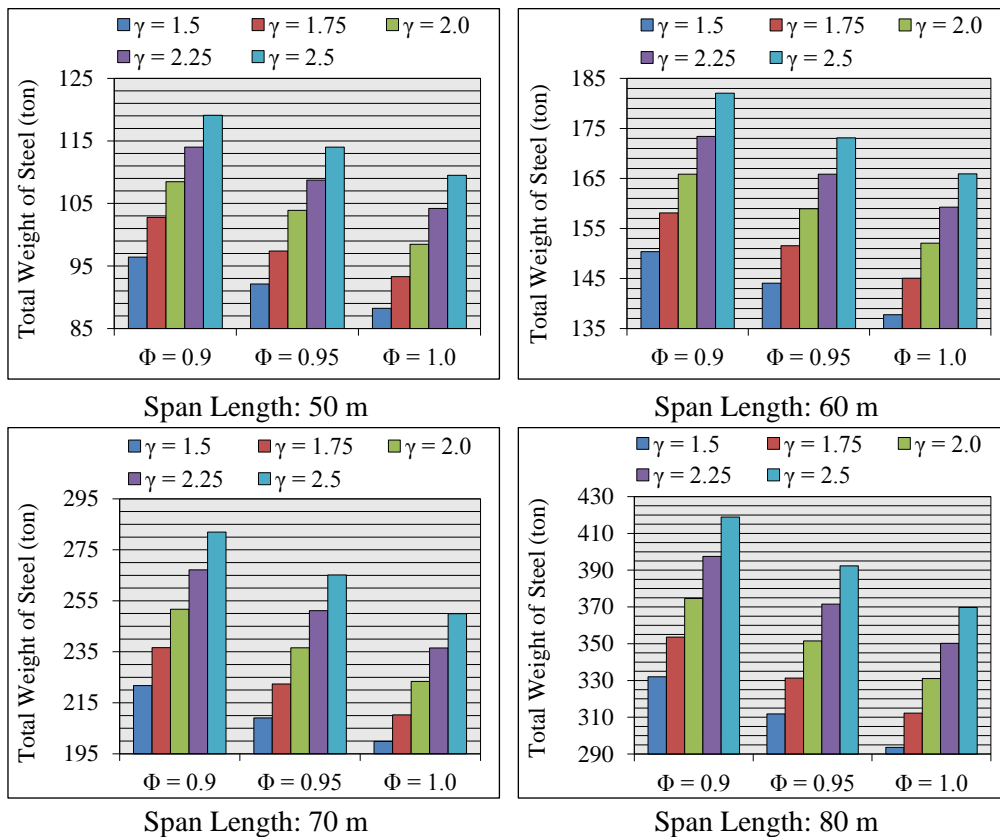


**Figure 5-5** Total Weight of Steel (HL93)

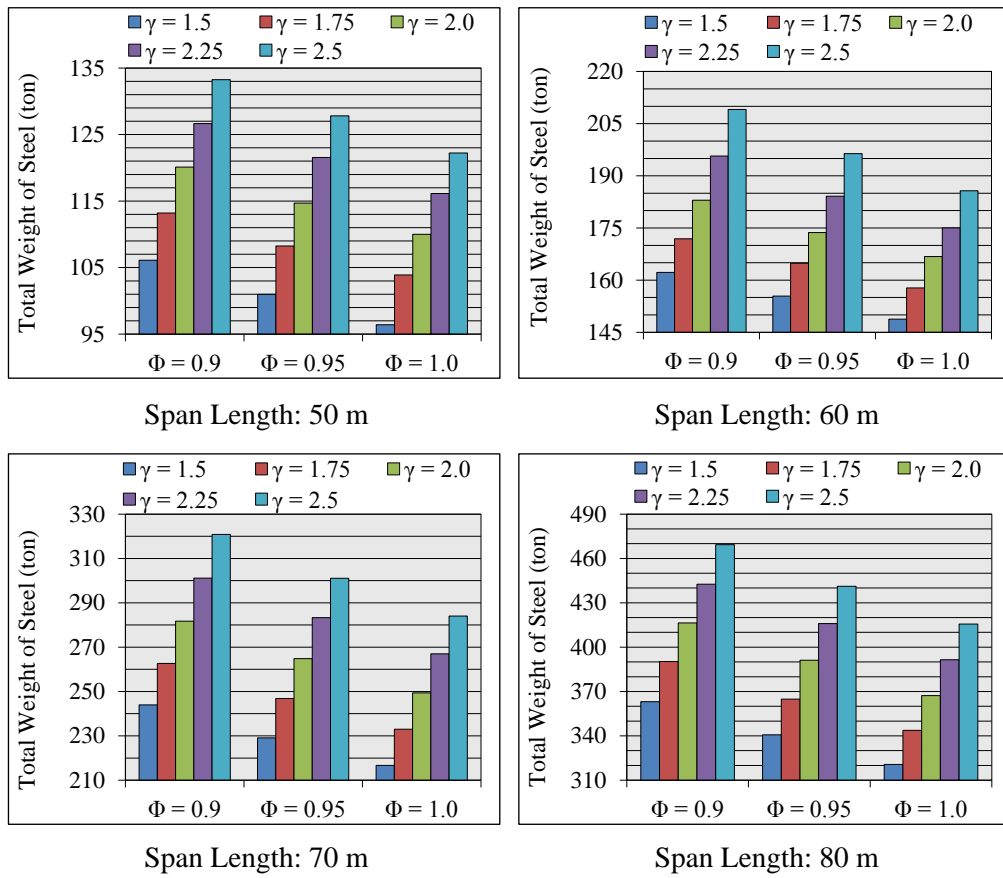


**Figure 5-6** Total Weight of Steel (AYK45)

As expected, the bridges designed with minimum resistance factor and maximum live load factor weigh much more than others. In following chapter, relationship between reliability and total weight of steel consumption will also be investigated.



## CHAPTER 6

### RELIABILITY EVALUATION

#### 6.1 Reliability Models

In general, parameters involved in engineering design involve uncertainties. Presence of these uncertainties results in difficulties in satisfying basic design requirements. Figure 6-1 presents a simple case with two main random variables, namely unfactored load (S) and resistance (R). Their randomness is expressed in terms of their means  $\mu_S$  and  $\mu_R$ , standard deviations  $\sigma_S$  and  $\sigma_R$ , and corresponding density functions  $f_S(s)$  and  $f_R(r)$ , respectively.

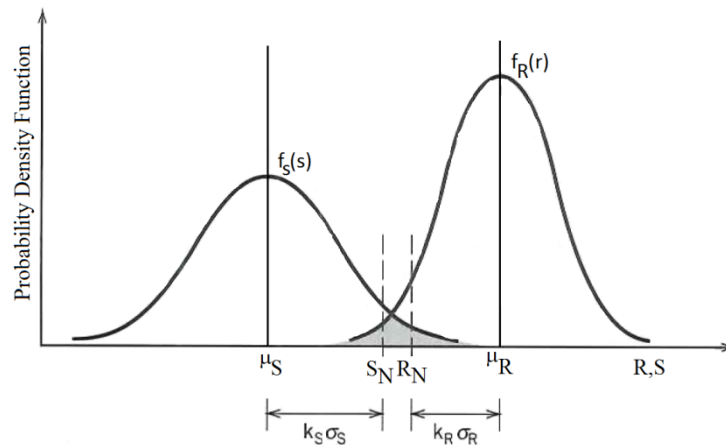


**Figure 6-1** Fundamentals of Reliability Analysis

The measure of reliability can be expressed as probability of survival as well as probability of failure,

$$\begin{aligned}
 p_f &= P(\text{failure}) = P(R < S) \\
 &= \int_0^\infty \left[ \int_0^s f_R(r) dr \right] f_S(s) ds \\
 &= \int_0^\infty F_R(s) f_S(s) ds
 \end{aligned}
 \tag{6-1}$$

where  $F_R(s)$  is the cumulative distribution function of  $R$  determined at  $s$ . That equation presented above is considered the basic equation in reliability-based design concept. When the load,  $S$  is equal to  $s$ , the probability of failure is  $F_R(s)$ , and due to the fact that load is a random variable; the integration should be performed to consider all the possible values of  $S$ , with respect to their corresponding likelihoods represented by the probability density function of  $S$  (Haldar and Mahadevan, 2000).

In practice, resistance and load depends on various basic random variables, such as the material properties, dimensional quantities, load effects, etc. The specific performance criterion, which is called limit state function or performance function or failure function, needs to be defined in terms of those basic random variables. It is described as:

$$M = R - S = g(\mathbf{X}) = g(X_1, X_2, \dots, X_n) \quad (6-2)$$

where  $M$  is the safety margin, which is a performance indicator, and  $\mathbf{X}$  is the vector of random variables. The failure surface or limit state is the case where  $g(\mathbf{X}) = M = 0$ . Failure surface forms a boundary between safe and unsafe zones. Positive values of  $M$  indicates safe region, whereas non-positive values of  $M$  indicates unsafe region. We can find probability of failure by carrying out the following integration,

$$p_f = \int \dots \int_{g(\cdot) < 0} f_X(x_1, x_2, \dots, x_n) dx_1 dx_2 \dots dx_n \quad (6-3)$$

where  $f_X(x_1, x_2, \dots, x_n)$  is the joint probability density function for the basic random variables  $X_1, X_2, \dots, X_n$  and the integration is carried out over the failure region, which is  $g(\cdot) < 0$ . In general, there are two main problems regarding that calculation of probability of failure: one of them is lack of data for obtaining joint probability density function, and the other one is that evaluation of multiple integrals is difficult. These difficulties are overcome by introducing approximate methods. In this thesis study, MVFOSM (Mean Value First Order Second Moment), AFOSM (Advanced First Order Second Moment), FORM (First Order Reliability Method) and SORM (Second Order Reliability Method) have been introduced and used, as such approximate methods.

### 6.1.1 First–Order Second–Moment Methods

First-order second moment methods are mean value first-order second-moment method (MVFOSM), advanced first-order second-moment method (AFOSM) and first-order reliability method (FORM). These methods use the information on first and second moments of random variables. In MVFOSM method, the distributional

information of random variables is ignored, whereas in AFOSM method, the information of the distribution is taken into consideration when random variables are normal, or taken as equivalent normal variates.

#### 6.1.1.1 Mean Value First-Order Second Moment Method

The method is originated from the study of Cornell (1969, as cited in Haldar and Mahadevan, 2000). It is based on a first-order Taylor series approximation of the failure function centered at the mean values of the random variables. Therefore, analysis of functions provides the mean and standard deviation of the failure function, i.e.,  $\mu_g$  and  $\sigma_g$ . These two parameters are used to build a measure of the reliability. The measure is called reliability index and it is an indicator of probability of failure as well as probability of survival. Reliability index is commonly denoted by the Greek letter  $\beta$ , and is formulated as the following:

$$\beta = \frac{\mu_g}{\sigma_g} \quad (6-4)$$

By multiplying Eq. (6-4) by  $\sigma_g$ , it becomes obvious that  $\beta$  is the number of standard deviations from the mean to the failure surface. The more standard deviations the failure surface is away from the mean, the safer the structure. In other words, the higher reliability index indicates the smaller probability of failure. To put it another way, the smaller values of the reliability index indicate that the failure surface is closer to the mean, which implies a higher failure probability.

If all random variables are normally distributed, probability of failure can be expressed in terms of reliability index as the following:

$$P_f = \Phi(-\beta) = 1 - \Phi(\beta) \quad (6-5)$$

where  $\Phi$  is standard normal cumulative distribution function. In Table 6-1, some reliability indices and their corresponding probability of failure are tabulated.

**Table 6-1** Reliability Index and the Corresponding Probability of Failure

Reliability Index, $\beta$	Probability of Failure, $P_f$
0	0.5
1	0.159
2	0.0228
3	0.00135
4	0.0000317
5	0.000000287
6	0.00000000987

Considering failure function is linear in the basic variables  $X_1, X_2, \dots, X_n$ , then it can be stated as

$$g(\mathbf{X}) = a_0 + a_1X_1 + \dots + a_nX_n \quad (6-6)$$

Mean value of failure function can be calculated as

$$\mu_g = g(\mu_X) = a_0 + a_1\mu_{X_1} + \dots + a_n\mu_{X_n} \quad (6-7)$$

and variance of the function is

$$\sigma_g^2 = a_1^2\sigma_{X_1}^2 + \dots + a_n^2\sigma_{X_n}^2 + \sum_{i=1}^n \sum_{j=1, j \neq i}^n \frac{\partial g}{\partial X_i} \frac{\partial g}{\partial X_j} Cov(X_i, X_j) \quad (6-8)$$

where  $Cov(X_i, X_j)$  is covariance of  $X_i$  and  $X_j$ , and is equal to  $\rho_{X_i X_j} \sigma_{X_i} \sigma_{X_j}$ , in which  $\rho_{X_i X_j}$  is correlation coefficient between  $X_i$  and  $X_j$ . If the variables are uncorrelated,  $\rho_{X_i X_j}$  is equal to 0. Note that the mean and standard deviation obtained are exact due to the fact that  $g(\mathbf{X})$  is linear.

In case  $g(\mathbf{X})$  is nonlinear, the result of the mean and standard deviation would not be exact, and approximate values of those can be obtained by using a linearized function, which is constructed by expanding failure function in Taylor series centered at the mean values and keeping only the linear terms. Hence, linearized function will be

$$g(\mathbf{X}) = g(\mu_X) + \sum_{i=1}^n \frac{\partial g}{\partial X_i} (X_i - \mu_{X_i}) \quad (6-9)$$

where  $\partial g/\partial X_i$  is evaluated at mean values. From the equation, approximate values of  $\mu_g$  and  $\sigma_g$  are obtained by

$$\mu_g \cong g(\mu_{X_1}, \dots, \mu_{X_n}) \quad (6-10)$$

$$\sigma_g^2 \cong \sum_{i=1}^n \sum_{j=1}^n \frac{\partial g}{\partial X_i} \frac{\partial g}{\partial X_j} Cov(X_i, X_j) \quad (6-11)$$

However, neglecting higher order terms may introduce significant error. Another shortcoming is that the mean point expansion lacks failure function invariance property. In other words, mechanically equivalent formulations of the same failure criterion may give different reliability index values. That means that reliability index is affected by how the failure function is formulated. This is a problem not only for nonlinear forms of failure functions but even in certain linear forms, e.g., when the loads counteract one another (Ellingwood et al., 1980).

Furthermore, calculation of the reliability index on the basis of linearization of non-linear failure function depends on the selection of linearization point. Instead of so-called mean point  $(\mu_{X_1}, \dots, \mu_{X_n})$ , another point on the failure surface would be more reasonable. Experience shows that an expansion centered at the mean point should not be used (Thoft-Christensen et al., 1982).

#### 6.1.1.2 Advanced First-Order Second Moment Method

Advanced first-order second moment method is also referred to as Hasofer-Lind method, which was proposed by Hasofer and Lind in 1974 for normal variables (as cited in Haldar and Mahadevan, 2000). Hasofer and Lind's reliability index denoted as  $\beta_{HL}$  is defined as the minimum distance from the origin of the axes to the failure surface in the standardized z-coordinate (reduced coordinate) system (Thoft-Christensen et al., 1982; Haldar and Mahadevan, 2000).

In this method, all random variables are assumed to be uncorrelated. Next, the first step is to standardize all random variables as the following:

$$Z_i = \frac{X_i - \mu_{X_i}}{\sigma_{X_i}}, \quad i = 1, 2, \dots, n \quad (6-11)$$

where  $\mu_{X_i}$  and  $\sigma_{X_i}$  are the mean and standard deviation of the random variable  $X_i$ , and  $Z_i$  is a random variable with zero mean and unit standard deviation. By the equation above, the failure surface in the x-coordinate system is transformed to a failure surface in the z-coordinate system (also referred as to the transformed or reduced coordinate

system). The point having the minimum distance to the origin on the failure surface is called design point, coordinates of which is denoted as  $\mathbf{z}^*$ . In Figure 6-2, a two-dimensional example is shown. As illustrated,  $g(\mathbf{Z}) = 0$  is a nonlinear failure function in the transformed coordinates.

By definition,  $\beta_{HL}$  can be formulated as

$$\beta_{HL} = \min \left( \sum_{i=1}^n z_i^2 \right)^{\frac{1}{2}} \quad (6-12)$$

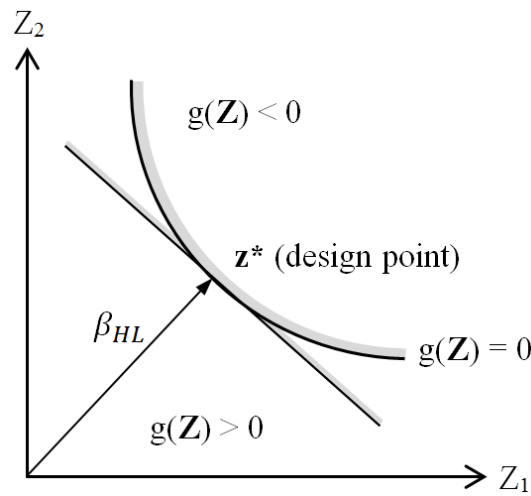


**Figure 6-2** Hasofer-Lind Reliability Index: Nonlinear Failure Function

One can obtain the minimum distance by using the following expression (Thoft-Christensen et al., 1982):

$$\beta_{HL} = - \frac{\sum_{i=1}^n z_i^* \left( \frac{\partial g}{\partial Z_i} \right)}{\sqrt{\sum_{i=1}^n \left( \frac{\partial g}{\partial Z_i} \right)^2}} \quad (6-13)$$

where  $(\partial g / \partial Z_i)$  is the  $i$ th partial derivative calculated at the design point with coordinates  $(z_1^*, \dots, z_n^*)$ . The design point in the  $z$ -coordinate is given by:

$$z_i^* = -\alpha_i \beta_{HL} \quad (i = 1, 2, \dots, n) \quad (6-14)$$

in which

$$\alpha_i = - \frac{\left(\frac{\partial g}{\partial Z_i}\right)}{\sqrt{\sum_{i=1}^n \left(\frac{\partial g}{\partial Z_i}\right)^2}} \quad (6-15)$$

An algorithm was developed by Rackwitz (1976, as cited in Haldar and Mahadevan, 2000) to evaluate  $\beta_{HL}$  and  $z_i^*$  as the followings:

- Step 1. Define the appropriate failure function.
- Step 2. Assume initial values of the design point  $x_i^*, i = 1, 2, \dots, n$ . Mean values of random variables may be used as the initial design point. Get the reduced variates  $z_i^* = (x_i^* - \mu_{X_i})/\sigma_{X_i}$ .
- Step 3. Compute  $(\partial g/\partial Z_i)$  and  $\alpha_i$  at  $z_i^*$
- Step 4. Calculate the new design point  $z_i^*$ , in terms of  $\beta_{HL}$ , as in Equation (6-14).
- Step 5. Substitute the new  $x_i^*$  in the failure function  $g(\mathbf{z}^*) = 0$  and solve for  $\beta_{HL}$ .
- Step 6. Recalculate  $z_i^*$  by using the  $\beta_{HL}$  value in Step 5 via  $z_i^* = -\alpha_i \beta_{HL}$ .
- Step 7. Repeat Step 3 through 6 until  $\beta_{HL}$  converges.

Some significant remarks can be drawn by comparing the MVFOSM and AFOSM proposed by Hasofer and Lind. The reliability indices MVFOSM does not use any information related to the distribution of random variables; on the other hand, AFOSM proposed by Hasofer and Lind is applicable when they are normally distributed. The most remarkable difference is that the design point is not on the failure surface in the MVFOSM method, while the design point is on the failure surface in the AFOSM (Hasofer-Lind) method.

### 6.1.1.3 First-Order Reliability Method

The shortcoming of the Hasofer-Lind method, which is applicable only for normally distributed variables, necessitates transformation of nonnormal variables into equivalent normal variables.

Rackwitz and Fiessler (1976, as cited in Haldar and Mahadevan, 2000) determined mean  $\mu_{X_i}^N$  and standard deviation  $\sigma_{X_i}^N$  of equivalent normal variable by considering that the cumulative probability as well as the probability density ordinate of the equivalent normal distribution are equal to those of the corresponding nonnormal distribution at the design point ( $\mathbf{x}^*$ ) on the failure surface.

Equating the CDFs and PDFs as indicated above at the failure point  $x_i^*$ , one gets

$$\Phi\left(\frac{x_i^* - \mu_{X_i}^N}{\sigma_{X_i}^N}\right) = F_{X_i}(x_i^*) \quad (6-16)$$

$$\frac{1}{\sigma_{X_i}^N} \phi\left(\frac{x_i^* - \mu_{X_i}^N}{\sigma_{X_i}^N}\right) = f_{X_i}(x_i^*) \quad (6-17)$$

where  $F_{X_i}(x_i^*)$  and  $f_{X_i}(x_i^*)$  are the original CDF and PDF of  $X_i$  evaluated at  $x_i^*$ ,  $\Phi(\cdot)$  and  $\phi(\cdot)$  are CDF and PDF of standard normal distribution.

First equality yields that  $\mu_{X_i}^N = x_i^* - \Phi^{-1}[F_{X_i}(x_i^*)]\sigma_{X_i}^N$  and it can be obtained from the second one together with first equality that  $\sigma_{X_i}^N = \phi\{\Phi^{-1}[F_{X_i}(x_i^*)]\}/f_{X_i}(x_i^*)$ .

Having obtained  $\mu_{X_i}^N$  and  $\sigma_{X_i}^N$ , the same algorithm described in previous section can be used as if all the random variables were normally distributed. Note that solving the failure function for  $\beta$ , as stated in Step 5 of the algorithm, may be difficult in case of complicated nonlinear failure function. In that case, Newton-Raphson method can be used to find  $\beta$ . This alternative Newton-Raphson type recursive algorithm is suggested by Rackwitz and Fiessler in 1978 (as cited in Haldar and Mahadevan, 2000).

### 6.1.2 Second-Order Reliability Method

Considering two different failure surfaces, one of which is linear and the other one is nonlinear, as illustrated in Figure 6-3, it is clear that the minimum distances from the origin of the axes to the failure surfaces are the same, namely their reliability indices calculated based on FORM method are identical, although their failure domains are different. However, failure probability of failure function with larger failure domain, which is linear one in this case, should be more than that of failure function with smaller failure domain. FORM method does not consider the curvature of nonlinear failure function. Hence, SORM method was developed to overcome this shortcoming.

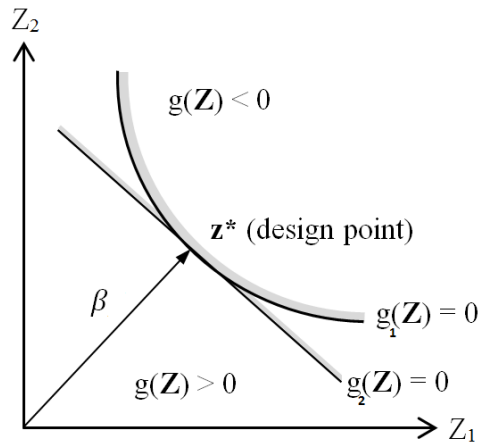


**Figure 6-3** Nonlinear and Linear Failure Functions

Breitung (1984) formed a simple closed-form solution for the probability calculation by a second-order approximation using the asymptotic approximation theory as the following:

$$p_{f_2} \approx \Phi(-\beta_{FORM}) \prod_{i=1}^{n-1} (1/\sqrt{1 + \beta_{FORM}\kappa_i}) \quad (6-18)$$

where  $\kappa_i$  is the principal curvature of the failure function at the design point. He showed that this second-order probability approximation asymptotically approaches the first-order approximation as  $\beta_{FORM} \rightarrow \infty$  with  $\beta_{FORM}\kappa_i$  is fixed.

To use the formula provided above, it is essential to compute the principal curvature  $\kappa_i$  of the failure function at the design point. To do so, first it is necessary to rotate equivalent normal random variables around origin so that the last variable coincides with the vector  $\alpha$ , the unit gradient vector of the failure function at the design point. A 2-dimensional example is illustrated in Figure 6-4, in which  $Y_i$  are equivalent normal variables and  $Y_i'$  are rotated variables. The transformation  $\mathbf{Y}$  into  $\mathbf{Y}'$  is an orthogonal transformation:  $\mathbf{Y}' = \mathbf{R}\mathbf{Y}$ .

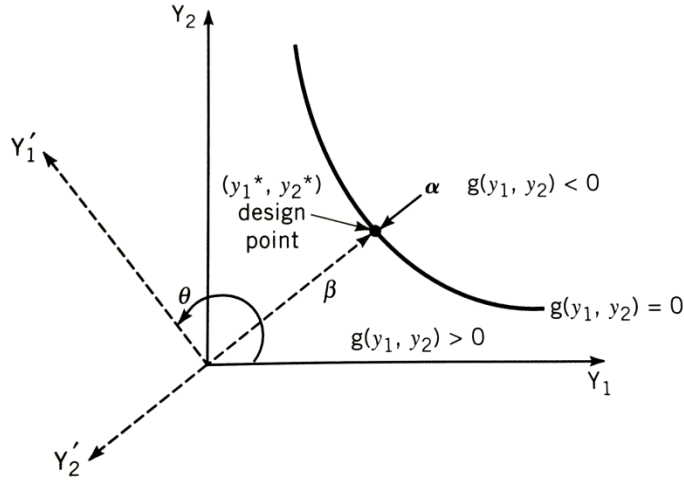


**Figure 6-4** Rotation of Coordinates (Haldar and Mahadevan, 2000)

Matrix  $\mathbf{R}$  can be constructed by first forming  $\mathbf{R}_0$  matrix and then applying Gram-Schmidt (G-S) orthogonalization procedure, which is not going to be detailed here, to this matrix.  $\mathbf{R}_0$  matrix is formed as follows:

$$\mathbf{R}_0 = \begin{bmatrix} 1 & 0 & \cdot & \cdot & \cdot & 0 \\ 0 & 1 & 0 & \cdot & \cdot & 0 \\ \alpha_1 & \alpha_2 & \cdot & \cdot & \cdot & \alpha_n \end{bmatrix} \quad (6-19)$$

After applying G-S method to  $\mathbf{R}_0$ , one can obtain matrix  $\mathbf{R}$ . Then a matrix  $\mathbf{A}$ , elements of which are denoted as  $a_{ij}$ , is evaluated as the following:

$$a_{ij} = \frac{(\mathbf{RDR}^t)_{ij}}{|\nabla G(\mathbf{y}^*)|}, \quad i = 1, 2, \dots, n-1 \quad (6-20)$$

In which  $\mathbf{D}$  is the  $n \times n$  2<sup>nd</sup> derivative matrix of the failure function in the standard normal space computed at the design point, and  $|\nabla G(\mathbf{y}^*)|$  is the length of gradient vector in the standard normal space. After obtaining matrix  $\mathbf{A}$ , the principal curvatures  $\kappa_i$  are eigenvalues of matrix  $\mathbf{A}$ . Now, formula given by Breitung (1984) can be used to compute second-order approximate of the probability of failure.

To compare FORM, a reliability index based on FORM can be calculated as the inverse cumulative standard normal distribution function of the probability of failure.

$$\beta_{SORM} = -\Phi^{-1}(p_{f_2}) \quad (6-20)$$

## 6.2 Failure Function

Failure function can be expressed as  $g = R - Q$ , in which  $R$  stands for flexural resistance capacity and  $Q$  stands for load effect. That  $g$  is less than zero means structure fails and the probability of failure can be defined as  $P_F = P(R - Q < 0) = P(g < 0)$ .

Load effect  $Q$  is expressed as the following:

$$Q = D_1 + D_2 + D_3 + D_4 + LL (1+IM) GDF \quad (6-21)$$

where  $D_1$ ,  $D_2$ ,  $D_3$  and  $D_4$  are dead load components,  $LL$  is live load,  $IM$  is dynamic load factor and  $GDF$  is girder distribution factor. These load components are explained in Chapter 3.

For the flexural resistance capacity  $R$ , please refer to Chapter 4. However, note that in Chapter 4, nominal resistance capacity is introduced. In failure function, resistance should be multiplied by professional factor,  $PF$ , which is also explained in Chapter 4.

## 6.3 Target Reliability Index

After obtaining a database and deciding methodology to determine reliability index, the next step is to choose a target reliability index,  $\beta_T$  for the load and factor calibration. The reliability level that is guaranteed is selected as a goal for the components. The purpose in the calibration of load and resistance factors is to satisfy uniform reliability indices so that calculated  $\beta$  will be as close as possible to that  $\beta_T$ . Therefore, the advantage of the calibrated LRFD format from a reliability viewpoint is uniform reliability indices over different spans, and load effects (Moses, 2001).

Optimum reliability can be determined by minimizing total expected cost. The total cost involves the cost of design and construction, and the expected cost of failure. The cost of failure includes not only the cost of replacement or repair but also the cost of shortage of use, and legal costs (liability in case of injuries). Due to economic concerns, it is reasonable to consider primary and secondary components separately in bridges because the consequences of failure of these components are different. Target reliability index for secondary components is lower than that for primary components. A main structural element, failure of which results in the collapse of the whole structure, is a primary component. Girders are the primary components in case of bridges (Nowak and Szerszen, 2000).

In calibration of AASHTO LRFD (Nowak, 1999), target reliability index was chosen based on reliability level of existing structures, which were selected from different regions of the United States. It was determined as 3.5.

Adopting a target reliability index is out of scope of this study. Therefore, an imaginary target reliability index, which is 4.00, is selected for this study.

#### 6.4 Load and Resistance Factors

In design, different sets of load and resistance factors are tried in order to achieve predefined target reliability index. It is obvious that using higher load factor and lower resistance factors results in safer design. To see change in reliability index, three different resistance factors, which are 0.90, 0.95 and 1.00, and 5 different live load factors, which are 1.50, 1.75, 2.00, 2.25 and 2.50, are used. That makes a total 15 different sets of load and resistance factor combination. After designs are utilized based on these different sets of load and resistance factors, reliability analysis is conducted for each. Different methods are used in reliability analysis as indicated before. Minimums of values given by these methods are accepted as reliability indices. In Table 6-2 to Table 6-5, reliability indices obtained for different span lengths are listed for different set of load and resistance factors and these are plotted in Figure 6-5 to Figure 6-8.

**Table 6-2** Reliability Indices for Different Sets of Load and Resistance Factors (HL93) (Based on the Statistics of Live Load from Overall Case)

Live Load (LL) and Resistance (R) Factors	Span Length (m)				Average $\beta$
	50	60	70	80	
LL: 1.50; R: 0.90	2.83	2.91	2.89	2.90	2.88
LL: 1.50; R: 0.95	2.58	2.65	2.63	2.62	2.62
LL: 1.50; R: 1.00	2.35	2.39	2.45	2.34	2.38
LL: 1.75; R: 0.90	3.12	3.19	3.15	3.17	3.16
LL: 1.75; R: 0.95	2.88	2.94	2.90	2.89	2.91
LL: 1.75; R: 1.00	2.64	2.70	2.66	2.63	2.66
LL: 2.00; R: 0.90	3.39	3.45	3.39	3.42	3.41
LL: 2.00; R: 0.95	3.17	3.22	3.15	3.15	3.17
LL: 2.00; R: 1.00	2.92	2.97	2.91	2.89	2.92
LL: 2.25; R: 0.90	3.64	3.69	3.62	3.65	3.65
LL: 2.25; R: 0.95	3.41	3.45	3.38	3.38	3.41
LL: 2.25; R: 1.00	3.19	3.22	3.15	3.13	3.17
LL: 2.50; R: 0.90	3.86	3.85	3.83	3.86	3.85
LL: 2.50; R: 0.95	3.64	3.68	3.60	3.60	3.63
LL: 2.50; R: 1.00	3.44	3.46	3.37	3.35	3.40

**Table 6-3** Reliability Indices for Different Sets of Load and Resistance Factors (HL93) (Based on the Statistics of Live Load from Extreme Case)

Live Load (LL) and Resistance (R) Factors	Span Length (m)				Average $\beta$
	50	60	70	80	
LL: 1.50; R: 0.90	3.43	3.41	3.43	3.36	3.40
LL: 1.50; R: 0.95	3.11	3.09	3.10	3.02	3.08
LL: 1.50; R: 1.00	2.80	2.77	2.77	2.70	2.76
LL: 1.75; R: 0.90	3.80	3.75	3.75	3.68	3.75
LL: 1.75; R: 0.95	3.49	3.45	3.44	3.35	3.43
LL: 1.75; R: 1.00	3.20	3.15	3.14	3.03	3.13
LL: 2.00; R: 0.90	4.14	4.06	4.05	3.97	4.06
LL: 2.00; R: 0.95	3.87	3.78	3.75	3.65	3.76
LL: 2.00; R: 1.00	3.55	3.49	3.45	3.34	3.46
LL: 2.25; R: 0.90	4.45	4.34	4.33	4.23	4.34
LL: 2.25; R: 0.95	4.16	4.06	4.03	3.93	4.05
LL: 2.25; R: 1.00	3.89	3.79	3.75	3.63	3.76
LL: 2.50; R: 0.90	4.71	4.70	4.58	4.47	4.62
LL: 2.50; R: 0.95	4.45	4.33	4.30	4.18	4.31
LL: 2.50; R: 1.00	4.20	4.07	4.02	3.89	4.05

**Table 6-4** Reliability Indices for Different Sets of Load and Resistance Factors (AYK45) (Based on the Statistics of Live Load from Overall Case)

Live Load (LL) and Resistance (R) Factors	Span Length (m)				Average $\beta$
	50	60	70	80	
LL: 1.50; R: 0.90	3.85	3.91	3.86	3.88	3.88
LL: 1.50; R: 0.95	3.61	3.66	3.61	3.60	3.62
LL: 1.50; R: 1.00	3.38	3.41	3.36	3.32	3.37
LL: 1.75; R: 0.90	4.18	4.23	4.16	4.18	4.19
LL: 1.75; R: 0.95	3.95	4.00	3.91	3.91	3.94
LL: 1.75; R: 1.00	3.73	3.75	3.67	3.64	3.70
LL: 2.00; R: 0.90	4.48	4.46	4.44	4.46	4.46
LL: 2.00; R: 0.95	4.25	4.29	4.20	4.20	4.23
LL: 2.00; R: 1.00	4.03	4.06	3.96	3.93	4.00
LL: 2.25; R: 0.90	4.75	4.72	4.71	4.72	4.73
LL: 2.25; R: 0.95	4.54	4.49	4.47	4.46	4.49
LL: 2.25; R: 1.00	4.32	4.33	4.22	4.20	4.27
LL: 2.50; R: 0.90	5.00	4.97	4.95	4.96	4.97
LL: 2.50; R: 0.95	4.79	4.72	4.70	4.70	4.73
LL: 2.50; R: 1.00	4.57	4.53	4.48	4.46	4.51

**Table 6-5** Reliability Indices for Different Sets of Load and Resistance Factors  
(AYK45) (Based on the Statistics of Live Load from Extreme Case)

Live Load (LL) and Resistance (R) Factors	Span Length (m)				Average $\beta$
	50	60	70	80	
LL: 1.50; R: 0.90	4.53	4.41	4.40	4.29	4.41
LL: 1.50; R: 0.95	4.31	4.14	4.11	3.99	4.14
LL: 1.50; R: 1.00	4.02	3.86	3.83	3.69	3.85
LL: 1.75; R: 0.90	4.89	4.74	4.74	4.60	4.74
LL: 1.75; R: 0.95	4.63	4.49	4.46	4.32	4.48
LL: 1.75; R: 1.00	4.39	4.23	4.19	4.03	4.21
LL: 2.00; R: 0.90	5.20	5.20	5.03	4.89	5.08
LL: 2.00; R: 0.95	4.97	4.80	4.77	4.62	4.79
LL: 2.00; R: 1.00	4.73	4.56	4.51	4.34	4.54
LL: 2.25; R: 0.90	5.47	5.48	5.30	5.14	5.35
LL: 2.25; R: 0.95	5.26	5.24	5.05	4.88	5.11
LL: 2.25; R: 1.00	5.03	4.84	4.80	4.62	4.82
LL: 2.50; R: 0.90	5.71	5.73	5.54	5.37	5.59
LL: 2.50; R: 0.95	5.51	5.50	5.30	5.12	5.36
LL: 2.50; R: 1.00	5.30	5.27	5.06	4.88	5.13

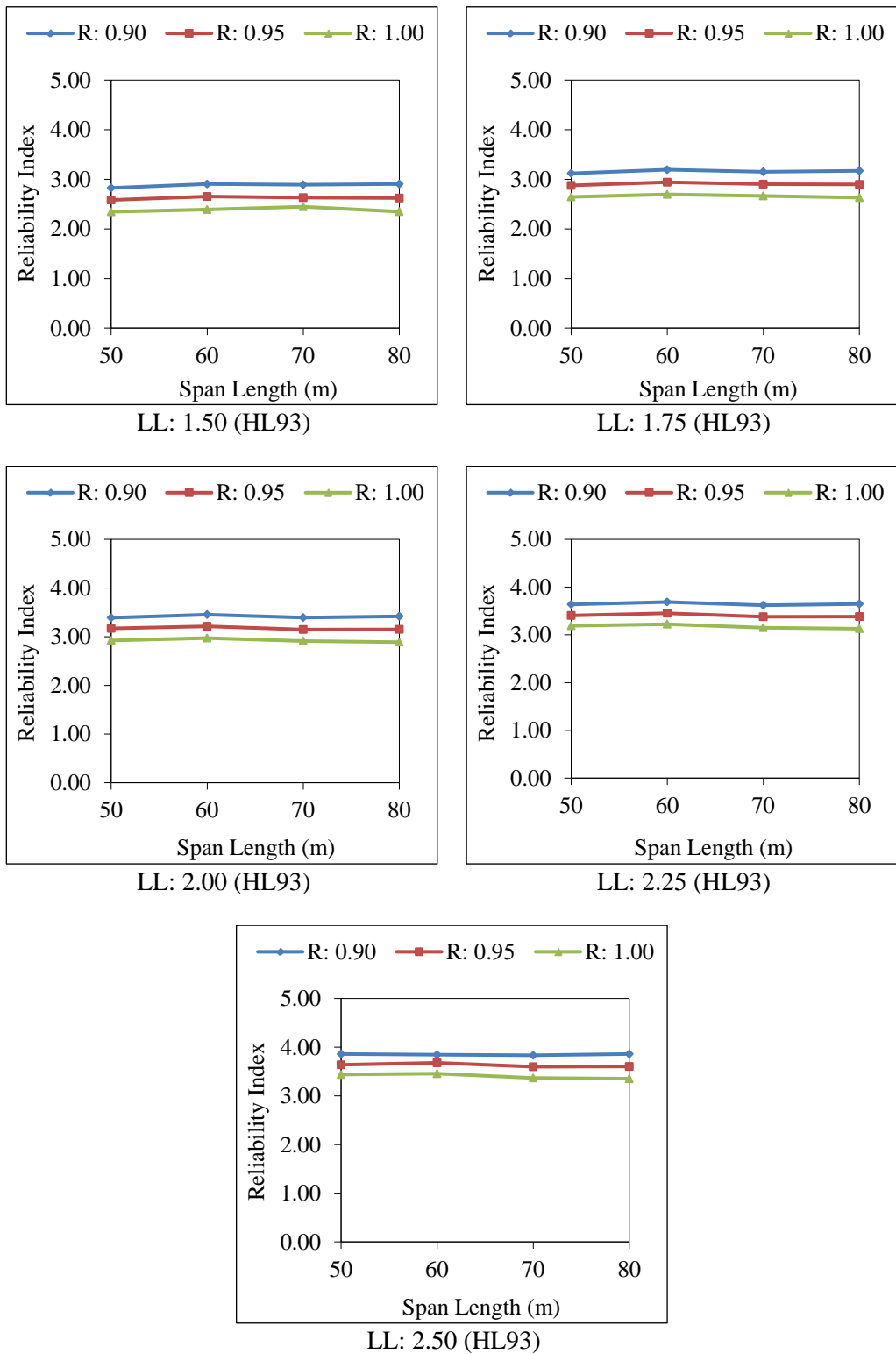
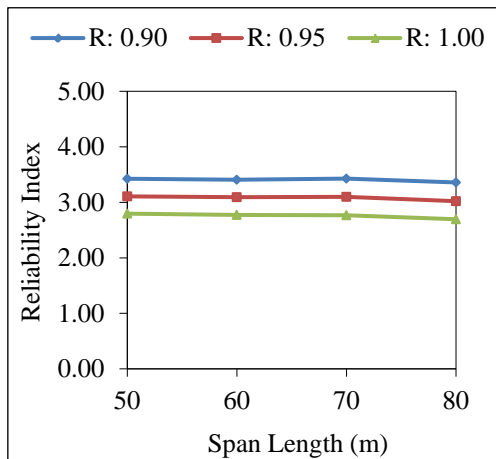
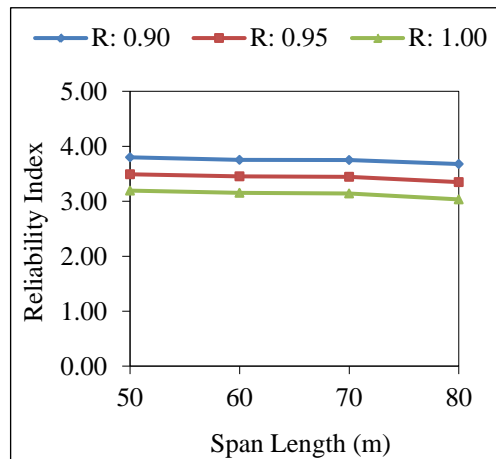


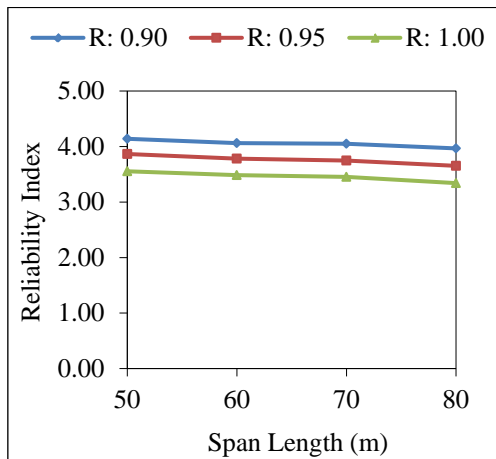
**Figure 6-5** Reliability Indices for Different Sets of Load and Resistance Factors (HL93) (Based on Statistics of Live Load from Overall Case)



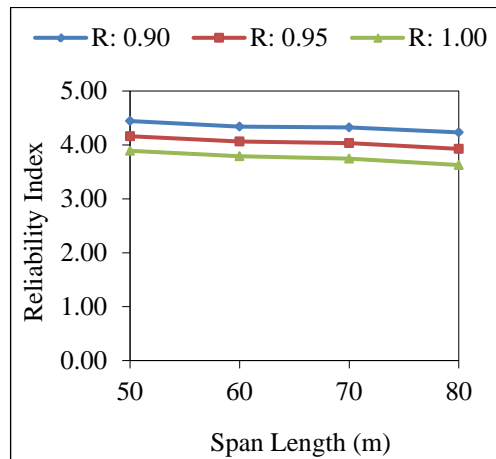
LL: 1.50 (HL93)



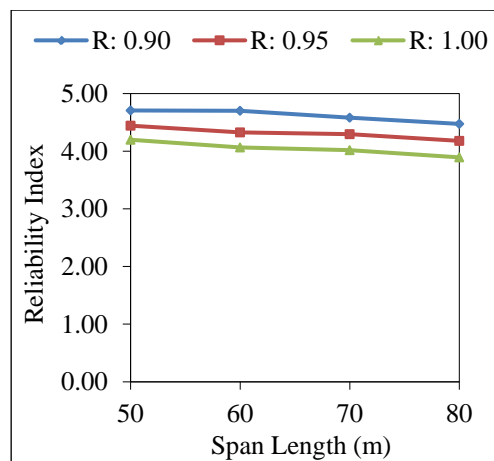
LL: 1.75 (HL93)



LL: 2.00 (HL93)

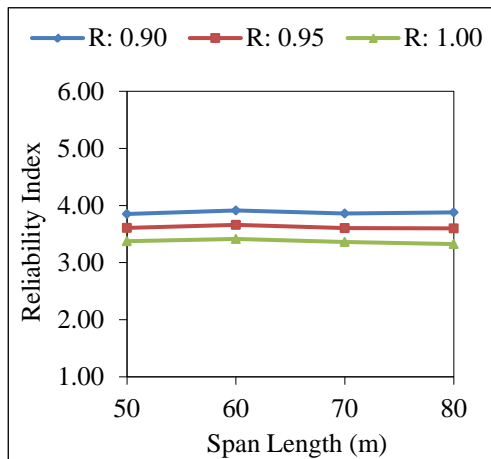


LL: 2.25 (HL93)

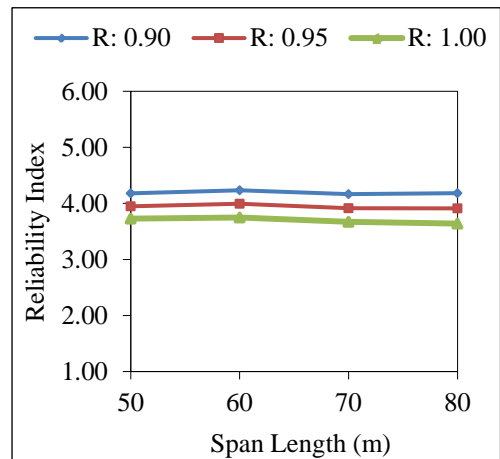


LL: 2.50 (HL93)

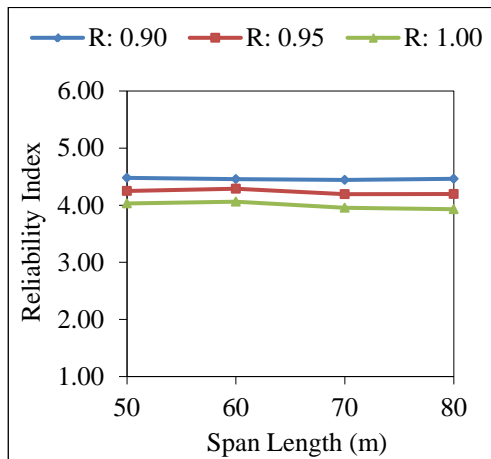
**Figure 6-6** Reliability Indices for Different Sets of Load and Resistance Factors (HL93) (Based on Statistics of Live Load from Extreme Case)



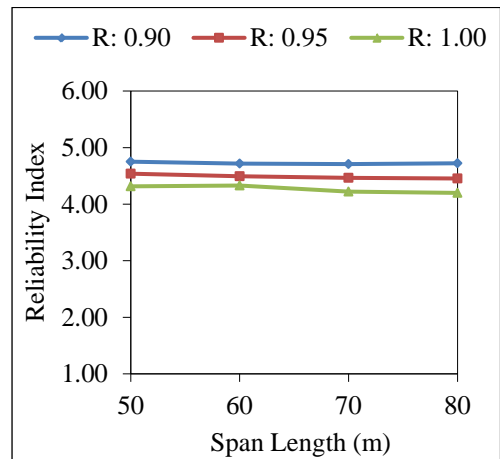
LL: 1.50 (AYK45)



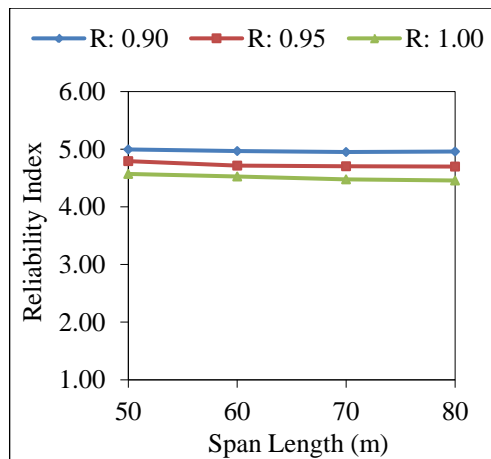
LL: 1.75 (AYK45)



LL: 2.00 (AYK45)

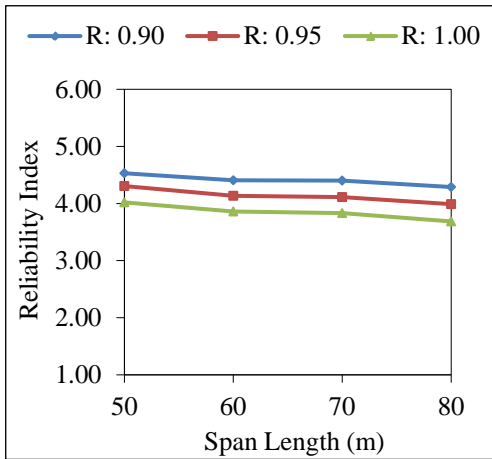


LL: 2.25 (AYK45)

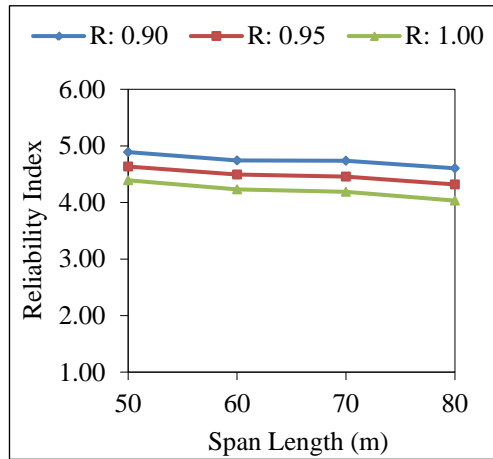


LL: 2.50 (AYK45)

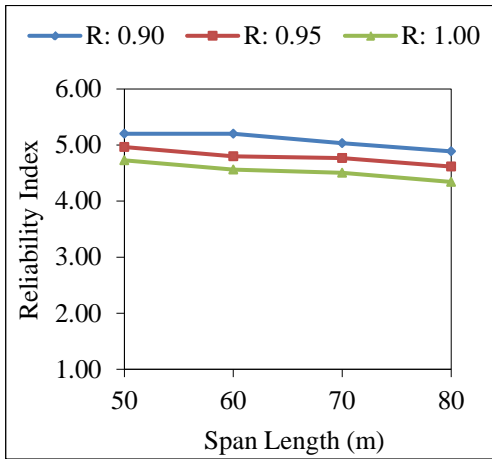
**Figure 6-7** Reliability Indices for Different Sets of Load and Resistance Factors (AYK45) (Based on Statistics of Live Load from Overall Case)



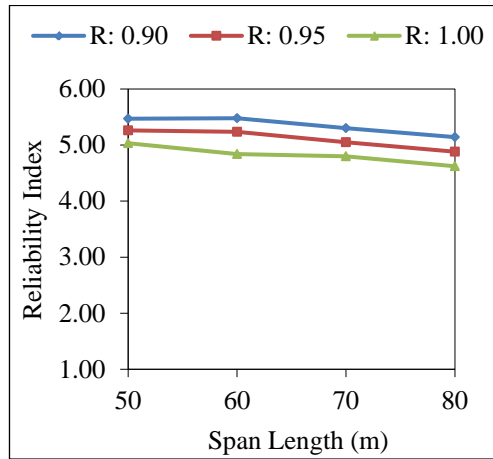
LL: 1.50 (AYK45)



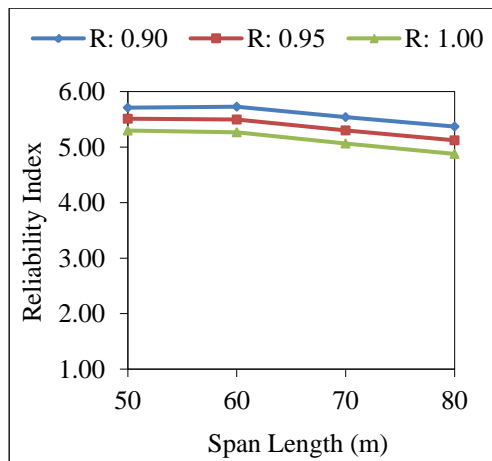
LL: 1.75 (AYK45)



LL: 2.00 (AYK45)



LL: 2.25 (AYK45)



LL: 2.50 (AYK45)

**Figure 6-8** Reliability Indices for Different Sets of Load and Resistance Factors (AYK45) (Based on Statistics of Live Load from Extreme Case)

The results indicate that reliability indices computed using live load’s statistical parameters obtained from “overall case” are less than those computed live load’s using statistical parameters obtained from “extreme case”. The difference is approximately 12% for AYK45 and 15% for HL93.

According reliability analyses based on statistics obtained from “extreme case”, target reliability index is achieved by either “LL: 2.00” and “R: 0.90” or “LL: 2.25” and “R: 0.95” or “LL: 2.50” and “R: 1.00” for HL93 loading; and “LL: 1.75” and “R: 1.00” for AYK45 loading.

When reliability analyses are utilized by using statistics determined from “overall case”, it is seen that target reliability index is not achieved by trial set of load and resistance factors for HL93 loading. Therefore, a higher live load factor or a less resistance factor should be used in order to satisfy target reliability index. Whereas, target reliability index is achieved by “LL: 1.75” and “R: 0.90” for AYK45 loading.

### 6.5 Comparison of Results of Different Reliability Analysis Methods

In order to see differences of reliability indices obtained from different analysis methods, reliability indices of girders designed for HL93 with live load factor of 1.50 and resistance factor of 0.90 are tabulated in Table 6-6 and plotted in Figure 6-9, as an example.

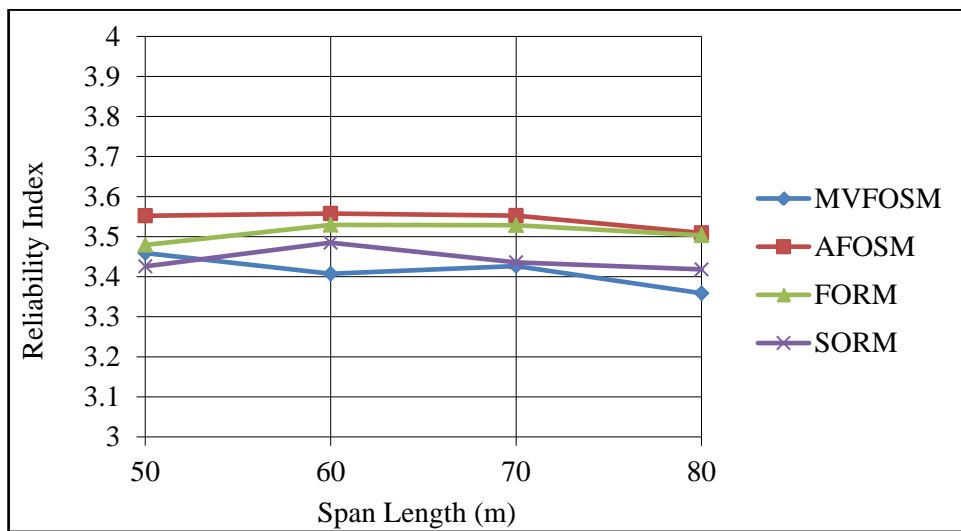


**Figure 6-9** Comparison of Results of Different Reliability Analysis Methods (HL93; R: 0.90, LL: 1.50) (Based on Extreme Case)

**Table 6-6** Comparison of Results of Different Reliability Analysis Methods (HL93; R: 0.90, LL: 1.50) (Based on Extreme Case)

Span (m)	MVFOSM	AFOSM	FORM	SORM
50	3.46	3.55	3.48	3.43
60	3.41	3.56	3.53	3.49
70	3.43	3.55	3.53	3.44
80	3.36	3.51	3.50	3.42

Comparison is also made based on ratios of results obtained from one method to another one and shown in Figure 6-10. Note that a perfect match between the two methods is indicated by a 100 percent value.

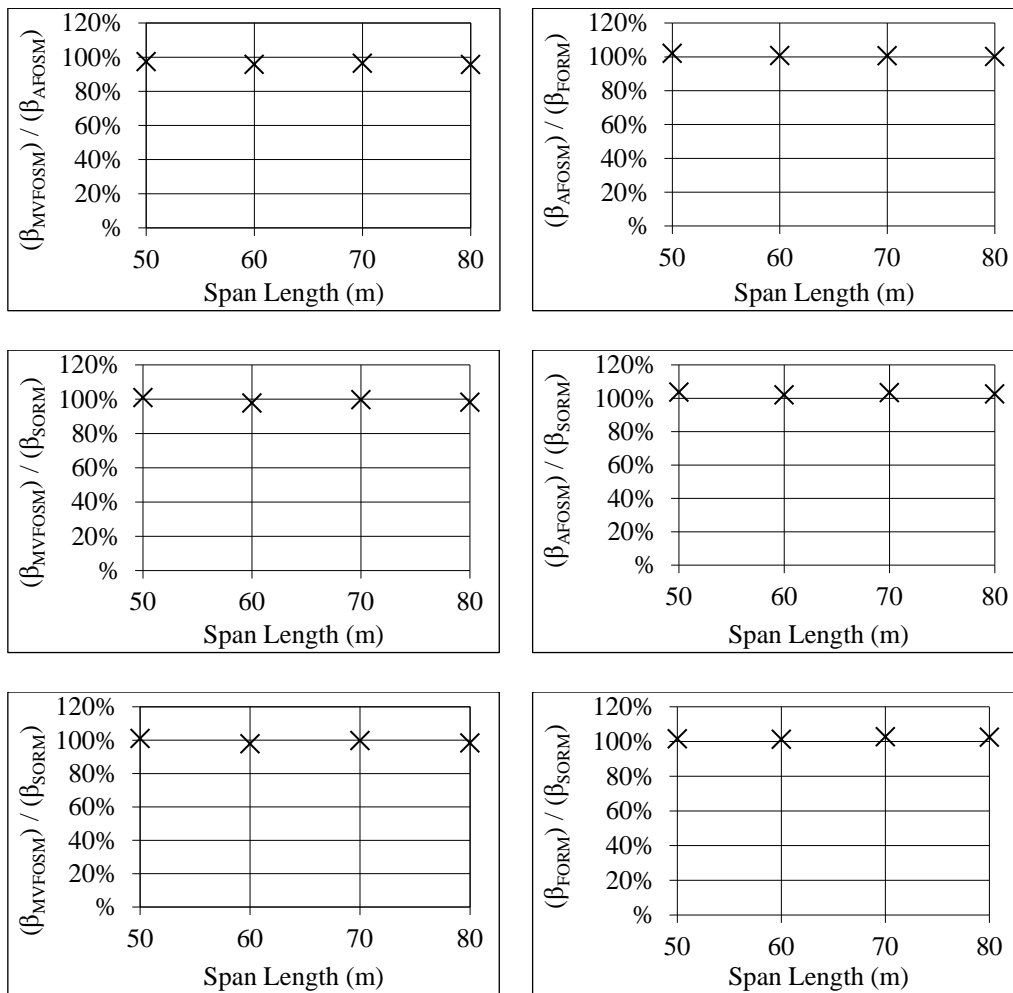


**Figure 6-10** Comparison of Results of Different Reliability Analysis Methods (HL93; R: 0.90, LL: 1.50) (Based on Extreme Case)

Results indicate that reliability indices obtained from different analysis methods are not different much. As stated before, minimums of values given by these methods are used.

### 6.6 Change in Reliability Indices with respect to Total Steel Weight

It is clearly visible that increasing load factor and decreasing resistance factor result in a higher reliability index together with heavier girder weight. Therefore, it is useful to see how much increasing reliability index affects the total weight of steel used, which directly relates to expected construction cost. In this way, it can be concluded that higher reliability index may be chosen as a target provided that higher reliability index is obtained by little increase in total weight of steel. In Figure 6-11 to Figure 6-14, change in reliability indices with respect to total weight of steel is shown for HL93 and AYK, respectively.

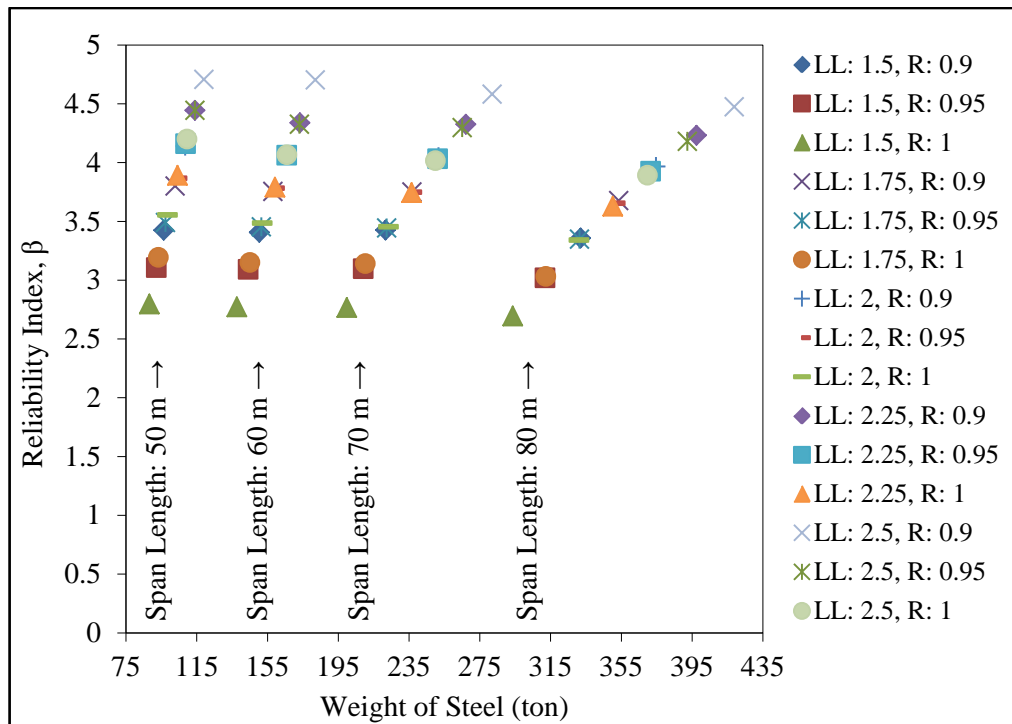


**Figure 6-11** Change in Reliability Indices with Respect to Total Steel Weight (HL93) (Extreme Case)

For example, reliability index of 70 m long girder designed with LL: 2.00 and R: 0.9 for HL93 is about 4.00 and total weight of steel used is 251.7 tons. If reliability index of 4.50 is wanted to be achieved, LL: 2.50 and R: 0.9 may be used, which results in

total weight of steel of about 282 tons. Namely, increasing reliability index of 4.00 to 4.50 brings about an increase of 12% in total weight of steel used.

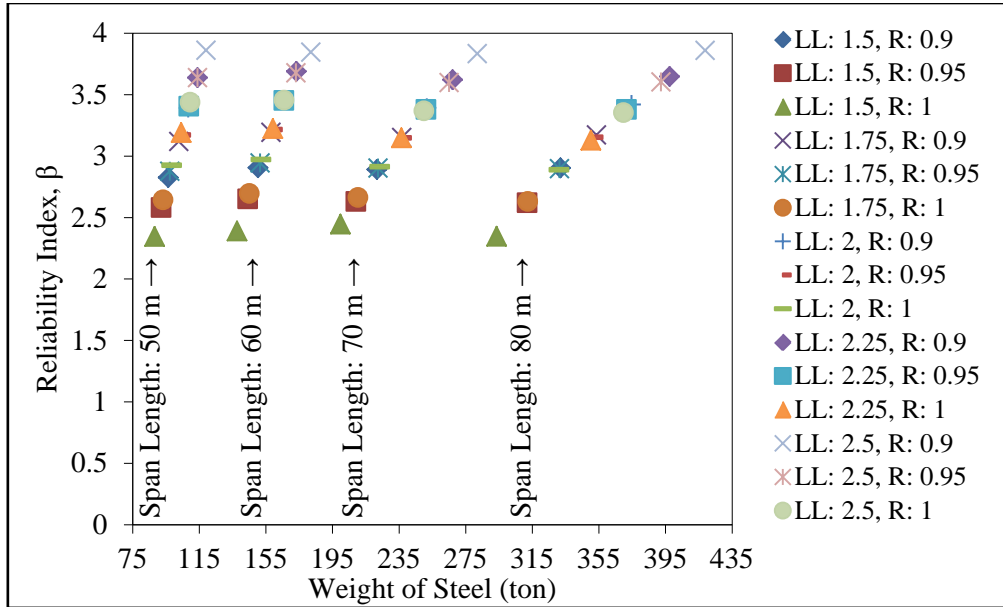


**Figure 6-12** Change in Reliability Indices with Respect to Total Steel Weight (HL93) (Overall Case)

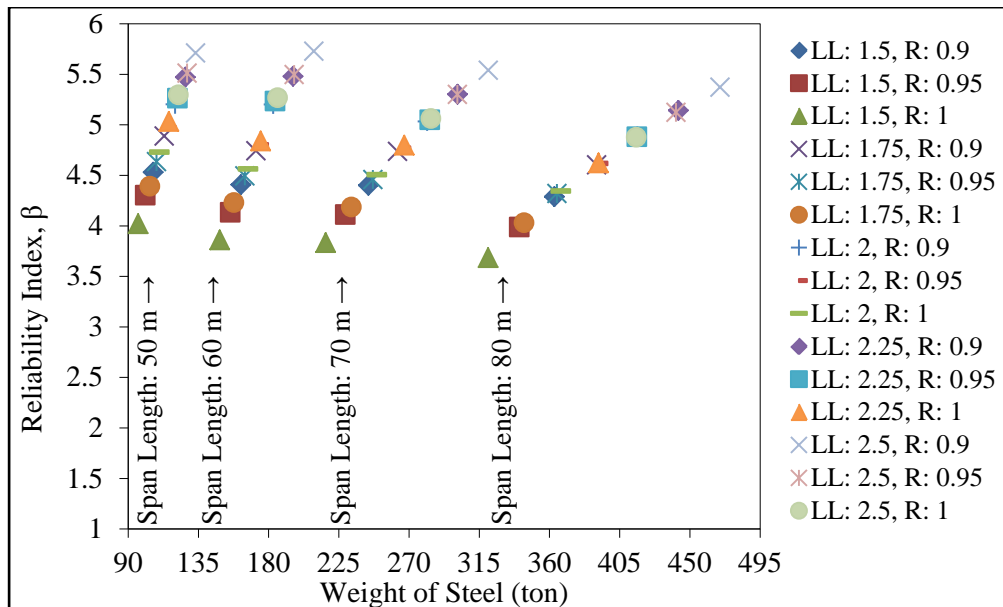


**Figure 6-13** Change in Reliability Indices with Respect to Total Steel Weight (AYK45) (Extreme Case)

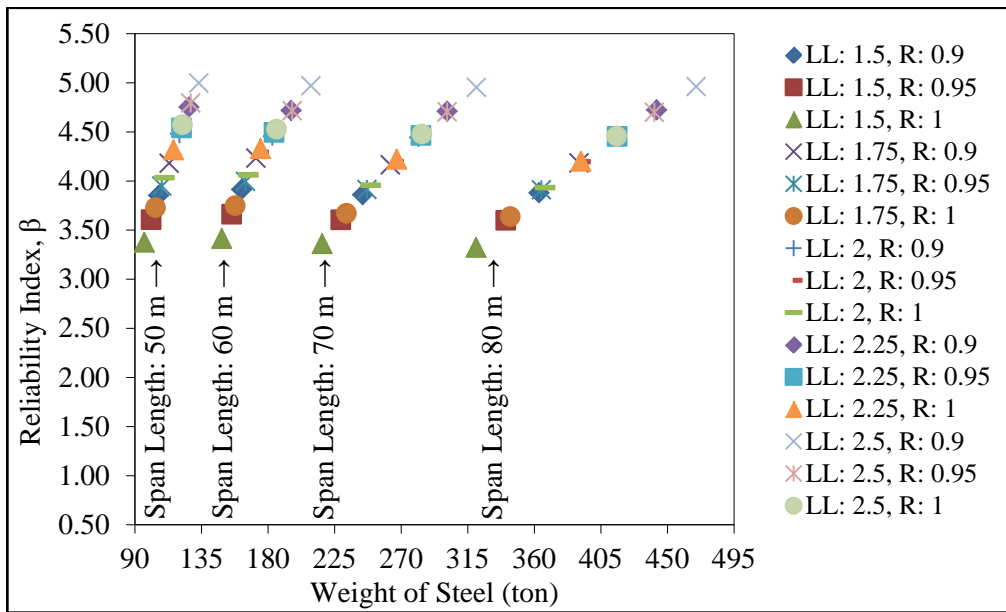


**Figure 6-14** Change in Reliability Indices with Respect to Total Steel Weight (AYK45) (Overall Case)



## CHAPTER 7

### CONCLUSION

#### 7.1 Summary and Concluding Comments

In Turkey, design method of highway bridges tends to shift to LRFD concept from LFD. For this reason, General Directorate of Highways of Turkey has decided to use a modified version of AASHTO LRFD. Therefore, load and resistance factors are calibrated based on conditions in Turkey. In addition, a new live load model is proposed.

A total of 120 simply supported composite steel plate girders are flexurally designed based on different resistance and live load factors as well as live load models, namely AYK45 and HL93. In design of steel girders, requirements of AASHTO LRFD are used except for load and resistance factors. Live load factors are chosen as 1.50, 1.75, 2.00, 2.25, and 2.50. Resistance factors are selected as 0.90, 0.95, and 1.00. Dead load factors are fixed at 1.25 for structural and nonstructural elements and 1.50 for asphalt. In this way, girders are designed for a total of 15 sets of load and resistance factors. The bridge span lengths vary from 50 m to 80 m with an increment of 10 m. Designs are utilized by using a macro-based Microsoft Excel spreadsheet, which is developed specifically for this study.

For the reliability analyses of designed girders, statistical parameters regarding load and resistance are quantified in terms of bias factor, coefficient of variation and type of probability distribution. For that purpose, available local data supplemented by information compiled from relevant international literature are used. For instance, statistical parameters regarding dead loads are decided based on Nowak's (1999) study. Nowak classifies dead load into four different components due to their different degrees of variation.

It seems that current live load model used in Turkey is not appropriate for span lengths more than about 50 meters. Therefore, a new live load model, which is called AYK45, is proposed to be used in Turkey. This live load model contains truck load combined with a lane load. It is very similar to live load model of AASHTO LRFD but heavier than that. In order to determine statistical parameters belonging to live load, a truck survey data conducted in different highway branches in Turkey in years between 2005 and 2006 is used. This survey data is as same as the survey data used in the study of Argınhan (2010). Argınhan had evaluated statistical parameters regarding HL93 for Turkey. Three cases are considered for extrapolation purposes, namely overall, upper

tail and extreme cases. In previous studies of different researchers, extreme case was used to determine statistical parameters. However, in this study, in addition to statistical parameters obtained from extreme case, those obtained from overall case are also taken into consideration due the fact that coefficient of variation obtained from overall case is higher, which reduces reliability indices.

After obtaining statistical parameters regarding load and resistance components, reliability indices for each design case are computed by different methods, namely mean value first – order second moment method, advanced first – order second moment method, first – order reliability method and second – order reliability method. Minimum reliability index of calculated ones is set as reliability index of corresponding set of load and resistance factors.

In the USA, reliability index of 3.50 was targeted in calibration of load and resistance factors. However, in Turkey, a reliability index of 4.00 was targeted. As illustrated in Figure 7-1, in case statistical parameters obtained from “extreme case” for live load, based on designed bridge girders, where AYK45 live load model is used, reliability index of 4.00 is obtained by using resistance and live load factors as “R: 1.00” and “LL: 1.75”, respectively. Whereas, in case of HL93 live load model, reliability index of 4.00 is obtained by using resistance and live load factors as either “R: 0.90” and “LL: 2.00” or “R: 1.00” and “LL: 2.50”. It is understandable that the same level of reliability is obtained by less amount of live load factor for AYK45 because it is heavier than HL93.

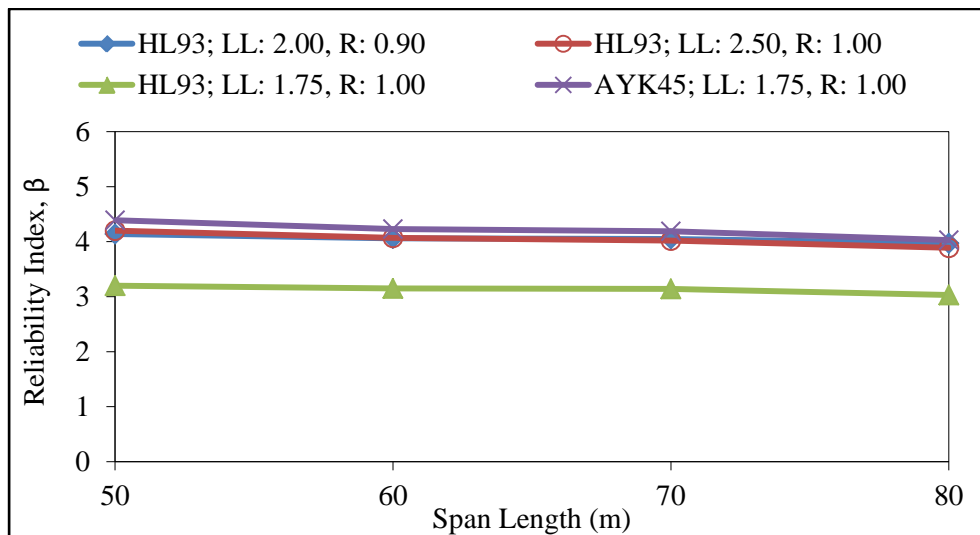


**Figure 7-1** Set of Load and Resistance Factors Considered and Corresponding Reliability Indices (Based on Statistical Parameters Obtained from Extreme Case for Live Load)

In case statistical parameters obtained from overall case for live load, it is seen that target reliability index is not satisfied by trial sets of load and resistance factors for HL93 loading. Therefore, a higher live load factor or a less resistance factor should be used in order to achieve target reliability index. In this case, target reliability index of 4.00 is achieved by “LL: 1.75” and “R: 0.90” for AYK45 loading.

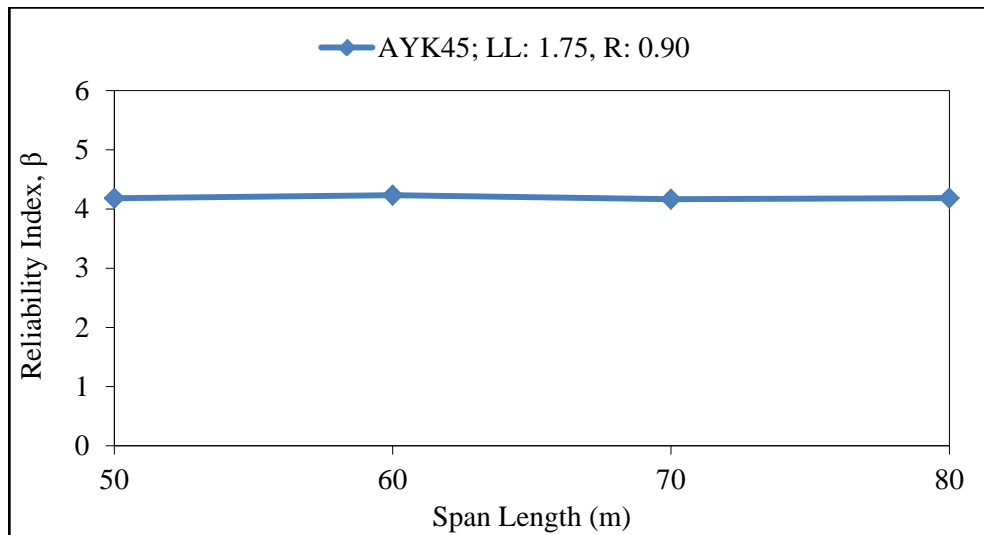


**Figure 7-2** Load and Resistance Factor Considered and Corresponding Reliability Index (Based on Statistical Parameters Obtained from Overall Case for Live Load)

It is seen that in design of steel plate girder bridges HL93 loading with live load and resistance factors of 1.75 and 1.00, respectively does not provide a safe design considering conditions in Turkey in case of target reliability index of 4.00. Hence, if HL93 live load model is wanted to be used in design of steel plate girder bridges in Turkey, either live load factor which is higher than 1.75 or resistance factor which is less than 1.00 should be selected so that target reliability index is achieved.

Whereas, the new proposed live load model, AYK45 with live load and resistance factors of 1.75 and 1.00, respectively satisfies the targeted reliability level based on live load’s statistical parameters obtained from extreme case (Figure 7-1). In case of using statistical parameters obtained from overall case, AYK45 loading satisfies the target reliability index when live load and resistance factors of 1.75 and 0.90, respectively are used (Figure 7-2). Therefore, it can be concluded that AYK45 loading is safe enough when live load factor of 1.75 is used. However, resistance factor should be decided. Based on different extrapolation approaches used in obtaining statistical parameters regarding live load, namely “overall case” and “extreme case”, resistance factors of 0.90 and 1.00, respectively should be used together with live load factor of

1.75. However, using resistance factor of 0.90, instead of 1.00, will result in an increase of about 10% in total weight of steel used as illustrated in Figure 7-3. So the higher authority should make the final decision.

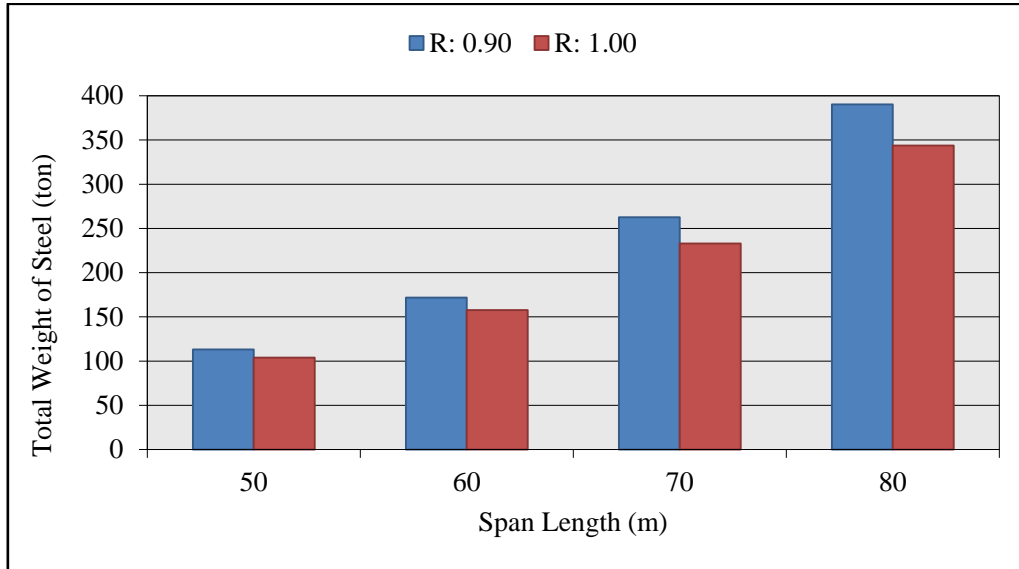


**Figure 7-3** Total Weight of Steel Used in Design of Bridge (AYK45, LL: 1.75)

## 7.2 Recommendations for Future Studies

The study conducted in here needs to be extended to other kinds of bridge types, namely reinforced concrete bridges, post-tensioned concrete bridges, suspension bridges, cable-stayed bridges, arch bridges and other types of girder bridges. Moreover, other kinds of failure modes such as axial tensile, axial compression, eccentric compression, negative flexure and shear need to be considered.

In addition, more reliable survey data should be used. As indicated, truck survey used in this study lacks of data regarding axle spacing of trucks, which is essential to compute moment effects. Although this issue was overcome by estimating the amount of axle spacing based on truck catalog search, exact values of axle spacing data, which is obtained from survey, would be more appropriate. Therefore, measuring the axle spacing in surveys should be seriously considered. Moreover, statistical parameters regarding yield strength of steel are obtained from international literature in this study. In future studies, obtaining local data is essential and more acceptable.

Source of load is another issue that must be taken into account. In this study, only live load is considered. However, wind load, temperature load, earthquake load and other types of loads also need to be considered for different limit states.

Besides girders, other components of bridges such as bracings, joints, piers, pier caps, abutments, foundations, piles may be taken into consideration.



## REFERENCES

- Altay, G., & Güneyisi, E. M. (2008). Türkiye'de Yapısal Çelik Sektörü ve Yeni Gelişimler.
- American Association of State Highway and Transportation Officials. (2007). *AASHTO LRFD Bridge Design Specifications*. Washington, DC.
- American Association of State Highway and Transportation Officials. (2010). *AASHTO LRFD Bridge Design Specifications*. Washington, DC.
- Ang, A. H.-S., & Tang, W. H. (1984). *Probability Concepts in Engineering Planning and Design, Vol. 2: Decision, Risk, and Reliability*. John Wiley & Sons Inc.
- Argınhan, O. (2010). *Reliability Based Safety Level Evaluation of Turkish Type Precast Prestressed Concrete Bridge Girders Designed in Accordance with the Load and Resistance Factor Design Method, M.Sc. Thesis*. Ankara: The Graduate School of Natural and Applied Sciences, METU.
- Barker, R. M., & Puckett, J. A. (2007). *Design of Highway Bridges: an LRFD Approach*. Hoboken, New Jersey: John Wiley & Sons, Inc.
- Breitung, K. (1984). Asymptotic Approximations for Multinormal Integrals. *Journal of Engineering Mechanics*, Vol.110: 357-366.
- Castillo, E. (1988). *Extreme Value Theory in Engineering*. Academic Press Inc.
- Ellingwood, B., Galambos, T. V., MacGregor, J. G., & Cornell, C. A. (1980). *Development of a Probability Based Load Criterion for American National Standard A58*. NPS Special Publication 577.
- Ersoy, U. (1999). *Reinforced Concrete*. Ankara: METU.
- European Ready Mixed Concrete Organization. (July 2013). *Ready-Mixed Concrete Industry Statistics: Year 2012*.
- Fırat, F. K. (2006). Türkiye'de Kullanılan Betonun Kalitesinin İstatistiksel Olarak İncelenmesi. *Yedinci Uluslararası İnşaat Mühendisliğinde Gelişmeler Kongresi, 11-13 Ekim 2006*. İstanbul: Yıldız Teknik Üniversitesi.

Fırat, F. K. (2007). *Development of Load and Resistance Factors for Reinforced Concrete Structures in Turkey, Phd. Thesis* . Ankara: The Graduate School of Natural and Applied Sciences, METU.

Güreş, H. Y. (2013). Çelik Yapı Sektörü 2012 Değerlendirmesi ile 2013 Beklentileri ve Hedefleri.

Haldar, A., & Mahadevan, S. (2000). *Probability, Reliability and Statistical Methods in Engineering Design*. John Wiley & Sons, Inc.

Hwang, E.-S., & Nowak, A. S. (1991). Simulation of Dynamic Load for Bridges. *Journal of Structural Engineering*, Vol.117, No.5: 1413-1434.

Kesler, C. (1966). Strength. In *Significance of Tests and Properties of Concrete and Concrete-Making Materials, ASTM STP 169A* (pp. 144-159). West Conshohocken, PA: ASTM International.

Kulicki, J. M., Prucz, Z., Clancy, C. M., Mertz, D. R., & Nowak, A. S. (2007). *Updating the Calibration Report for AASHTO LRFD Code: Final Report*. NCHRP 20-07/186, Transportation Research Board.

Kun, L., & Qilin, Z. (2012). Research for Calibration and Resistant Factors of LRFD Design of Steel Bridge in China. *Journal of Performance of Constructed Facilities*, Vol. 26, No.2: 212-219.

Kwon, O.-S., Kim, E., & Orton, S. (2011). Calibration of Live-Load Factor in LRFD Bridge Design Specifications Based on State-Specific Traffic Environments. *Journal of Bridge Engineering*, Vol. 16, No.6: 812-819.

Li, G. Q., & Li, J. J. (2007). *Advance Analysis and Design of Steel Frames*. John Wiley & Sons, Ltd.

Moses, F. (2001). *NCHRP Report 454: Calibration of Load Factors for LRFR Bridge Evaluation*. Washington, DC: National Academy Press.

Nassif, H. H., & Nowak, A. S. (1995). Dynamic Effect of Truck Loads on Girder Bridges. *Road Transport Technology - 4* (pp. 383-387). Ann Arbor: University of Michigan Transportation Research Institute.

Nowak, A. S. (1999). *NCHRP Report 368: Calibration of LRFD Bridge Design Code*. Washington, DC: National Academy Press.

Nowak, A. S., & Hong, Y.-K. (1991). Bridge Live-Load Models. *Journal of Structural Engineering*, Vol.117, No.9: 2757-2767.

Nowak, A. S., & Szerszen, M. M. (2000). Structural Reliability as Applied to Highway Bridges. *Prog. Struct. Engng Mater.*, 2:218-224.

Nowak, A. S., Kim, S., & Szerszen, M. M. (1999). Dynamic Loads for Steel Girder Bridges. *17th International Modal Analysis Conference*, (pp. 731-737).

Nowak, A. S., Park, C.-H., & Casas, J. R. (2001). Reliability Analysis of Prestressed Concrete Bridge Girders: Comparison of Eurocode, Spanish Norma IAP and AASHTO LRFD. *Structural Safety*, 23: 331-344.

Phuvoravan, K. (2006). Load Distribution Factor Equation for Steel Girder Bridges in LRFD Design. *Symposium on Infrastructure Development and the Environment*. Diliman, Quezon City, Philippines: University of the Philippines.

T.C. Bayındırlık Bakanlığı, Karayolları Genel Müdürlüğü. (1982). *Yol Köprüleri için Teknik Şartname*. Ankara: Karayolları Genel Müdürlüğü Matbaası.

Thoft-Christensen, P., & Baker, J. (1982). *Structural Reliability Theory and Its Applications*. Springer Verlag.

Türk Standardları Enstitüsü. (1980). *TS648: Çelik Yapıların Hesap ve Yapım Kuralları*. Ankara.

Türkiye Hazır Beton Birliği. (Nisan 2013). *2012 Yılı Hazır Beton Sektörü İstatistikleri*.



## APPENDIX A

### DESIGN EXAMPLE

A design example of 60 meter long composite steel plate girder designed with live load factor of 1.75 and resistance factor of 1.00 for AYK45 live loading is stated here.

#### Material Properties

Yield strength of steel,  $F_y = 345$  MPa

Elastic modulus of steel = 199955 MPa

Compressive strength of concrete,  $f'_c = 30$  MPa

Density of steel = 7850 kg/m<sup>3</sup>

Density of concrete = 2400 kg/m<sup>3</sup>

Density of Asphalt = 2250 kg/m<sup>3</sup>

#### Section Properties

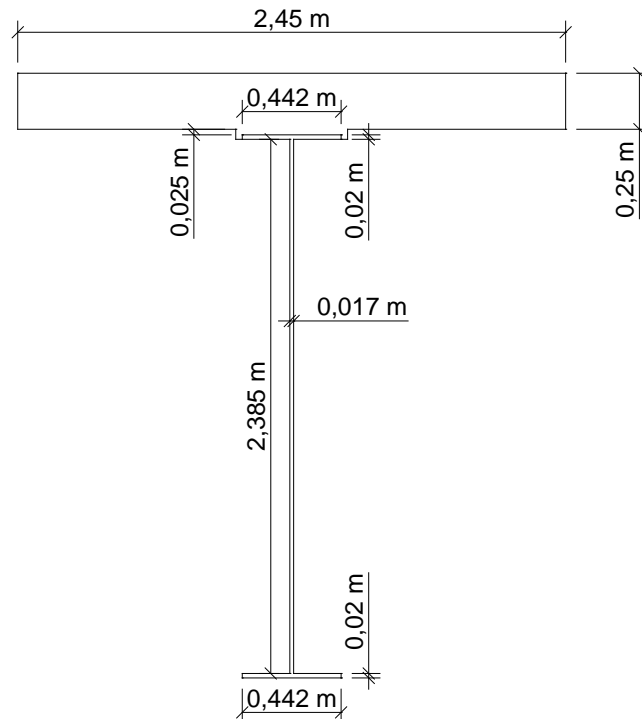


**Figure A-1** Cross-sectional Dimensions of Composite Steel Girder

Effective flange width,  $b_e = \text{Girder spacing} = 2.45 \text{ m}$   
 Cross-sectional area of steel girder,  $A = 0.058225 \text{ m}^2$   
 Moment of inertia of steel girder about centroid,  $I = 0.044785 \text{ m}^4$

### Member Proportion Checks

$$\frac{D}{t_w} = \frac{2.385}{0.017} = 140.3 < 150 \dots \text{OK}$$

$$\frac{b_f}{2t_f} = \frac{0.442}{2 \times 0.02} = 10.1 < 12 \dots \text{OK}$$

$$b_f = 0.442 > \frac{D}{6} = \frac{2.385}{6} = 0.398 \dots \text{OK}$$

$$t_f = 0.02 > 1.1t_w = 1.1 \times 0.017 = 0.0187 \dots \text{OK}$$

### Dead Load Effects

Four separate dead loads must be calculated. The first is the dead load of factory made elements,  $D_1$ . The second type of dead load is  $D_2$ , which represents the cast-in-place concrete. The third load,  $D_3$ , is caused by wearing surface. The fourth load,  $D_4$ , is the weight of the barriers. For design it is assumed that the barrier loads are distributed equally among the interior and exterior girders.

$$D_1: \text{Weight of steel girder} = 7850 \times 9.81 \times 0.058225 \times 10^{-3} = 4.48 \text{ kN/m}$$

$$D_2: \text{Weight of slab} = 2400 \times 9.81 \times 0.25 \times 2.45 \times 10^{-3} = 14.42 \text{ kN/m}$$

$$+ \text{Weight of haunch} = 2400 \times 9.81 \times 0.025 \times 0.5 \times 10^{-3} = 0.29 \text{ kN/m}$$

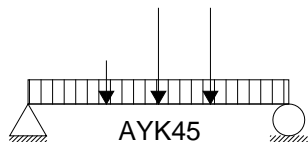
$$D_3: \text{Weight of asphalt} = 2250 \times 9.81 \times 0.06 \times 2.45 \times 10^{-3} = 3.24 \text{ kN/m}$$

$$D_4: \text{Weight of barriers (1/5 share)} = 2 \times 4.4 / 5 = 1.76 \text{ kN/m}$$

Moments ( $wL^2/8$ )

- $M_{D1} = 4.48 \times 60^2 / 8 = 2016 \text{ kNm}$
- $M_{D2} = (14.42 + 0.29) \times 60^2 / 8 = 6619 \text{ kNm}$
- $M_{D3} = 3.24 \times 60^2 / 8 = 1458 \text{ kNm}$
- $M_{D4} = 1.76 \times 60^2 / 8 = 792 \text{ kNm}$

### Live Load Effects



$$M_{\text{lane}} = 10 \times 60^2 / 8 = 4500 \text{ kNm}$$

$$M_{\text{truck}} = 6218.8 \text{ kNm}$$

Girder distribution factor,  $mg$ ,

$$K_g = n(I + Ae_g^2) = 7.6[0.044785 + 0.058225 \times (2.425/2 + 0.025 + 0.25/2)^2] = 1.16184 \text{ m}^2$$

$n = 7.6$  for  $f'_c = 30 \text{ MPa}$

$$mg_M^{SI} = 0.06 + \left(\frac{S}{4300}\right)^{0.4} \left(\frac{S}{L}\right)^{0.3} \left(\frac{K_g}{Lt_s^3}\right)^{0.1} = 0.06 + \left(\frac{2450}{4300}\right)^{0.4} \left(\frac{2450}{60000}\right)^{0.3} \left(\frac{1.16184 \times 10^{12}}{60000 \times 250^3}\right)^{0.1}$$

$$mg_M^{SI} = 0.373$$

$$mg_M^{MI} = 0.075 + \left(\frac{S}{2900}\right)^{0.6} \left(\frac{S}{L}\right)^{0.2} \left(\frac{K_g}{Lt_s^3}\right)^{0.1} = 0.075 + \left(\frac{2450}{2900}\right)^{0.6} \left(\frac{2450}{60000}\right)^{0.2} \left(\frac{1.16184 \times 10^{12}}{60000 \times 250^3}\right)^{0.1}$$

$$mg_M^{MI} = 0.562$$

$$mg = \max(mg_M^{SI}, mg_M^{MI}) = 0.562$$

$$M_{LL+IM} = mg \left[ M_{\text{truck}} \times \left(1 + \frac{IM}{100}\right) + M_{\text{lane}} \right] = 0.562[6218.8 \times (1 + 0.33) + 4500] = 7177 \text{ kNm}$$

### Load Combination

$$M_U = 1.25M_D + 1.5M_{DA} + 1.75M_{LL+IM}$$

$$M_U = 1.25(2016 + 6619 + 792) + 1.5(1458) + 1.75(7177)$$

$$M_U = 26530.5 \text{ kNm}$$

### Moment Carrying Capacity

Plastic forces,

- Slab,  $P_s = 0.85f'_c t_s b_e = 0.85(30)(0.25)(2.45) \times 10^3 = 15618.8 \text{ kN}$
- Tension flange,  $P_t = F_y b_t t_t = (345)(0.442)(0.02) \times 10^3 = 3049.8 \text{ kN}$
- Compression flange,  $P_c = F_y b_c t_c = (345)(0.442)(0.02) \times 10^3 = 3049.8 \text{ kN}$
- Web,  $P_w = F_y D t_w = (345)(2.385)(0.017) \times 10^3 = 13988 \text{ kN}$

Location of plastic neutral axis (PNA),

- $P_s + P_c > P_t + P_w \rightarrow$  PNA is in the compression flange
- $P_s < P_c + P_w + P_t$
- Distance from the PNA to the top of the compression flange,

$$Y = \left(\frac{t_c}{2}\right) \left[ \frac{P_w + P_t - P_s}{P_c} + 1 \right] = \left(\frac{0.02}{2}\right) \left[ \frac{13988 + 3049.8 - 15618.8}{3049.8} + 1 \right]$$

$$= 0.01465 \text{ m}$$

- PNA depth,  $D_p = 0.25 + 0.025 + 0.01465 = 0.28965 \text{ m}$

Compactness Check,

- $F_y = 345 \text{ MPa} < 70 \text{ ksi} (=483 \text{ MPa}) \dots \text{OK}$
- $D/t_w = 2.385/0.017 = 140.3 < 150 \dots \text{OK}$
- $2D_{cp}/t_w = 0/0.17 = 0 < 3.76\sqrt{E/F_y} = 3.76\sqrt{199955/345} = 90.5 \dots \text{OK}$

Note that  $D_{cp}$  is taken equal to zero unless PNA is in the web.

Plastic moment capacity,

$$M_p = \frac{P_c}{2t_c} [Y^2 + (t_c - Y)^2] + P_s d_s + P_w d_w + P_t d_t$$

$d_w$  = distance from PNA to centroid of web

$$d_w = 2.385 / 2 + 0.02 + 0.025 + 0.25 - 0.28965 = 1.19785 \text{ m}$$

$d_t$  = distance from PNA to centroid of tension flange

$$d_t = 0.02 / 2 + 2.385 + 0.02 + 0.025 + 0.25 - 0.28965 = 2.40035 \text{ m}$$

$d_c$  = distance from PNA to centroid of compression flange

$$d_c = 0.02 / 2 + 0.025 + 0.25 - 0.28965 = 0.00465 \text{ m}$$

$d_s$  = distance from the PNA to the midthickness of the concrete deck

$$d_s = 0.25 / 2 - 0.28965 = 0.16465 \text{ m}$$

$$M_p = \frac{3049.8}{2 \times 0.02} [0.01465^2 + (0.02 - 0.01465)^2] + 15618.8 \times 0.16465 + 13988 \times 1.19785 + 3049.8 \times 2.40035 = 26666.3 \text{ kNm}$$

Nominal flexural resistance,

$$D_p = 0.28965 \text{ m} > 0.1D_t = 0.1(2.7) = 0.27 \text{ m} \text{ (} D_t \text{ is total depth of composite section)}$$

$$\rightarrow M_n = M_p(1.07 - 0.7D_p/D_t) = 26666.3[1.07 - 0.7(0.28965)/2.7] = 26530.5 \text{ kNm}$$

### Design Check

$$\Phi_t M_n = 1.00(26530.5) = 26530.5 \text{ kNm}$$

$$M_U = 26530.5 \text{ kNm}$$

$$M_U = \Phi_t M_n \dots \text{OK}$$